"Synthesis and Characterizations of Lead Free KNN Ceramics near Morphotropic Phase Boundaries"

by

Mausumi Pattanaik

Department of Physics

For the award of the degree of

M.Tech (R)

to be submitted to

National Institute of Technology, Rourkela

Rourkela 769008, India

August-2011

DECLARATION

I hereby declare that thesis entitled "***Synthesis and Characterizations of Lead Free KNN Ceramics near Morphotropic Phase Boundaries***" which is being submitted by me to National Institute of Technology for the award of degree of Mater of Technology (Res.) is original and authentic work conducted by me in the Department of Physics, National Institute of Technology, Rourkela under the supervision of Prof. Pawan Kumar, Department of Physics, National Institute of Technology, Rourkela. No part or full form of this thesis work has been submitted elsewhere for a similar or any other degree.

Mausumi Pattanaik
Department of physics
National Institute of Technology
Rourkela-769008

DEPARTMENT OF PHYSICS
NATIONAL INSTITUTE OF TECHNOLOGY
ROURKELA-769008

CERTIFICATE

This is to certify that the thesis on **"Synthesis and Characterizations of Lead Free KNN Ceramics near Morphotropic Phase Boundaries"** submitted by **Mausumi Pattanaik**, to the National Institute of Technology, Rourkela in partial fulfillment of the requirements for the award of the degree of **Master of Technology (Res.) in Physics** is a record of bonafide research work carried out by her under my supervision and guidance .Her thesis in my opinion is worthy of consideration for the award of degree of Master of Technology in accordance with the regulation of the institute.

The results embodied in this thesis have not been submitted to any other university or institute for the award of degree.

Prof . Pawan Kumar
Department of Physics
National Institute of Technology
Rourkela-769008

ACKNOWLEDGEMENT

It is with a feeling of great pleasure that I would like to express my most sincere heartfelt gratitude to Prof. Pawan Kumar, Dept. of Physics, NIT, Rourkela for suggesting the topic for my thesis report and for his ready and able guidance throughout the course of preparing the report. I thank you Sir for your help, inspiration and blessings.

I express my sincere thanks to Prof. S.Jena, Head of the Department of Physics, NIT, Rourkela for providing me the necessary facilities in the department.

I would also take this opportunity to express my gratitude and sincere thanks to my honorable teachers , my Lab mates and the research scholars of Department of Physics ,NIT, Rourkela for their invaluable advice, constant help, encouragement, inspiration and blessings.

Submitting this thesis would have been a Herculean job, without the constant help, encouragement, support and suggestions from my friends and seniors especially Prakas Palei , Naresh Kumar Reddy and Sridevi Swain.

I would like to thank my parents and other family members, specially my brother for their support in all my life and their love, which has been a constant source of strength for everything I do.

I would also express my sincere thanks to laboratory Members of Department of Physics, Department of Ceramic Engineering and Material and Metallurgical Engineering, N.I.T. Rourkela.

Mausumi Pattanaik

Abstract

Ferroelectric oxides are a group of advanced electronic materials with a wide variety of properties useful in applications such as capacitors, memory devices, resonators and filters, infrared sensors, microelectromechanical systems, optical waveguides and modulators. Among the oxide based perovskite-structured ferroelectric system lead zirconate titanate (PZT) emerged as one of the useful material in various applications. But due to the toxicity of lead and serious environmental concerns there is an urgent need to develop lead free alternatives to replace the currently dominant lead based piezoelectric such as PZT.

Among non lead based ferroelectric systems Sodium Potassium Niobate($K_XNa_{1-X}NbO_3$ / KNN) based ferroelectric ceramics has recently emerged as a promising materials in radio frequency (rf) and microwave applications due to high dielectric tunability , low dielectric loss , relatively high curie temperature and piezoelectric coefficient. KNN system posses 3MPBs when X= 0.50,0.31 and 0.18. Near these MPB regions the compositions of KNN system are expected to exhibit better electrical properties .Till now the emphasis is around compositions close to 50/50 MPB. It is also difficult to sinter KNN ceramics because of its hygroscopic nature. This thesis presents results on growth and structural and electrical characterization of KNN ceramics near its 3MPB regions. In the current work emphasis has been given on low temperature synthesis of KNN ceramics near the three MPB regions using partial co-precipitation method and their characterizations. Using partial co precipitation method we have synthesized different compositions near the 3 MPB regions. Calcination temperature for single perovskite phase formation was optimized to ~700^0C, which is much lower than the same system synthesized by solid state synthesis route (SSSR). The structural and electrical properties of different compositions near the 3 MPB regions were studied in detail .It was

found that $K_{0.5}Na_{0.5}NbO_3$ MPB composition showed better density (~ 4.4g/cc), piezoelectric coefficient (d_{33} ~ 71 pC/N) and ferroelectric properties (P_s~ 14.271 μC/cm^2, E_c~ 9.8389KV/cm^2, P_r~ 10.9336 μC/cm^2) . Therefore to further improve the electrical properties of this composition, we have synthesized this MPB composition by using combustion synthesis process using urea as fuel and carried out sintering in oxygen atmosphere.

Through combustion method single perovskite phase of $K_{0.5}Na_{0.5}NbO_3$ (KNN) system was synthesized at relatively low calcination temperature (450°C) by using urea as fuel. The sintering of the KNN sample was performed at 1120^{o}C for 2h in the oxygen rich environment. SEM micrograph showed the dense and non-uniform distribution of grains with grain size ~1.45μm. The experimental density, piezoelectric (d_{33}) and ferroelectric(P_r) of the oxygen sintered KNN samples was found to be ~ 4.398g/cc, ~84pC/N and ~ 8.31 μC/cm^2 respectively , which is higher than the same system sintered in air by mixed oxide method.

Key words: Perovskite; Dielectric properties; Ferroelectric properties; piezoelectric properties; KNN; Morphotropic Phase Boundary.

Contents

LIST OF FIGURES

LIST OF TABLES

Chapter 1

Introduction, Literature Survey and Objective of Work

Introduction

This chapter provides a brief description of the phenomenon of ferroelectricity and piezoelectricity. The literature review section emphasizes on alkali niobate type lead free system and their solid solutions.

1.1 Ferroelectrics

Ferroelectricity is a phenomenon which was discovered in 1921. The name refers to certain magnetic analogies. But it has no connection with iron (ferrum) at all. Ferroelectricity has also been called Seignette electricity, as Seignette or Rochelle Salt (RS) was the first material found to show ferroelectric properties such as a spontaneous polarization on cooling below the Curie point, ferroelectric domains and a ferroelectric hysteresis loop. More concentration in the research on ferroelectric materials came in the 1950's leading to the widespread use of barium titanate ($BaTiO_3$) based ceramics in capacitor applications and piezoelectric transducer devices. Then after, many other ferroelectric ceramics including lead titanate ($PbTiO_3$), lead zirconate titanate (PZT), lead lanthanum zirconate titanate (PLZT), and relaxor ferroelectrics like lead magnesium niobate (PMN) have been developed and utilized for a variety of applications. Many new applications have also emerged due to the development of ceramic processing and thin film technology. Because of the continuous succession and development of new materials and technology, these materials led to new significant number of

industrial and commercial applications. Ferroelectric ceramics have found the biggest use in the areas such as dielectric ceramics for capacitor applications, ferroelectric thin films for non volatile memories, piezoelectric materials for medical ultrasound imaging and actuators, and electro-optic materials for data storage and displays [1].

Broad applications of ferroelectric materials are due to the properties like:

- High dielectric constant
- Unique piezoelectric, pyroelectric and electro-optic co-efficient
- Non-volatility
- Switching polarization

1.2 Crystalline structure and ferroelectric materials

On the basis of the symmetry elements of translational position and orientations, there are 230 space groups. Ignoring translational repetition, these 230 groups break down into 32 classes known as the 32 point groups, which are based on orientation only [2, 3]. Any point may be defined by coordinates x, y, and z, with respect to the origin of symmetry. A centrosymmetric crystal is a crystal in which the movement of each point at x, y & z to a new point at -x, -y & -z does not cause a recognizable difference. This implies that centrosymmetric crystals are non-polar and thus do not possess a finite polarization or dipole moment. Out of the 32 classes (or point groups), 11 classes are centrosymmetric and 21 classes are non-centrosymmetric. The later possesses no centre of symmetry which is the necessary requirement for the occurrence of piezoelectricity. However, one of the 21 classes, though classified as the non centrosymmetric class, possesses other combined symmetry elements,

thus rendering no piezoelectricity. Therefore, only 20 classes of non-centrosymmetric crystals exhibit piezoelectric effects, means polarization can be induced by a mechanical stress. Again, out of 20 piezoelectric classes 10 classes possess spontaneous polarization and hence can have piezoelectric as well as pyroelectric effects. There is a subgroup within these 10 classes that possesses spontaneous polarization and reversible polarization known as ferroelectrics. Fig 1.1 shows the inter-relationship of piezoelectric and subgroups on the basis of symmetry[4].

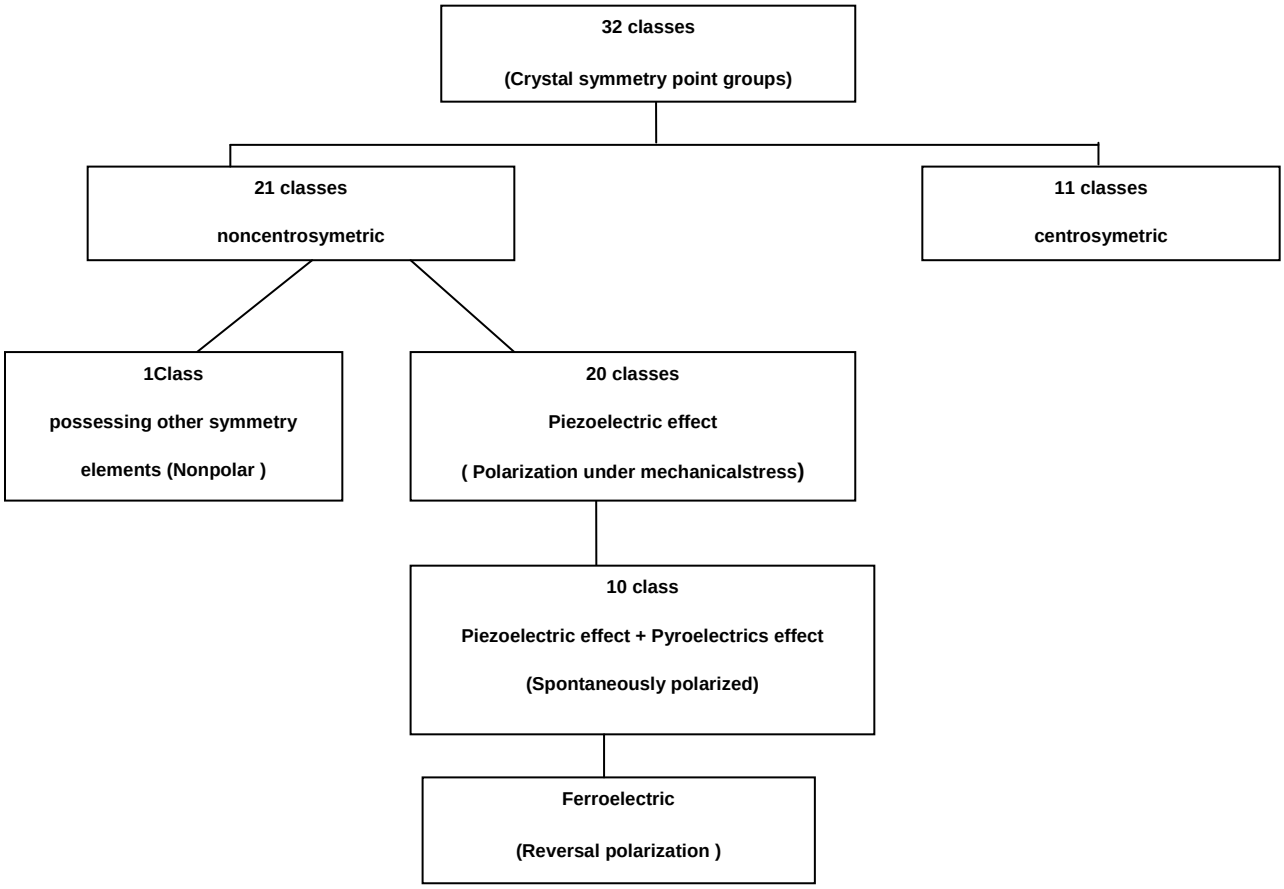

Figure 1.1 Classification of crystals showing the classes with piezoelectric, pyroelectric and ferroelectric effects.

Therefore, ferroelectricity is one of the most fascinating properties of dielectric solids. These are the certain special type of polar dielectrics in which the permanent electric dipoles are oriented in a specific direction even in the absence of the applied external electric field. Materials exhibiting ferroelectric properties must be either single crystals or polycrystalline solids composed of crystallites. A ferroelectric material must also have the following special properties.

- ✓ Spontaneous polarization
- ✓ Ferroelectric hysteresis (non-linear P vs. E curve)
- ✓ Curie transition temperature

1.3 General properties of ferroelectrics

1.3.1 Spontaneous polarization

Spontaneous polarization is defined as the value of the dipole moment per unit volume or the value of the charges per unit area on the surface perpendicular to the axis of spontaneous polarization in the absence of an external field. Only the crystals with a unique polar axis show spontaneous polarization vector along the axis. Generally the maximum value of remnant polarization is considered as the spontaneous polarization for a material at a given temperature. The spontaneous polarization is a function of temperature as shown in Fig1.2. As the temperature increases the thermal energy causes the dipoles to get disoriented. So the spontaneous polarization decreases with increasing the temperature and vanishes at a particular temperature called Curie temperature [4,5].

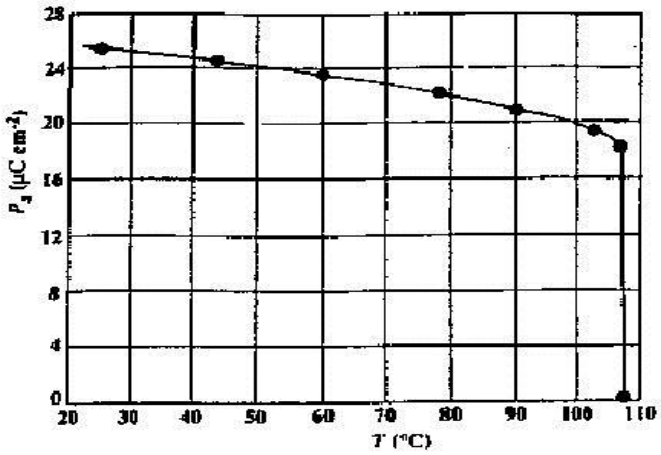

Figure 1.2 Variation of spontaneous polarization with temperature of BT ferroelectric ceramics[4].

1.3.2 Ferroelectric domain and hysteresis loop

The polarization (P)versus the electric field (E) behavior for a ferroelectric is non-linear and it exhibits a hysteresis loop similar to that of ferromagnetic material. Whenever the ferroelectric material subjected to an electric field the electric dipoles tend to get oriented in the direction of the electric field. There is a tendency for most of the dipoles to remain oriented in the field direction even in the absence of external electric field. This can be explained on the basis of the concept of ferroelectric domains. The ferroelectric domains are defined as the small microscopic regions in material within which all the dipoles are aligned in the same direction. Therefore each domain has one specific polarization direction .A ferroelctric single crystal has multiple ferroelectric domains which are separated by the interface called domain walls. A single domain can be obtained by domain wall motion which can be possible by the application of appropriate electric field. A strong field could lead to the reversal of the polarization in the domain, known as domain switching [5,6].

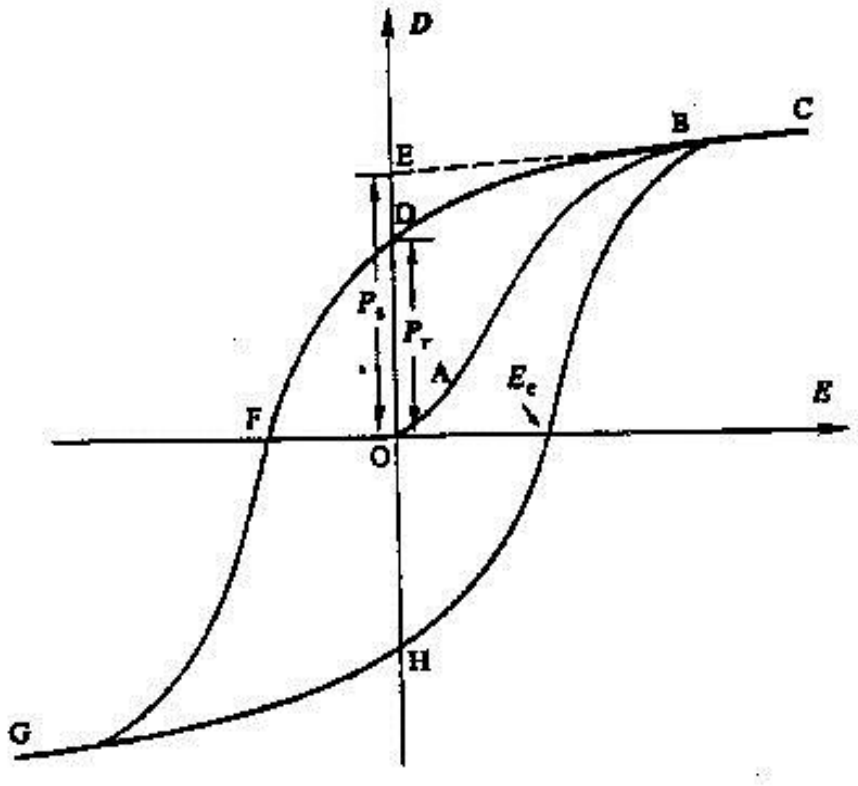

Figure 1.3 A polarization vs. electric field (P-E) hysteresis loop for a typical ferroelectric crystal[5,6]

The variation of the polarization with the applied electric field is shown in the Fig1.3. Initially the material is completely depolarized in the absence of the electric field due to the random orientation of the polarizations of the respective domains. As the electric field strength is increased the domain start to align in the positive direction of electric field by giving rise to the rapid increase of polarization (OB).At a very high field level the polarization reaches a saturation value (P_{sat}).The polarization does not fall to zero even when the field is removed, because of the alignment of some of the domains in positive direction. Hence the crystal will show a remnant polarization (P_r) .The crystal cannot completely depolarized until a field of magnitude (OF) is applied in the negative direction. The external field required to reduce the

polarization to zero is called the coercive field (E_c).If the field is increased more in negative direction, the direction of polarization flips and hence the hysteresis loop is obtained [5].

1.3.3 Ferroelectric Curie temperature and phase transition

All ferroelectric materials have a transition temperature called Curie temperature (T_c).At the Curie temperature the spontaneous polarization vanishes and at a temperature $T>T_C$ the crystal doesnot exhibit ferroelectricity, whereas for $T<T_C$ the crystal exhibit ferroelectricity. By decreasing the temperature across Curie point a ferroelectric crystal under goes a phase transition from a non-ferroelectric phase to ferroelectric phase. If more ferroelectric phases are present there, then the temperature at which the crystal changes from one ferroelectric to another ferroelectric structure is called transition temperature.[7]. Near the Curie point or transition temperatures, thermodynamic properties including dielectric, elastic, optical, and thermal constants show an anomalous behavior. This is due to a distortion in the crystal as the phase structure changes. The temperature dependence of the dielectric constant above the Curie point ($T > T_c$) in ferroelectric crystals is governed by the Curie-Weiss law

$$\varepsilon_r = \varepsilon_0 + C/(T-T_o) \qquad (1.1)$$

Where ε_r is the permittivity of the material

ε_o is the permittivity of the vacuum

C is the curie constant

T_o is the curie temperature, which is obtained by extrapolation.

Ferroelectrics are dominated by the displacive phase transition. In perovskite classes of ferroelectric materials, the temperature dependence of the permittivity varies for 1st and

2nd order phase transitions. Fig1.4 illustrates the temperature dependence of the permittivity for displacive ferroelectric materials exhibiting first or second order phase transitions. Second order phase transitions, which are common for rhombohedral compositions, are generally characterized by a broad peak in permittivity. Ferroelectrics undergoing first order phase transitions are typical tetragonal based structure. For first order transition $T_o<T_C$ while for second order phase transition $T_o=T_C$ [8].

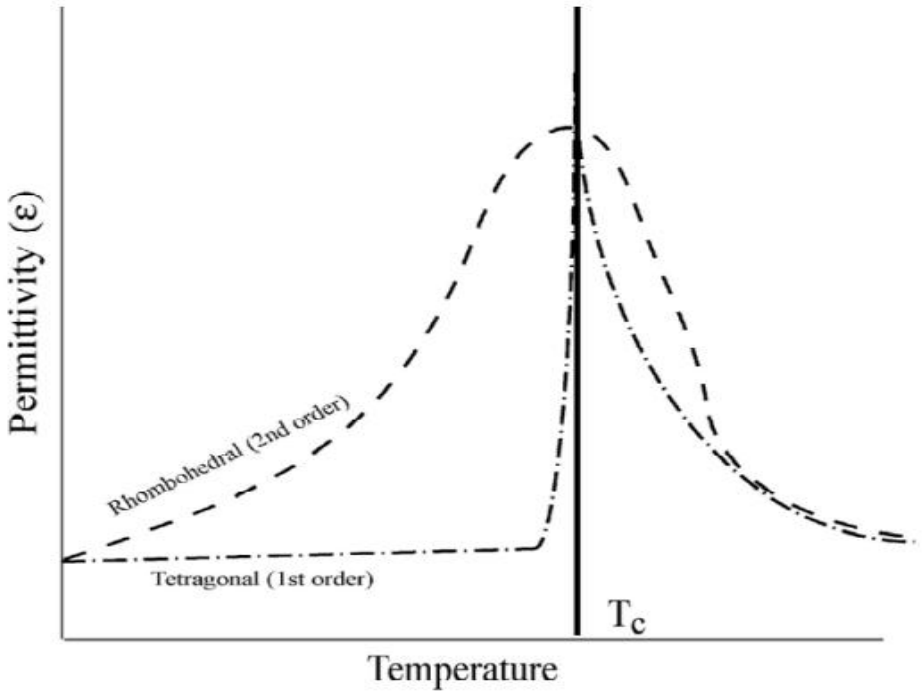

Figure1.4 Idealized permittivity of a ferroelectric material as a function of temperature [8].

For displacive transitions (e.g., $BaTiO_3$, $PbTiO_3$, $KNbO_3$), the Curie Constant is very high (~ 10^4 – 10^5 K) and the paraelectric phase is microscopically nonpolar. For

order-disorder transition (e.g., TGS, KH_2PO_4), the Curie constant is of the order of T_o and the paraelectric phase is nonpolar on macroscopic or thermally averaged.

1.3.4 Polarization mechanisms

In general, there are five different mechanisms of polarization which can contribute to the dielectric response of the ferroelectrics [9].

• **Electronic polarization (P_{ele}),** exists in all dielectrics. It is based on the displacement of the negatively charged electron shell against the positively charged core. The electronic polarizability P_{ele} is approximately proportional to the volume of the electron shell. Thus, in general P_{ele} is temperature-independent, and large atoms have a large electronic polarizability.

• **Ionic polarization (P_{ion}),** is observed in ionic crystals and describes the displacement of the positive and negative sublattices under an applied electric field.

• **Orientation polarization (P_{Or}),** describes the alignment of permanent dipoles. At ambient temperatures, usually all dipole moments have statistical distribution of their directions. An electric field generates a preferred direction for the dipoles, while the thermal movement of the atoms perturbs the alignment. The average degree of orientation is given by the Langevin function

$$\alpha_{or} = p^2 /(3k_B T) \qquad (1.2)$$

where k_B denotes the Boltzmann constant and T the absolute temperature.

• **Space charge polarization (P_{Sc}),** could exist in dielectric materials which show spatial inhomogeneities of charge carrier densities. Space charge polarization effects are not only of

importance in semiconductor field-effect devices, but also occur in ceramics with electrically conducting grains and insulating grain boundaries (so-called Maxwell-Wagner polarization**).**

• **Domain wall polarization (P_{Dw}),** plays a decisive role in ferroelectric materials and contributes to the overall dielectric response. The motion of a domain wall that separates regions of different oriented polarization takes place by the fact that favored oriented domains with respect to the applied field tends to grow.

The total polarization of dielectric material results from all the contributions discussed above. The contributions from the lattice are called intrinsic contributions, in contrast to extrinsic contributions.

$$P = P_{ele} + P_{ion} + P_{or} + P_{Sc} + P_{Dw} \qquad (1.3)$$

If the oscillating masses experience a restoring force, a relaxation behavior is found (for orientation, domain walls, and space charge polarization). Resonance effects are observedfor the ionic and electronic polarization. The dispersion of the dielectric function is shown in the following Fig.1.5.Generally the space charge polarization is caused by a drift of mobile ions or electrons which are confined to outer or inner interfaces. Depending on the local conductivity, the space charge polarization may occur over a wide frequency range from 1mHz up to few MHz. The polarization due to the orientation of electric dipoles takes place in the frequency ranges from 1mHz to a few GHz. It is often possible to distinguish between space charge and orientation polarization due to the temperature dependence nature of P_{or}. In the infrared region between 1THz to 10 THz, ionic polarization is observed due to the resonances of the molecular vibrations and hence the easy displacement of ions. But beyond infrared the displacement of the ions cannot respond fast enough due to its inertia properties .So the

contribution beyond infrared is only electronic polarization. The resonance of the electronic polarization is around 10^{15} Hz which can be investigated by optical methods [10, 5].

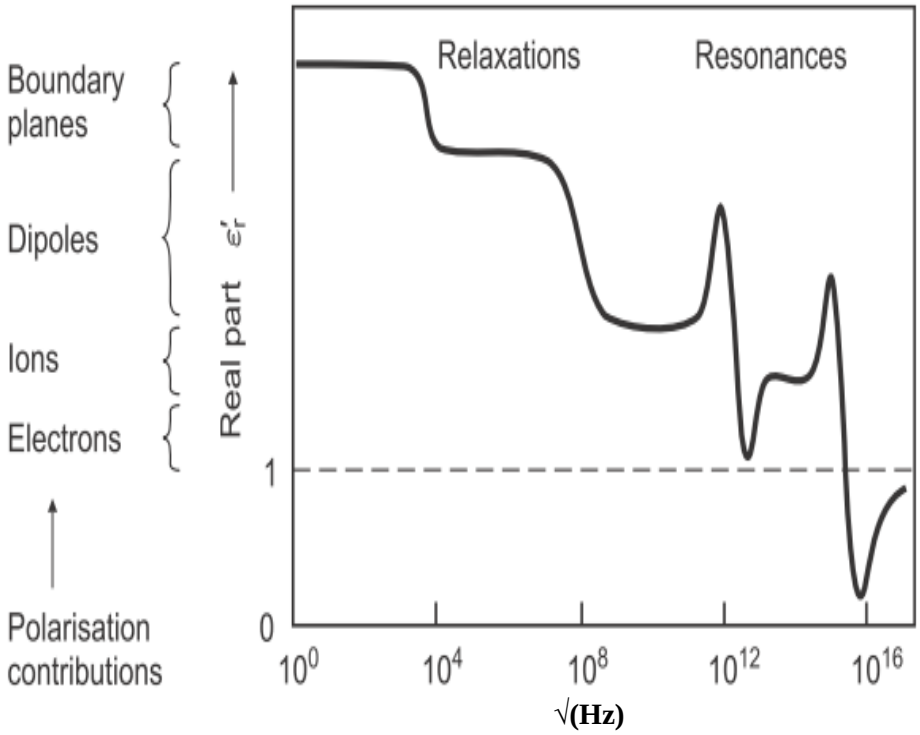

Figure 1.5 Frequency dependence of polarization processes[5].

1.4 Important ferroelectric material

Mainly there are four types of ferroelectric materials which are (1)the corner sharing octahedral,(2) compounds containing hydrogen bonded radicals, (3) organic polymers and (4) ceramic polymer composites **.**Among all of the four types of ferroelectric crystals corner sharing octahedral contain a large class of ferroelectric crystal in which perovskite structure type of compound is one. Perovskite piezoelectrics are of the great importance among all the piezoelectric ceramics. This structure has a general formula ABO_3 and may be described as a simple cubic unit cell with the corners occupied by a large cation ("A", such as Pb, Ba, Ca,

K, Na, etc.), a smaller cation ("B", such as Ti, Nb, Mg, Zr, etc.) and oxygens in the face centers.

How well a variety of cations can fit together to form the perovskite structure can be empirically predicted by the following relationship:

$$t = R_A + R_B / \sqrt{2}(R_B + R_0) \qquad (1.4)$$

where t is called "tolerance factor" and R_A , R_B and R_O the ionic radii of the A, B cations and oxygen ions, respectively. If the bonding between all the ions in the perovskite structure is ideally ionic, for a perfectly fit perosvkite structure, the tolerance factor is 1.0. The empirical rule of using t to predict the structure of a perovskite material is that when $0.95 < t < 1.0$, the structures are cubic, those with $t < 0.95$ tend to be slightly distorted but non-ferroelectric, and those with t slightly greater than 1 are ferroelectric.[8,10,11].

A typical perovskite material, barium titanate ($BaTiO_3$), was the first piezoelectric ceramic in which ferroelectric behavior was discovered. It is widely used because of its substantially high coupling factors and relatively good operation temperature. The most popular ferroelectric materials are described in the following sections.

1.4.1Barium titanate ($BaTiO_3$,BT)

Barium titanate ($BaTiO_3$) has a paraelectric cubic phase above its Curie point of about 130^0 C. In the temperature range of 130^0 C to 0^0 C the ferroelectric tetragonal phase with a c/a ratio of ~ 1.01 is stable,with spontaneous polarization along one of the [001] directions in the original cubic structure. Between 0^0 C and -90^0 C, the ferroelectric orthorhombic phase is stable with the polarization along one of the [110] directions in the original cubic structure. By

decreasing the temperature below -90^0 C, the phase transition from the orthorhombic to ferroelectric rhombohedral phase leads to polarization along one of the [111] cubic directions. The spontaneous polarization on cooling $BaTiO_3$ below the Curie point T_c is due to changes in the crystal structure. The paraelectric cubic phase is stable above 130^0 C with the center of positive charges (Ba^{2+} and Ti^{4+} ions) coinciding with the center of negative charge (O^{2-}). On cooling below the Curie point T_c, a tetragonal structure develops where the center of Ba^{2+} and Ti^{4+} ions are displaced relative to the O^{2-} ions, leading to the formation of electric dipoles. The developed spontaneous polarization is the net dipole moment produced per unit volume for the dipoles pointing in a given direction [6,12]. A cubic ABO_3 ($BaTiO_3$) perovskite-type unit cell and three dimensional network of corner sharing octahedra of O^{2-} ions is shown in Fig 1.6.

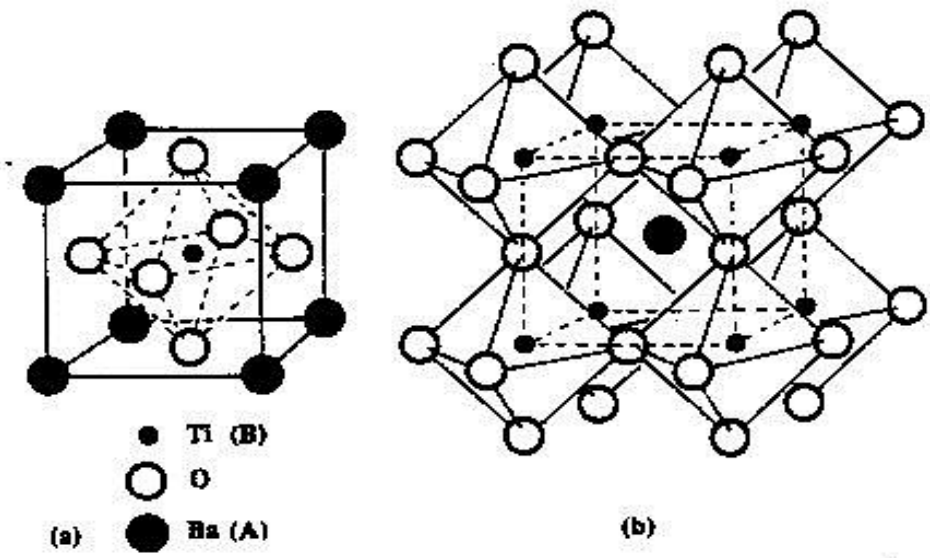

Figure 1.6 (a) A cubic ABO_3 ($BaTiO_3$) perovskite-type unit cell and (b) three dimensional network of corner sharing octahedra of O^{2-} ions [12].

$BaTiO_3$ is the first piezoelectric transducer ceramic ever developed, due to its high dielectric constant and low dielectric loss. But in recent years, it has shifted away from

transducers to an almost exclusive use as high-dielectric constant capacitors of the discrete and multilayer (MLC) types. The reasons for this are primarily two-fold: (1) its relatively low T_c of 130°C, which limits its use as high-power transducers, and (2) its low electromechanical coupling factor in comparison to PZT (0.52 vs 0.48), which limits its operational output. The values of the dielectric constant depend on the synthesis route, which means purity, density, grain size etc [13,14]. The dielectric constant is also dependent on temperature, frequency and dopants. Fig. 1.7 shows the temperature dependence of the dielectric constant measured with a small field along the pseudo-cubic edge. In this figure, only the values of the dielectric constant in the tetragonal phase have a clear meaning, as they were measured on carefully selected single domain crystals with the proper orientation.

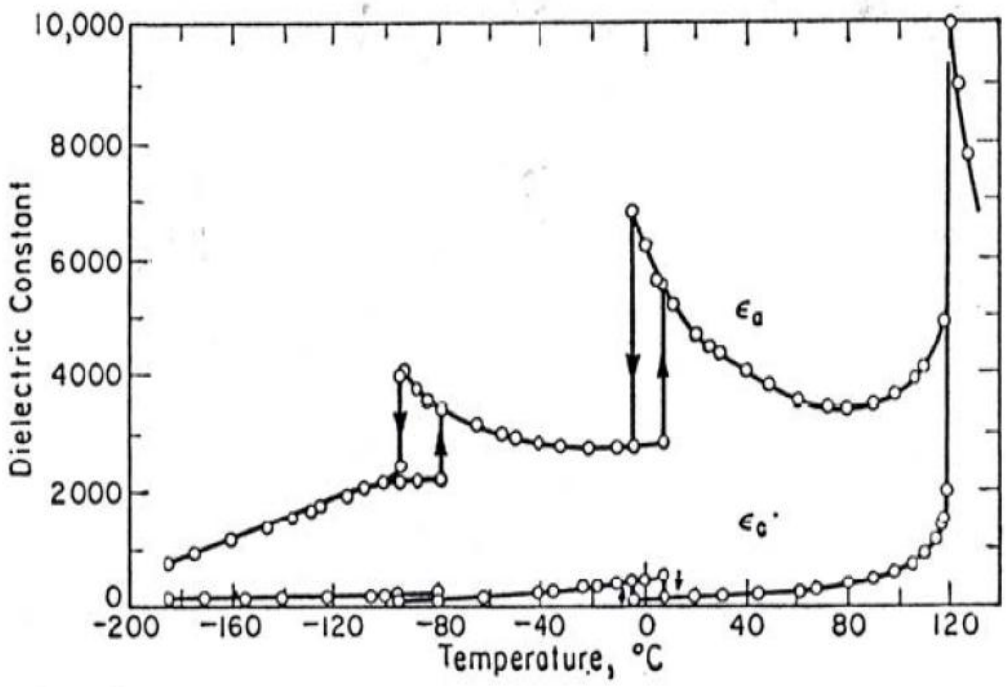

Figure 1.7 Dielectric constants of $BaTiO_3$as a function of temperature[13]

1.4.2 Lead titanate ($PbTiO_3$, PT)

Lead titanate is a ferroelectric material having a structure similar to $BaTiO_3$ with a high Curie point (490^oC). On decreasing the temperature across the Curie point a phase transition from the paraelectric cubic phase to the ferroelectric tetragonal phase takes place. Lead titanate ceramics are difficult to fabricate in the bulk form as they undergo a large volume change on cooling below the Curie point. Hence, pure $PbTiO_3$ ceramics crack and fracture during fabrication, because it is leading to a strain of > 6% at the time of a cubic (c/a = 1.00) to tetragonal (c/a = 1.064) phase transformation .The spontaneous strain developed during cooling can be reduced by modifying the lead titanate with various dopants such as Ca, Sr, Ba, Sn, and W to obtain a crack free ceramic. One representative of modified lead titanate composition, that has been extensively investigated recently is $(Pb_{0.76}Ca_{0.24})$ $((Co_{0.50}W_{0.50})_{0.04}Ti_{0.96})O_3$ with 2 mol. % MnO added to it. This composition has a decreased c/a ratio and Curie point of 255 ^oC). [15,16]

1.4.3 Lead zirconate titanate (PZT) &lanthanum PZT (PLZT)

PZT is a solid solution of $PbZrO_3$ and $PbTiO_3$ and the compositions around $Pb(Zr_{0.52}Ti_{0.48})O_3$ are of technical importance. PZT and modified PZT are materials of choice for transducer applications [13,17, 18] because they (1) possess higher electromechanical coupling coefficients than $BaTiO_3$, (2) have higher T_c values, which permit higher temperature of operation or higher temperature of processing during fabrication of the devices, (3) can be easily poled, (4) possess a wide range of dielectric constants, (5) are relatively easy to sinter at lower temperatures than $BaTiO_3$, and (6) form solid-solution compositions with many different constituents, thus allowing a wide range of achievable properties[13].

1.4.4 Bismuth layer-structure ferroelectrics (BLSF)

The two most important piezoelectric materials with the $(Bi_2O_2)^{2+}$ layer structure are bismuth titanate ($Bi_4Ti_3O_{12}$) and lead bismuth niobate ($PbBi_2Nb_2O_9$). The family of bismuth layer-structured ferroelectrics (BLSF) is very attractive from the viewpoint of their applications [19] .BLSF are characterized by their low ε, high T_c, and a large anisotropy in the electromechanical coupling factor (k_t /k_p or k_{33} /k_{31}) [20]. Therefore, the BLSF ceramics are seen as superior candidates for lead-free piezoelectrics for high-T_c piezoelectric sensors, filters, resonators and/or pyroelectric sensors with large figures of merit.

Bismuth titanate $Bi_4Ti_3O_{12}$(BIT), is a well-known BLSF material**.** The BIT layer structure is characterized by bismuth oxide ($(Bi_2O_2)^{2+}$) layers positioned between perovskite like layers. This crystal structure promotes a plate like morphology with the $(Bi_2O_2)^{2+}$ layers parallel to the plane of the platelets. BIT is monoclinic in the ferroelectric phase but is generally represented using an orthorhombic setting with the c-direction perpendicular to the layers and the major component of the spontaneous polarization in the a-direction of the perovskite plane. Cummins and Cross reported anisotropic spontaneous polarizations in BIT single crystals (50 μC/cm^2 along the a-axis and 4μ C/cm^2 along the c-axis). On the other hand, fully reliable piezoelectric properties of BIT ceramics have not been reported because of some problems such as low resistivity and large coercive field [21]. To solve these problems, Nb^{5+} and V^{5+} ions were doped into BIT ceramics to obtain higher resistivities. The highest d_{33} of 20 pC/N was achieved with a composition corresponding to $Bi_4Ti_{2.86}Nb_{0.14}O_{12}$ with a T_c of 655^o C. The crystal structure of $Bi_4Ti_3O_{12}$ is shown in Fig 1.8. A few bismuth oxide layered perovskite materials, such as $SrBi_2Nb_2O_6$ (SBN), $SrBi_2Ta_2O_9$ (SBT), and

$SrBi_2(Nb,Ta)_2O_9$ (SBTN), $SrBi_4Ti_4O_{15}$ have attracted an attention in the research community, because they are fatigue-free, lead-free and possess ferroelectric properties independent of film thickness for FeRAM application [22].

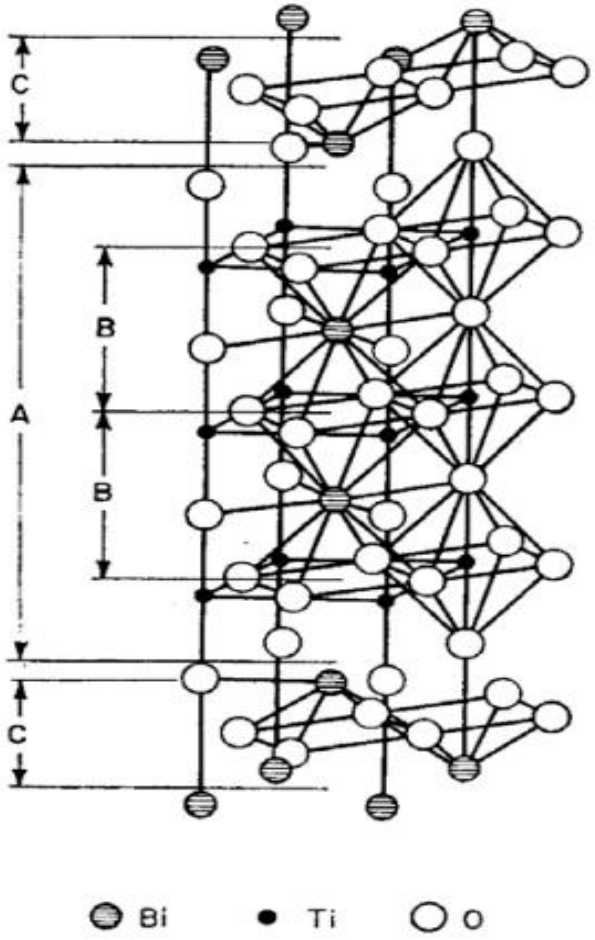

Fig.1.8 Crystal structure of $Bi_4Ti_3O_{12}$: C denotes $Bi_2O_2^{2+}$ layers and B denotes units of hypothetical perovskite structure and A denotes the perovskite multiple layer height[22].

1.5 Piezoelectricity

Some materials have the ability to produce electricity when subjected to mechanical stress. This is called the piezoelectric effect. The stress can be caused by hitting or twisting the material just enough to deform its crystal lattice without fracturing it. The effect also works in the opposite way i,e when a small electric current is applied, the material shows a slight deformation . Piezoelectricity was discovered more than one hundred years ago and has many applications today. The piezoelectric effect was first discovered in 1880 by Pierre Curie and Jacques Curie, two French physicists who were also brothers. Pierre Curie would later share the Nobel prize with his wife, Marie Curie, and Henri Becquerel for their work on radiation. The Curie brothers only discovered that piezoelectric materials can produce electricity, not that electricity can deform them. The next year, Gabriel Lippmann discovered this reverse effect. After these exciting discoveries different practical devices began to appear. Today, it is known that many materials such as quartz, topaz, cane sugar, Rochelle salt, and bone have this effect. This effect is used in electronic clocks, gas ovens, inkjet printers, and many other appliances. It also used in scientific instruments which require extremely precise movements, like microscopes**.**

Only the materials that have no center of symmetry in their crystalline structures possess piezoelectricity. For the direct piezoelectric effect, when a mechanical stress T is applied to the piezoelectric material, the charge generated is proportional to the force. The general equations that relate the electric and elastic variables can be written as:

$$D = dT + \varepsilon^T E \qquad (1.5)$$

where D is dielectric displacement (electric flux density per unit area) and d is called piezoelectric charge constant (or "piezoelectric constant" in short) that has unit of Coulombs/Newton. It can be understood as induced polarization per unit stress ε^T is the permittivity while the stress remains constant.

There is also a reverse effect, in which the applied electric field produces a proportional strain S.The induced strain S can be expressed in terms of the applied electric field and can be written as

$$S = s^E T + dE \qquad (1.6)$$

In this case s^E is the elastic compliance and remains constant under the electric field ,where as d has a unit of meters/Volt, which is different from that in case of the direct effect. For both effects the proportionality constant is the piezoelectric constant d which has numerically identical value for for both direct and reverse effects shown in equations (1.5) and (1.6).

Piezoelectric materials relates the properties like electric displacement and strain to both mechanical and electrical states of material .The properties like displacement and strain are the directional quantities ,hence they are usually specified with subscript to identify the condition under which they are determined. Therefore, d is actually a tensor and many other physical properties of piezoelectric materials have two subscripts (1, 2 or 3) that indicate the directions of two related quantities. By convention, the subscript 3 denotes the poling direction of the material, whereas 1 and 2 are two arbitrarily chosen orthogonal axes in the plane normal to 3. So piezoelectric charge constant is represented as d_{ij} in which the first subscript denotes the direction of polarization generated in the material or the direction of the applied electric field.

The second subscript denotes the direction of the applied stress or the induced strain. For example, d_{33} represents that the induced polarization is in direction 3 when the stress is applied in the direction -3. Similarly d_{31} represents the induced strain along direction 1 (perpendicular to direction 3) per unit electric field applied along direction 3. So typical relationships for these coefficients are

$$D_{33} = d_{33}T_3 \quad \text{(Direct effect)} \qquad (1.7)$$

$$S_{33} = d_{33}\, E_3 \quad \text{(Converse effect)} \qquad (1.8)$$

Where d coefficients are numerically equal in both equations, which are usually expressed as $\times 10^{-12}$C/N for direct effect and $\times 10^{-12}$ m/V for converse effect [1,8].

Piezoelectric coupling factor

The efficiency of energy conversion within a piezoelectric transducer is an important parameter .The electromechanical coupling factor (k) is measure of the efficiency of the electrical-mechanical energy conversion of a piezoelectric element and is defined as the

$$k^2 = \frac{Outputmechanicalenergy}{Inputelectricalenergy}$$

$$\text{Or } k^2 = \frac{Outputelectricalenergy}{Inputmechanicalenergy} \qquad (1.9)$$

The square of k measures the fraction of the mechanical energy delivered into the piezoelectric element converted to electrical energy (or vice versa).The coupling factors are the tensor quantities . A specific coupling factor (k_{ij}) is associated with each piezoelectric coefficient (d_{ij}). In practice, the conversion of one form of energy into another is never be full, therefore k^2 is always smaller than 1 ($k < 1$).The magnitude of the piezoelectric coupling for

non-ferroelectric material is typically very small(k<0.1).However the piezoelectric coupling achieved in certain ferroelectrics is much higher (0.4≤ k ≤0.7) [1,8] .The actual expression of k is dictated by the shape of the piezoelectric element. For example, for a thin piezoelectric ceramic disc, the planar coupling factor, k_p is used to express radial coupling, i. e. the coupling between an electric field parallel to the direction along which, the ceramic is polarized and the mechanical response that causes radial vibrations, relative to the poling direction. k_p is related to the piezoelectric constant d_{ij} and the dielectric constant $\varepsilon_3$with the following relation

$$k_p = d_{33} / \sqrt{2/(S_{11}^E + S_{12}^E)\varepsilon_3^T} \qquad (1.10)$$

1.6 Literature survey

1.6.1 Lead-based piezoelectric materials

Most of the piezoelectric materials used today are lead-based. The PZT family mentioned earlier is the most common one. This is the binary solid solution of $PbZrO_3$ an antiferroelectric (orthorhombic structure) and $PbTiO_3$ a ferroelectric structure (tetragonal perovskite structure).PZT has the perovskite structure with the Ti^{+4} and Zr^{+4} ions at B site at random. The PZT phase diagram is shown in Fig.1.9 .The phase diagram shows that at high temperature PZT has the cubic perovskite structure which is paraelectric and on cooling below the curie point the structure under goes a phase change from the ferroelectric tetragonal phase to rhombohedral phase. PZT dominates the field of piezoelectrics because of its strong piezoelectric effect, especially at the compositions near the morphotropic phase boundary [$Pb(Zr_{0.52}Ti_{0.48})O_3$], where two ferroelectric phases tetragonal and rhombohedral

coexist at the room temperature. The morphotropic phase boundary of PZT is almost vertical in the phase diagram, as shown in Fig1.9 which maintains the excellent piezoelectric properties across a wide temperature range [8].

Besides PZT, some newer generations of lead-based piezoelectrics that exhibit exceptional piezoelectric properties have also been created by combining $PbTiO_3$(PT) with some lead-based ferroelectrics such as $Pb(Zn_{1/3}Nb_{2/3})O_3$ (PZN) and $Pb(Mg_{1/3}Nb_{2/3})O_3$(PMN) to form solid solutions. Moreover, these materials also show very high dielectric constants at room temperature owing to the broadening of the permittivity peak around the Curie temperature. PZT ceramics with MPB composition can also be doped with different ions and form "hard and soft" PZT's depending upon the requirements for certain applications [1, 8].

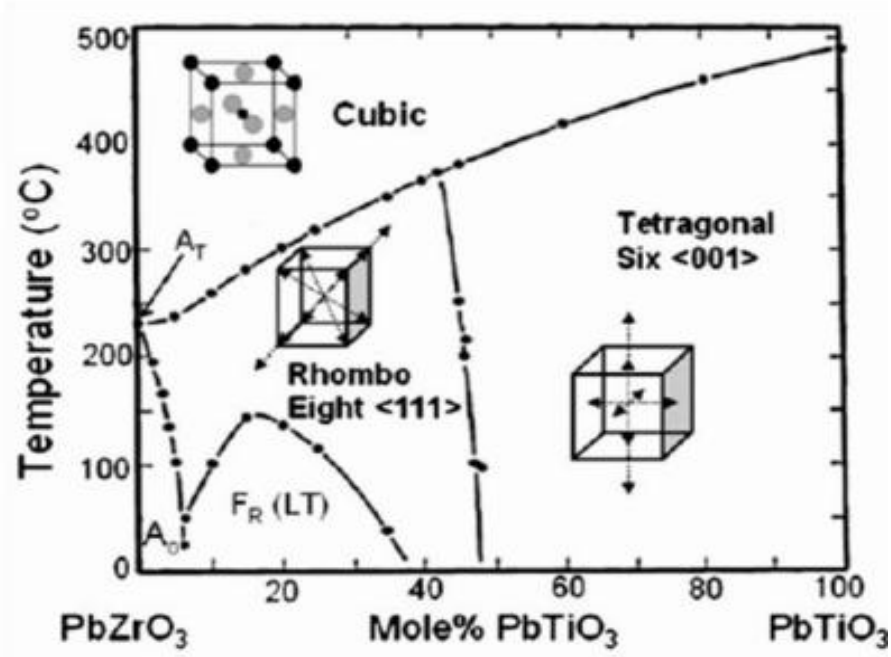

Figure 1.9 The phase diagram of PZT[8].

1.6.2. Current lead-free ferroelectrics

The most commonly used piezoelectric ceramics like $PbZr_xTi_{1-x}O_3$(PZT), $PbMg_{1/3}Nb_{2/3}O_3$-$PbTiO_3$(PMN-PT), and $PbZn_{1/3}Nb_{2/3}O_3$ -$PbTiO_3$ (PZN-PT) demonstrate high electromechanical properties (d_{33} is up to 700pC/N for PZT and 1500-2500 pC/N for the PMN-PT or PZN-PT) near their morphotropic phase boundaries **(**MPB) [23-25]. Due to high electromechanical properties, lead-based piezoelectric materials have an extensive use in different piezoelectric applications like actuators, sensors, and ultrasonic transducers. Except excellent electromechanical properties ,these lead-based piezoelectric materials contain a large amount of lead (> 60 wt. %) as a toxic element during processing. [26].

There are lots of environmental issues with restoring and recycling of the lead-based materials. Since lead maintains itself for a long time in the environment, accumulates in living tissues and can damage the brain and nervous system. On the other hand, improper disposing of lead, such as disposing in open environment, could introduce it to the ecosystem and cause "acid rain". Environmental and safety concerns with respect to the utilization, recycling, and disposal of Pb-based ferroelectric materials have induced a new surge in developing lead-free ferroelectrics, particularly those with properties comparable to their lead-based counterparts. Moreover, the necessity for using transducers with lead-free materials and monitoring ultrasound devices, which requires the embedded system in the human body, is another driving force for the investigation of lead-free piezoelectric materials [7,27].

Lead-free piezoelectric ceramics are classified into ferroelectrics with bismuth layered-structure, tungsten bronze and perovskite structures[28] .Among the above structures the lead free piezoelectrics with perovskite structure have the great importance

because of its simple structure with general formula ABO_3. . Lead-free piezoelectric materials with perovskite structure include the ferroelectric materials which are suitable for actuator and high power applications. The pervoskite structure of lead free ceramic is given in Fig 1.10. In this structure, cations based on their valence states and coordination numbers, occupy the A- or B- sites. The structure may be described by the simple cubic unit cell with a large cation (A) on the corners, a small cation (B) on the body centered, and the Oxygen (O) on the center of the faces [8, 29].

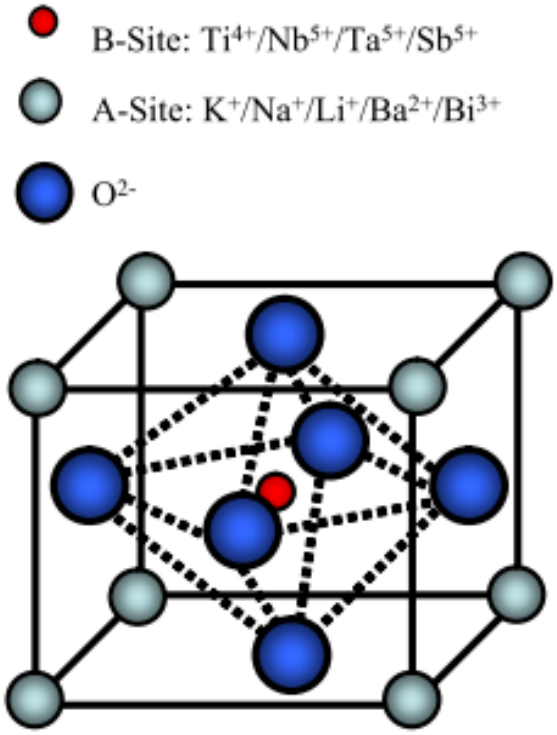

Figure 1.10 perovskite structure of lead free ceramics[8,29]

Bismuth sodium titanate $(Bi_{1/2}Na_{1/2})TiO_3$ and its solid solutions, $BaTiO_3$ (BT) and $KNaNbO_3$ -based ceramics ,$K_{1/2}Na_{1/2}NbO_3$ -$LiTaO_3$ (KNN-LT) are some examples of lead-free piezoelectric ceramics with perovskite structure[29]. BT is expected to be one of the superior candidates for lead free ferroelectrics, however the T_C of BT is too low~ 135^{o}C and

numerous poly-morphic phase transitions limit its overall usefulness. BNT along with its solid solution and alkali niobate compounds have received considerable attention due to their better piezoelectric properties and coupling coefficients than any other non-lead based piezoceramics. In BNT the depolarization temperature occurs at 200^0C and it has relatively high T_C. But this ceramic is difficult to fabricate in a dense body [29]. The system of $(Bi_{1/2}\ Na_{1/2})TiO_3$ -$(Bi_{1/2}\ K_{1/2})TiO_3$ -$BaTiO_3$ has shown the good electromechanical properties of d_{33}(191 pC/N), thickness coupling coefficient (k_t :56%), and T_c of 301˚C, which are expected to be reached to higher values in the grain-oriented condition [8,29,30]. On the other hand, $KNaNbO_3$ -based ceramics has also shown the d_{33} of 300pC/N and T_c is of ~ 400˚C and is comparable with some of the conventional PZT ceramics [13, 19, 29, 30].

Fig 1.11 (a) and (b) explicitly summarize the dielectric permittivity and the piezoelectric coefficients as a function of Curie temperature for different current lead-free ferroelectric systems in contrast to those of the PZT[31]. From the above figures one may notice that the dielectric and piezoelectric properties are normally enhanced by lowering the Curie temperature (T_C) for PZT-based materials. Except that for piezoelectric applications high Curie temperature is strongly desired in order to provide a wide temperature range of operation and ensuring the stability of the material performance. It is clear that among different perovskite materials KNN can have the properties which can be comparable with the PZT. But from the Fig 1.11 (a & b), one may notice that high piezoelectric coefficient and dielectric permittivity normally comes at the price of lowering the Curie temperature. Among lead free ferroelectrics KNN-based materials present a clear-cut advantage of high piezoelectric performance by maintaining high Curie temperature.

Potassium niobate (KN) ceramic with ferroelectric orthorhombic symmetry at room temperature has the phase transitions similar to $BaTiO_3$ but with higher T_c (~ 435ºC). $NaNbO_3$ (NN) ceramic is an orthorhombic anti-ferroelectric at room temperature with T_c ~ 355 ºC [30, 32].

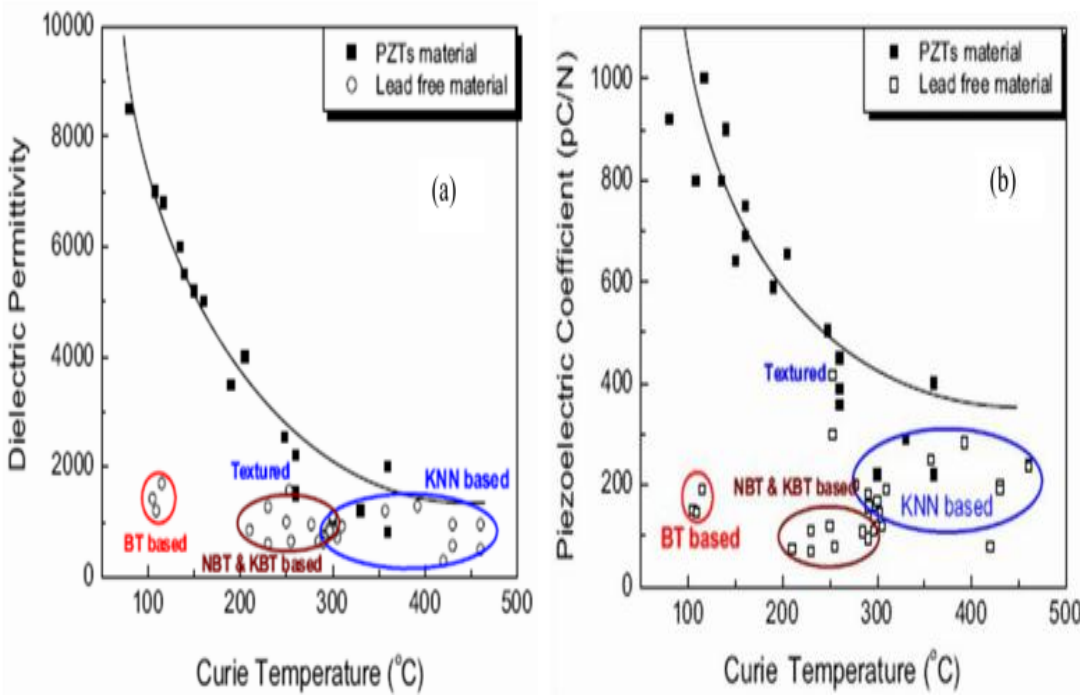

Figure-1.11 Property comparisons between PZT materials and lead-free materials :(a) dielectric permittivity as a function of Curie temperature; (b) piezoelectric coefficient as a function of temperature[31].

1.6.3 Potassium niobate ($KNbO_3$)

Matthias reported ferroelectricity in $KNbO_3$ (KN) system for the first time [3], where the point group of KN is assigned to mm2 with orthorhombic structure at room temperature. Phase transitions in potassium niobate are similar to $BaTiO_3$ (BT) and follow the same sequence of symmetry during cooling I,e cubic, tetragonal, orthorhombic and rhombohedral. However transitions in KN system are occurred at higher temperatures. Three out of four polymorphs in KN are ferroelectrics and have the curie point ~ 435^0C which represents the ferroelectric to paraelectric transformation temperature. Fig1.12 shows the permittivity-temperature behavior of the $KNbO_3$ single crystal with thermal hysteresis upon heating/cooling.

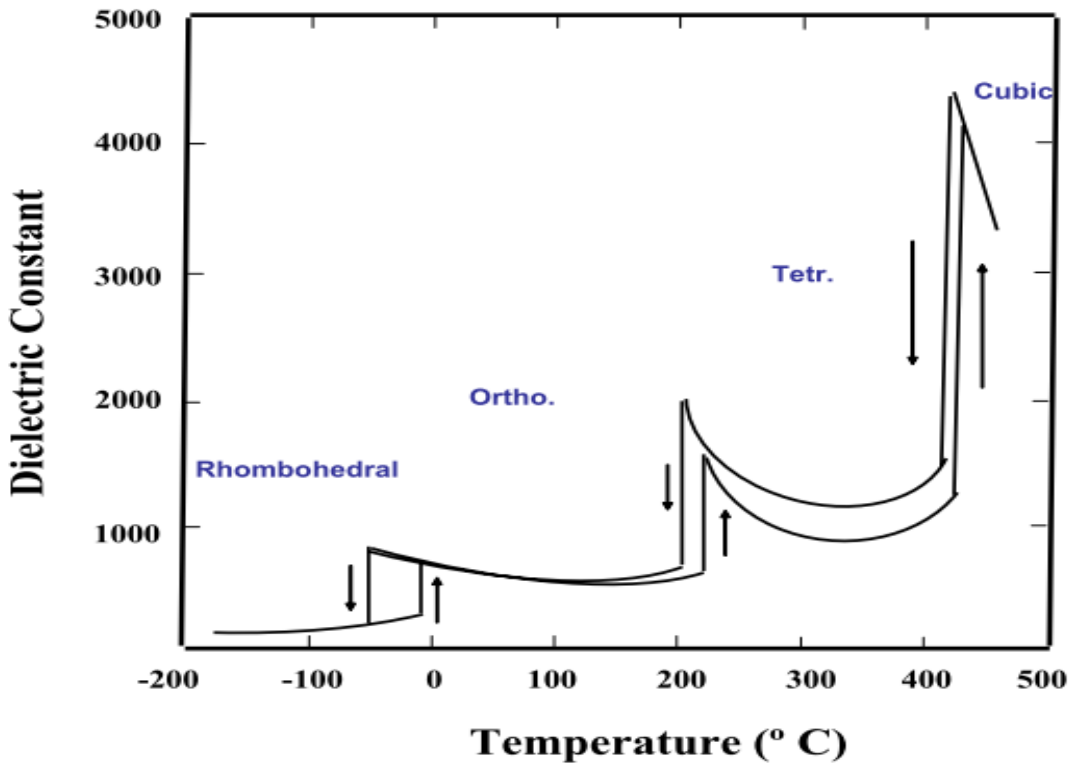

Figure 1.12 Dielectric constant temperature behavior of $KNbO_3$ single crystal[3]

In KNN system, number of other phases is also present in addition to the perovskite. Among them some are hygroscopic in nature which is the source of instability of the KN system. So processing of either single crystal or bulk ceramic of KN is difficult. Fig1.13 shows the phase diagram of K_2CO_3 -Nb_2O_5 where numerous phases coexist besides the perovskite phase [9]. Recent finding on higher piezoelectric properties along the [111] direction of tetragonal KN single crystal has highlighted the importance of the KN system, as KN does not have the problem of low temperature phase transitions [9, 33].

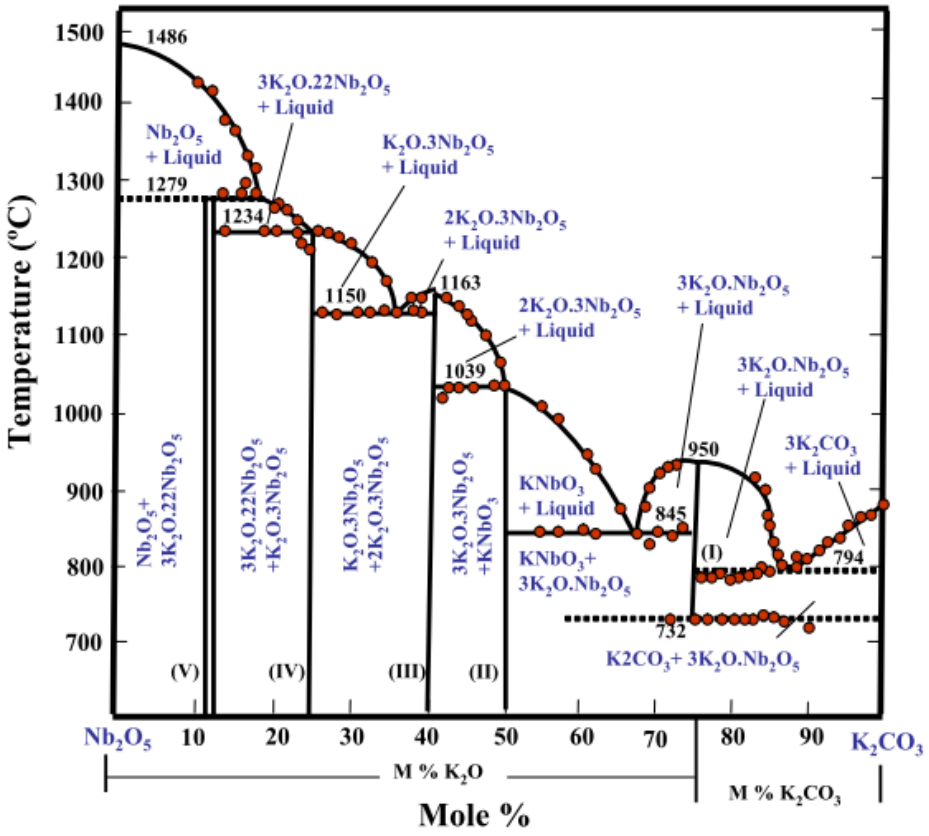

Figure 1.13 Phase diagram of K $_2$O-Nb_2O_5 (K_2CO_3 is used instead of K_2O for the part of diagram)[3]

In fact, upon heat treatment there is higher tendency of potassium niobate formation other than 1:1 ratio. High volatility of K_2O at sintering temperature also leads to non-stoichiometric KN composition. In order to solve this problem, leaching of the calcined powder with 2 % K_2CO_3 solution has been suggested [32], which dissolves the formed second phase(s) and retains the perovskite phase.

In the form of tetragonal structure, single crystal of $KNbO_3$ has a spontaneous polarization (P_s) of 30 μC/cm^2, while in the orthorhombic structure, it is 22 μC/cm^2. Room temperature properties of $KNbO_3$ ceramics are poor due to the difficulty in processing and sensitivity of these materials to the humidity (hygroscopic effect). Poled ceramics of the $KNbO_3$ have shown relative permittivity (at 1 MHz) of 430, dielectric loss of 2%, and planar coupling coefficient of 0.3 [9,34].

1.6.4 Sodium niobate ($NaNbO_3$)

Matthias reported sodium niobate (NN) as a room temperature ferroelectric material similar to potassium niobate. The compounds reported in the Na_2O-Nb_2O_5 system have the following Na:Nb ratios; 1:10, 1:7, 1:4 , 1:1, 3:1. At 1:1 compound of $NaNbO_3$ shows ferroelectric below room temperature where at/above it was non-polar and anti-ferroelectric. Sodium niobate at room temperature is orthorhombic anti-ferroelectric with space group of Pbam [9]. In this structure a & b axes are rotated 45º with respect to the simple cell and c axis is four times bigger than that of a simple perovskite cell. The monoclinic pseudo-rhombohedral phase (field-enforced phase) is a low temperature ferroelectric phase, which has the same polar axis direction as orthorhombic c- axis and orthorhombic phase is

the second field-enforced ferroelectric phase in pure sodium niobate. The induced external electric field lowers the length of c axis by half with respect to room temperature c-axis of orthorhombic anti-ferroelectric phase where the b axis acts as a polar axis. This phase can demonstrate a normal ferroelectric hysteresis loop under a high electric field. Fig.1.14 shows the low temperature-electric field behavior of $NaNbO_3$ single crystal [9].

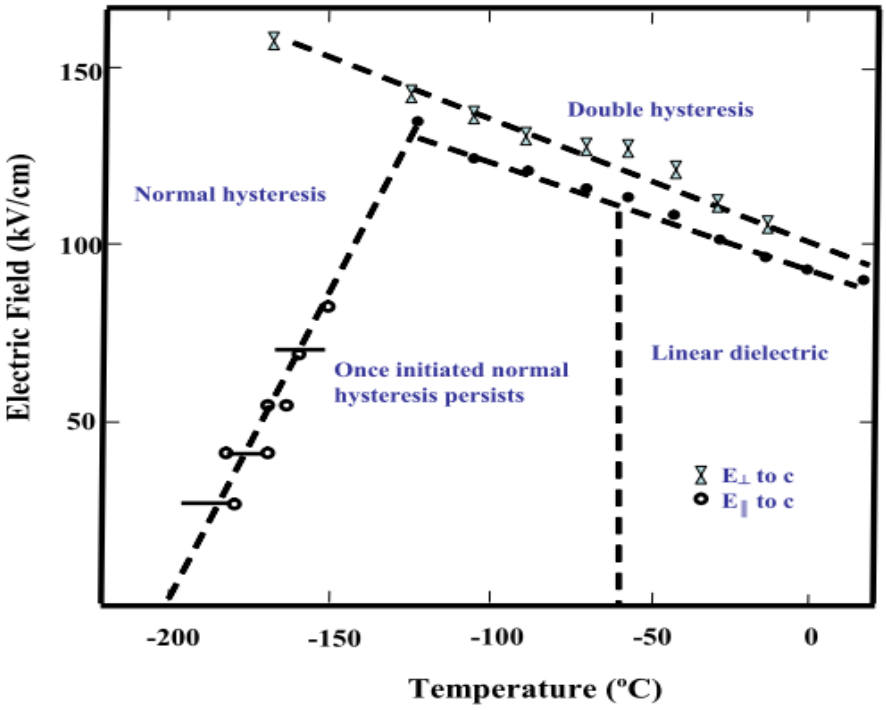

Figure 1.14 Effect of electric field on phase transition of $NaNbO_3$ single crystal [9]

The anti-ferroelectric Curie point for $NaNbO_3$ is around 355 ºC with four non-cubic phases. All four phases are considered paraelectric and are tetragonal or pseudo-tetragonal in which two have c >a and other two have c < a. At temperatures about 640 ºC, all of these phases transform to simple cubic. Fig.1.15shows the lattice parameter changes upon temperature increment and crystal structures formed in single crystal $NaNbO_3$ [35]. It was

observed that anti-ferroelectric NN at room temperature can be transformed to ferroelectric phase under a high external electric field [36,37]. Also the addition of potassium to NN develops the ferroelectric phase at room temperature and reduces the required electric field for ferroelectricity. It was observed that the minimum of 0.6 atomic percent of K^+ in the sodium niobate induced a ferroelectric phase with spontaneous polarization of 33μC/cm^2.At the same time, potassium cation has complete solid solubility in $NaNbO_3$ while the other materials such as lead titanate ($PbTiO_3$) or lead zirconate ($PbZrO_3$) show the limited solid solubility with lower spontaneous polarizations.

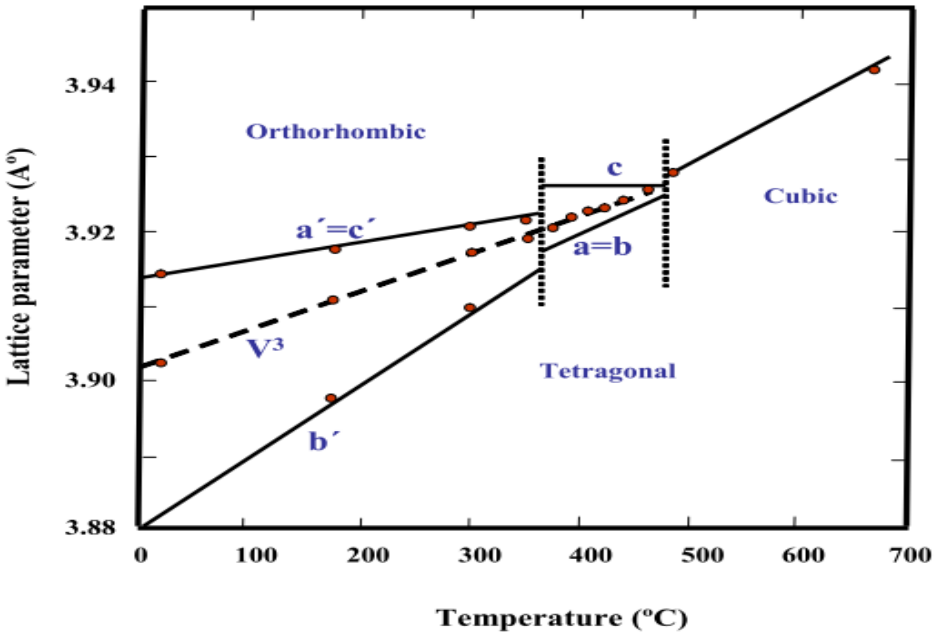

Figure 1.15 Phase transformations and lattice parameter changes in $NaNbO_3$single crystal[9]

1.6.5 Potassium sodium niobate ($K_xNa_{1-x}NbO_3$; KNN)

Potassium sodium niobate, $K_xNa_{1-x}NbO_3$ (abbreviated as KNN hereinafter), is a good candidate to replace PZT family because of its high Curie temperature and good piezoelectric properties. KNN is a solid solution of $NaNbO_3$ and $KNbO_3$. The addition of KN to NN results

in a ferroelectric phase with a high T_c (exceeding 400ºC) and is accompanied by a decrease in critical electric field needed to induce a ferroelectric phase transition as compared to that of pure NN [36,38]. The phase diagram of the $KNbO_3$ -$NaNbO_3$ system is given in Fig.1.16.By substituting a small amount of K^+ cation on the A-site of NN forms the same ferroelectric phase which can be produced at higher electric fields [9].Fig. 1.16 shows that the substitution of K^+ helps the stabilization of ferroelectric perovskite phase and reduces the formed metastable structures . On the other hand, substitution of the Na^+ cation in A-site position of $KNbO_3$ (left side of the phase diagram) does not change two high temperature phase transitions; however, it decreases the low temperature (orthorhombic-rhombohedral) phase transition [13,19].Phase diagram of KNN shows three morphotropic phase boundaries at around 52.5 mol%, 67.5 mol% and 82.5 mol% of $NaNbO_3$ separating two different orthorhombic phases, respectively(marked by the dash lines in Fig1.16) [39]. In 1959, the dielectric and piezoelectric properties of (1-x)$KNbO_3$ -x$NaNbO_3$ ceramic were reported and it was found that the piezoelectric properties of (1-x)$KNbO_3$ -x$NaNbO_3$ ceramics show less variation with change in composition than that for the PZT system. Around the MPB at 50 mol%$NaNbO_3$,namely, $Na_{0.5}K_{0.5}NbO_3$, piezoelectric performance was found maximum [19].

A major problem of undoped KNN is that it is fairly difficult to sinter in air using the conventional uniaxial pressing technique due to the limited phase stability of KNN system up to 1140^0C. Above this temperature high volatility of the potassium component occurred [40,41]. In addition to this, slight changes in stoichiometry can lead to the formation of an extra phase which make the final sample to disintegrate quickly once exposed to humidity [40-42]. However, atmospheric firing is strongly desired for industrial production of ceramics. So

to improve the sintering of this material, various techniques were used. It was reported in 1962 that hot pressing greatly increased the sintered density from 4.25 g/cm^3 to 4.46 g/cm^3 and the d_{33} was improved to 160pC/N [19]. Spark plasma sintering is also an another process, from which dense KNN ceramics can be synthesized [13,43] .Although these processes yields high densities, better properties as compared to conventionally sintered KNN, but it requires careful investigation and optimization of sintering parameters to result high quality and reproducible ceramics. Except that these processes are more expensive as compared to conventional sintering [42,44].

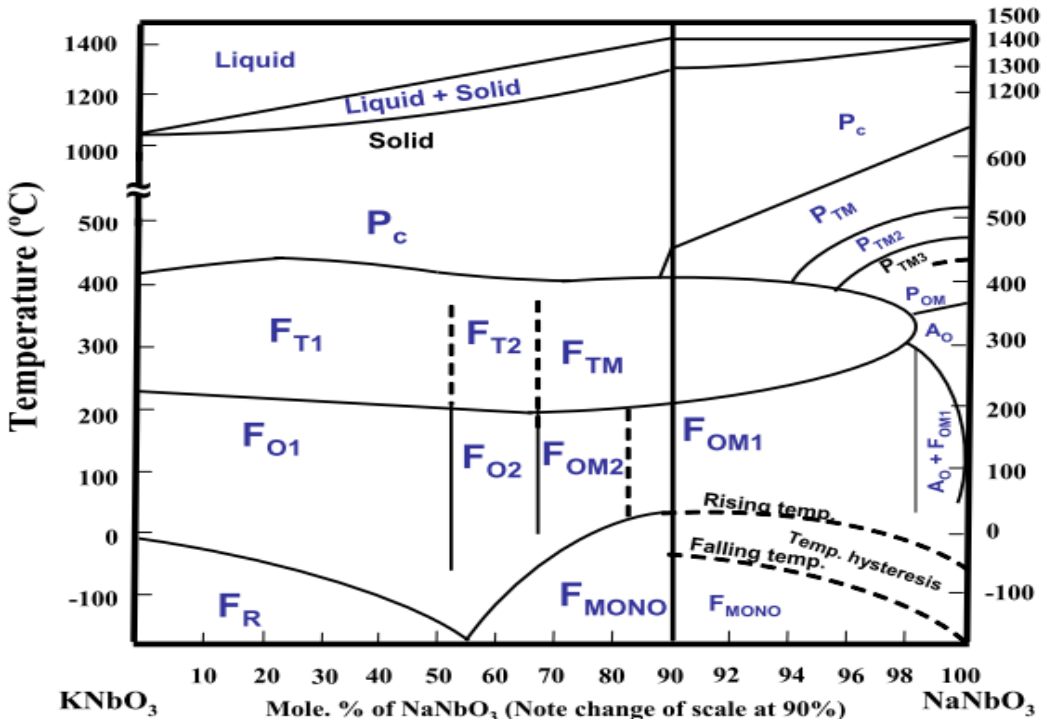

Figure 1.16 Phase diagram of the $KNbO_3$ - $NaNbO_3$ system[19]

In recent years different sintering aids like CuO, $K_4CuNb_8O_{23}$ (KCN) and $K_{5.4}Cu_{1.3}Ta_{10}O_{29}$ (KCT) are used to improve the density of the KNN system [45-48].CIP(Cold isopressing) was also used to obtain the green compacts in those studies and the

dielectric and piezoelectric properties did not show improvements even with the increase in sintered density of the ceramic. To effectively increase the piezoelectric performance of KNN system, few other materials have been used to form perovskite solid solutions with this KNN system such as NKN-$SrTiO_3$, NKN-$(Bi_{0.5}K_{0.5})TiO_3$, NKN-$BaTiO_3$, NKN-$LiTaO_3$, NKN-$LiNbO_3$ and NKN-$LiSbO_3$.These systems create morphotropic phase boundaries where an enhancement of the piezoelectric property was observed. From the literature, different synthesis process of the KNN based bulk material, its piezoelectric and dielectric properties are summarized in table 1.1[49-53].

Table-1.1 Summary of the piezoelectric and dielectric properties reported for all the current KNN-based bulk materials

	ε_r	Tanδ	d_{33} (pC/N)	T_C (°C)	K_p
NKN	290	0.04	80	420	0.35
NKN (hot pressed)	420	0.035	160	420	0.46
Spark Plasma sintering	~700	---	~148	395	---
Chemical synthesis	407	0.035	125	375	0.40
NKN-$LiTaO_3$(5%)	570	0.04	200	430	0.36
NKN-$SrTiO_3$ (5%)	950	---	200	277	0.37
NKN-$BaTiO_3$ (2%)	1000	0.04	104	358	0.295
NKN-$LiSbO_3$ (5%)	1288	0.019	283	392	0.5
Coating method with sintering aid	256	---	105	---	---

1.7 Objective of the work

Keeping the environmental concern in mind, a great deal of work has been carried out in the search of lead free ferroelectric materials based on the most studied perovskite compounds such as BT, KNN and NBT to replace PZT based material . But it is still important and challenging to design and synthesize new lead free ferroelectric systems with high performance and high T_C. According to the reported work, it is clear that the KNN family currently shows superior properties than that of the other lead free systems. Like PZT system, in KNN system three morphotropic phase boundaries (MPB) exist when Na mole % is around 52.5, 67.5 and 82.5. The compositions near these MPBs are expected to exhibit better electrical properties. In KNN system, the $K_{0.5}Na_{0.5}NbO_3$ composition is the most studied. Since, MPB is a region therefore any composition within this region can show better electrical properties. Also, compositions near other two MPBs of KNN system are not studied in detail. A new processing method that can improve the sintering of KNN is used in the present work.

Therefore, to realize the goal of this thesis, the specific research objectives were set as follows:

- Optimize the modified synthesis route for getting single perovskite phase and develop a new ceramic processing technique to overcome the sintering difficulty of KNN based materials. The approach used in this study is partial co-precipitation method which lowers the processing temperature of the KNN system and uses Na_2CO_3 , K_2CO_3 and NbO_3 as starting precursors.
- Single phase synthesis of different compositions near three MPB regions of KNN system.

- Detail study of phase formation, microstructure, dielectric & ferroelectric properties of compositions near three MPB regions of KNN system.
- propose a composition with better electrical properties among different MPB compositions.
- To further study the effect of Combustion synthesis technique on the composition with better electrical properties.

References

[1] Haertling G. J. Am. Ceram. Soc. 1999, 2, 797.

[2] Nye J.F. Physical Properties of Crystals (Oxford University Press, Oxford, 1960).

[3]Smith C.S. Macroscopic Symmetry and Properties of Crystals (Academic Press New York 1958)

[4] Kao K. C. Dielectric phenomena in solids (Elsevier Academic Press 2004).

[5] Vijaya M.S.; Rangarajan G. Material science (Tata McGraw-Hill Publishing India 2003).

[6] Vonhippel A. Rev. Mdern Phy.1950,22, 221.

[7] Nottleton R.E. Ferroelectrics1970 , 87, 2 .

[8] Jaffe B.; Cook,W. R.; Jaffe, H. C. Piezoelectric Ceramics (Academic Press New York 1971).

[9] Wang D. ; Fotinich Y.; Carman G. P. J. Appl. Phys. 1998,83, 5342 .

[10] Waser R.; Böttger U.; Tiedke S. Polar Oxides: Properties, Characterization, and Imaging, (WILEY-VCH Verlag GmbH & Co 2005).

[11] Wood E. A. Acta Crystallographica 1951,4, 353.

[12] Keith M. L.; Roy R. Am. Mineralogist 1954,39,1.

[13] Jaeger R. E.; Egerton L. J. Am. Ceram. Soc. 1962, 45, 209.

[14] Cao W.; Cross L.E. Phys.Rev. B.1991 ,44, 5 .

[15] Rittenmyer K.M. ; Ting R.Y. Ferroelectrics, 1990,110,170.

[16] Yamamoto T.; Saho M.; Okazaki K.; Goo E. Jap.J.Appl.Phy.1987, 57,2 .

[17] Kelly J. M., "A Study of Electromechanical Properties of PMN-PT Ceramics and Analysis of the Effects of Loss on Frequency Response of Piezoelectric Ceramics", Rutgers University, Ph.D. Thesis, 1998

[18] Egerton L.; Dillon D.M. J. Am. Ceram. Soc., 1959,42, 438.

[19] Takenaka T. ; Nagata H. J.Eur. Ceram Soc. 2005,25, 2693 .

[20] Elliot S. The Physics and Chemistry of Solids (John Wiley and Sons,Chichester,1998).

[21] Cummins S. E.; Cross L. E. J. Appl. Phys. 196839, 22, 68 .

[22] Noguchi Y. ; Miyayama M. Appl. Phys. Lett. 2001,78, 1903 .

[23] Park S. E.; Shrout T. R. IEEE Transactions on Ultrasonic, Ferroelectrics, and Frequency Control.1997, 44, 1140.

[24] Yamashita Y. ; Hosono Y. ; Harada K.;Yasuda N. IEEE Transactions on Ultrasonic, Ferroelectrics, and Frequency Control.2002, 2, 184.

[25] Yin J.; Jiang B.; Cao W. IEEE Transactions on Ultrasonic, Ferroelectrics, and Frequency Control.2000, 47, 285.

[26] Lv Y.G.; .Zhang C.L; Wu L.; Zhao M. L.; Xu J.P. mater. res. bull. 2009, 44, 284.

[27] Li H. "Sodium Potassium Niobate-based Lead-free Piezoelectric Ceramics: Bulk and Freestanding Thick Films" Drexel University,Phd thesis , june 2008

[28] Matsubara M. ; Yamaguchi T.; Kikuta K.; Hirano S.I. Jpn.J. Appl.Phys. 2004,43,7159.

[29] Takenaka T.;NagataH. ; Hiruma Y.; Yoshii Y.;Matumoto K. J.electroceramics. 2007, 19, 259.

[30] Smolenski G. A.;Isupov V. A;AgranovskayaA. I., Krainik,N. N. Sov..Phys.Solid State.1961,2, 2651.

[31] HaiboY.; Ying L; Fen W.; Hongjie L. Mat. Manu.Proc. 2008, 23, 489.

[32] Uchino K; Ferroelectric Devices(Marcel Decker, Inc. New York 2000).

[33] Wada S. ; Seike A. ; Tsurumi T. Jpn. J. Appl. Phy. 2001, 40, 5690.

[34] Kakimoto K.; Masuda I. ; Ohsato H. J. Eur.Ceram. Soc. 2005, 25, 2719.

[35] Shirane G.; Newnham R.; Pepinsky R. Phys. Rev. 1954, 96, 581.

[36] Cross L. E. Nature 1958, 181, 178.

[37] Molak A.; Onodera A.; Yamashita H. Jpn. J. Appl. Phys. 1992, 31,3221

[38] Cross L. E.; Nicholson B. J. Philos. Mag. 1955, 46, 212.

[39] Tennery V. J.; Wang K. W. J. App. Phy. 1968,39, 4750.

[40] Zupei Y.; yunfie C.; Bing L. ;Lingling w. Matt. Sci. and Eng.2006,432,292.

[41] Maeder M. D; Damjanovic D. ; Setter N. J. Electroceramics. 2004, 13, 385.

[42] Hansu B.; Dragan D.; Nava S. J. Eur. ceram. soc. 2006, 26,861.

[43]Li J.F.; Wang K. ; Zhang B.P.; Zhang L.M. J. Am. Ceram. Soc.2006, 89,706.

[44] Jarupoom P.; Pengpat K.; Eissayeam S.; Intatha U.; Rujijanagul G.; Tunkasiri T.; Ferr. Lett. 2008, 35, 119.

[45] Takao H.; Saito Y.; Aoki Y.; Horibuchi K. J. Am. Ceram. Soc.2006, 89, 1951.

[46] Li E.; Kakemoto H.; Wada S.; Tsurumi T. J. Am. Ceram. Soc. 2007,90, 1787.

[47] Matsubara M.; Yamaguchi T.; Sakamoto W.; Kikuta K.; Yogo T.; Hirano S. J. Am. Ceram. Soc. 2005,88, 1190.

[48]Nobre M. A. L.; Lanfredi S. Catalysis Today 2003,78, 529.

[49] GuoY. P.; Kakimoto K.; Ohsato H. Solid State Commun.2004,129, 279.

[50]Wang R.; Xie R.J.; Hanada K.; Matsusaki K.; Bando H.; Itoh M. phys. status solidi A. 2005,202, R57

[51] Cho K. H.;Park H. Y.;Ahn C. W.;Nahm S.; Uchino K.;Park S. H.;Lee H. G.;Lee H. J. J.Am. Ceram.Soc.2007,90, 1946.

[52] Zuo R. Z.;Fang X. S.;Ye C.;Li L. T. J. Am. Ceram.Soc. 2007,90, 2424.

[53] Zang G.Z.;Wang J.F.;Chen H.C;Su W.B; Wang C.M; QiP.; Ming B.Q.; Du J.;Zheng L.M.; Zhang S.; Shrout T. R.; Appl. Phy.Lett.2006,88, 212908.

Chapter 2

Experimental and Characterization Techniques used in the present work

Introduction

In this chapter the basic principles and various experimental techniques used in the present thesis work are explained. The characterization techniques include thermo gravimetric analysis / differential scanning calorimetery (TGA/DSC), density measurement, X-ray diffraction (XRD) analysis, scanning electron microscopy (SEM), dielectric constant and dielectric loss measurements, ferroelectric PE-hysteresis loop and piezoelectric charge coefficient measurement technique.

2.1 Thermo gravimetric analysis

Thermo gravimetric technique is used to determine the materials thermal stability and its fraction of volatile components by monitoring the weight change at the time of heating of the specimen .The measurement is normally carried out in air or in an inert atmosphere, such as He/Ar, and the changes in weight is recorded as a function of increase of temperature of test samples . Sometimes the measurement is performed in Neon oxygen atmosphere to slow down the oxidation. Such analysis relies on a high degree of precision in three measurements: weight, temperature, and temperature change. The result from thermo gravimetric analysis is usually reported graphically in the form of curves relating the mass loss from the sample against temperature during the chemical reaction processes. TGA is commonly employed in research and testing to determine degradation temperatures, absorbed moisture content of materials, the

level of inorganic and organic components in materials, decomposition points of explosives, and solvent residues. It is also often used to estimate the corrosion kinetics in high temperature oxidation process [1,2]

Differential scanning calorimetry or DSC is another thermo analytical technique in which the difference in the amount of heat required to increase the temperature of a test sample and reference sample is measured as a function of temperature. Both the test and reference sample are maintained at nearly the same temperature throughout the experiment. The basic principle of this technique is that when the test sample undergoes a physical transformation such as phase transitions, more or less heat will need to flow from it to the reference sample to maintain both at the same temperature. The heat flow in or out to the test sample depends on whether the process is endothermic or exothermic. When the test sample undergoes a phase transition from solid to liquid it requires more heat at the same rate as the reference sample. This absorption of heat corresponds to an endothermic peak in the DSC curve. Similarly when the test sample becomes crystallized, less heat is required to raise its temperature which corresponds to an exothermic peak on the curve. By observing the difference in heat flow between the test sample and reference sample, differential scanning calorimeters are able to measure the amount of heat absorbed or released during such transitions [1-3].

2.2 Calcination

Calcination is a chemical reaction process during which either the partial or complete phase of the compound is formed. It also helps in removing the unwanted gases and products during the decomposition of the constituent compounds. Calcination also helps in homogenizing the materials and reducing the shrinkage during the subsequent sintering

process of the finally shaped samples. In general, four physical processes are involved in the calcination of the raw materials:

(i) Linear expansion of the particles (< 400^0C) (ii) Solid phase reaction (400-750^0C) (iii) Contraction of product (750-850^0C) and (iv) Grain growth (>850^0C).

Phase formation of a compound takes place by solid-phase reaction, which involves the chemical reaction through atomic diffusion among grains at temperature below the melting points of the raw materials [4]. Usually, the calcination temperature is chosen high enough to cause complete reaction, but also low enough to cause subsequent grinding. In the materials, having volatile constituents, the calcination temperature must be kept low enough to avoid loss of the volatile parts. To lower the calcination temperature and avoid the loss of volatile constituents, alternating processing techniques such as MOD (sol-gel processing), Co-precipitation etc. are used [4]. Several non-conventional routes are also employed to reduce the calcination temperature, which results in better quality ferroelectrics at relatively lower sintering temperature.

2.3 Sintering

Sintering is the process in which the shaped materials are consolidated into strong and dense polycrystalline aggregates. During sintering at an appreciable temperature, the atomic motion is more violent and the area between grains in contact increases due to the thermal expansion of the grains and finally only one interface remains there between two grains. This corresponds to a state with much lower surface energy. In this state, the atoms on the grain surfaces are affected by neighbouring atoms in all directions, which results in densified ceramic [4]. At the beginning of the sintering process, but rather at high temperature, the lattice

distortion and internal strain are reduced by atomic diffusion and this is frequently called as 'the recovery process'. With the further increase in temperature, a recrystallization process occurs through atomic diffusion. During recrystallization, new crystal nuclei form and grow at grain boundaries and in other regions inside the grain with higher free energies. Meanwhile, some grains grow by swallowing up other grains. In the recrystallization stage, grain growth is usually realized through the motion of grain boundaries. In general, higher the sintering temperature, larger the grains would grow, as the grain growth is caused by atomic diffusion, which increases with the increase in sintering temperature. However, the density of a ceramic is affected by the sintering temperature and time in a more complex fashion. If the sintering temperature is too high or the sintering time is too long, the density of the lead based ceramics will be reduced owing to PbO evaporation at high temperatures. Since, the grain growth is caused by atomic diffusion, it follows that a higher sintering temperature and a larger hold time would result in larger grains. The oxide ceramics should be sintered in an oxidizing atmosphere or in air and a reducing atmosphere must be avoided. Therefore, no organic substances should be mixed with the semi-finished products, as they can produce a reducing atmosphere (i.e CO) during sintering [4].

2.4 X-Ray diffraction

X-ray diffraction is a versatile, non-destructive method to get information about the crystal structures of various materials and thin films. X-ray diffraction can be applied to any crystalline material, but the method is most sensitive to high Z elements, since the diffracted x-ray intensity is stronger from heavier nuclei. The power of XRD lies in the enormous amount of information that can be extracted from the data. An introductive treatment on the vast topic

of x-ray diffraction can be found in the book by Cullity [5,6]. Diffractometer is widely used for XRD analysis. In modern x-ray techniques, a series of peaks has been obtained, due to the use of the detector in the diffractometer. A typical diffractometer is shown in Fig 2.1.The powder diffractometer uses an x-ray detector to measure the positions of the diffracted beam .A convenient amount of incident ray is recorded at an angle of 2θ[2,6]

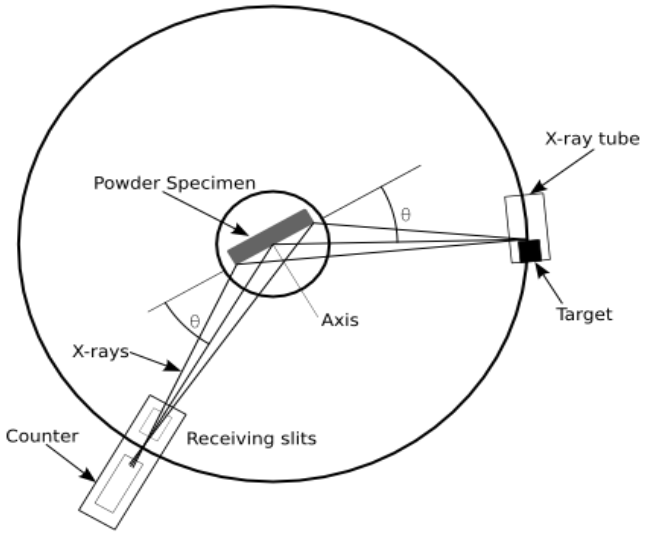

Figure 2.1Schematic diagram of an diffractometer[2,6]

The X-ray diffraction pattern is related to the crystal symmetry and can be used to monitor chemical reactions and structural properties such as phase purity and change of symmetry (phase transition). So the change of symmetry due to the change of crystal structure leads to the change in the x-ray diffraction pattern. This will affect the d-spacings within the lattice, which results the splitting or merging of peaks as shown in Fig 2.2 and Fig 2.3.This characteristic XRD pattern can be used to identify the symmetry and phase components of the materials [5,6].

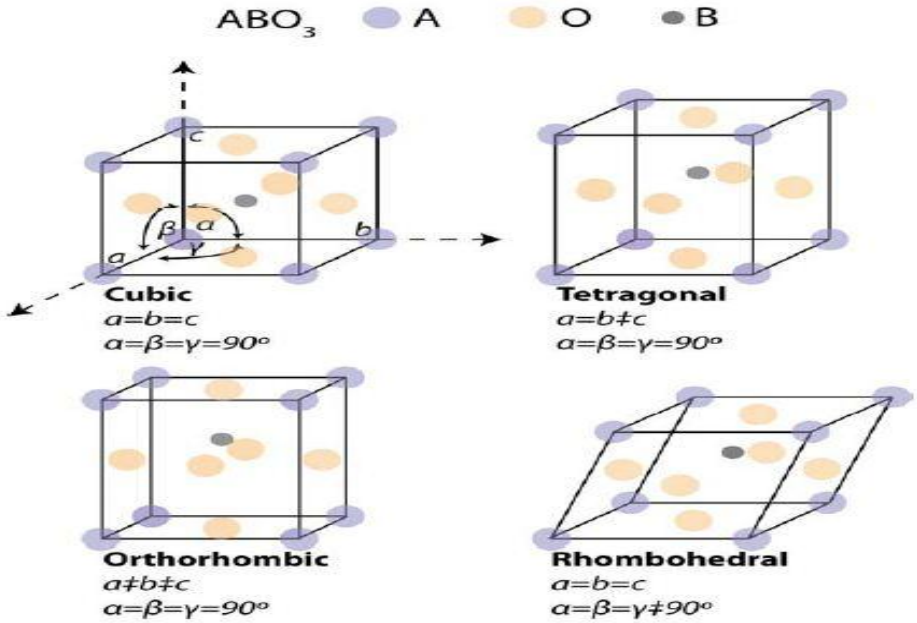

Figure 2.2 Illustration of various unit cell types with corresponding lattice parameters for a perovskite, ABO_3, structure [5,6].

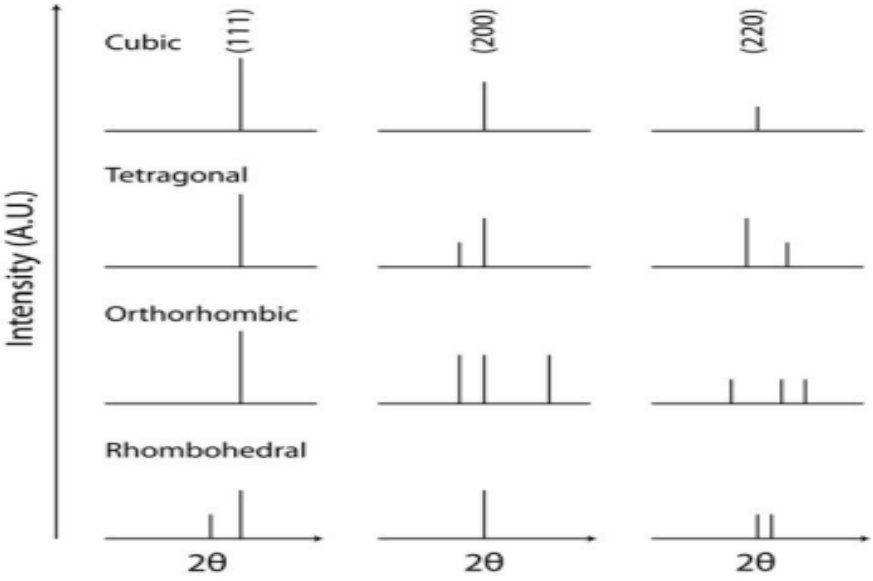

Figure2.3 Characteristic x-ray diffraction patterns for various symmetries showing the corresponding splitting with respect to the cubic (111), (200) and (220) reflections [6].

2.5 Scanning electron microscopy (SEM)

In this thesis work, the microstructures of the prepared ceramic samples are examined by using JEOL T-330 scanning electron microscope. A scanning electron microscope (SEM) is a type of electron microscope that images a sample by scanning it with a high-energy beam of electrons in a raster scan pattern. This technique is widely used to characterize the surface topography, morphology, compositions and crystallographic information of the samples. The fundamental principle of scanning electron microscopy (SEM) is mainly based on the accelerated electrons which carry significant amount of kinetic energy. This energy is dissipated as a variety of signals due to the electron-sample interactions . These signals include secondary electrons (that produce SEM images), backscattered electrons (BSE), diffracted backscattered electrons(used to determine crystal structures and orientations of minerals), photons (characteristic X-rays that are used for elemental analysis and continuum X-rays), visible light (cathode luminescence), and heat. Secondary electrons and backscattered electrons are commonly used for imaging the samples. Secondary electrons are most valuable for showing morphology and topography of the samples; whereas backscattered electrons are most valuable for illustrating contrasts in composition in multiphase samples (i.e. for rapid phase discrimination). X-ray generation is produced by inelastic collisions of the incident electrons with electrons in discrete orbital (shells) of atoms in the sample. Thus characteristic X-rays are produced for each element in a mineral that is "excited" by the electron beam. SEM analysis is considered to be "non-destructive"; that is, x-rays generated by electron interactions do not lead to volume loss of the sample, so it is possible to analyse the same materials repeatedly [7,8]. The schematic diagram of SEM is given in Fig 2.4

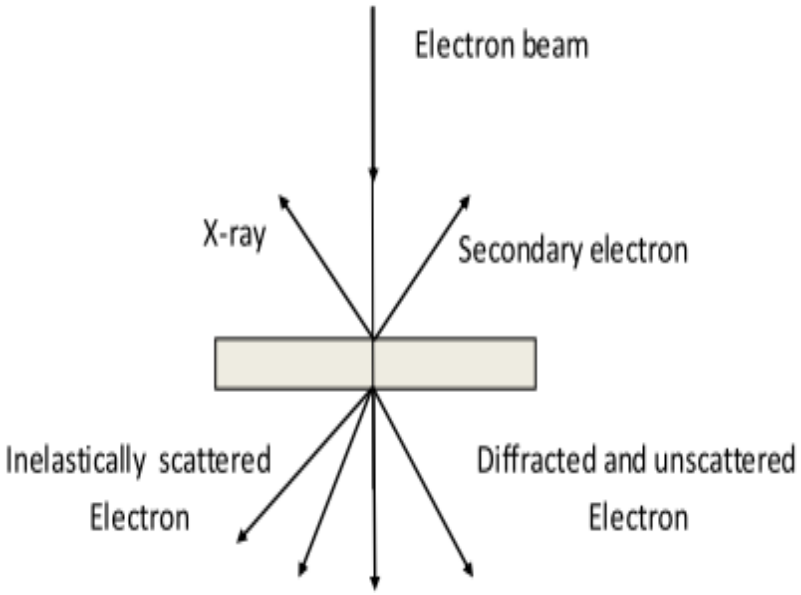

Figure 2.4 Schematic diagram of SEM [8].

The specimen under SEM investigation must be electrically conductive at least at the surface and electrically grounded to prevent the accumulation of electrostatic charge at the surface. The nonconductive specimen tends to charge accumulation when scanned by the electron beam and especially in secondary electron imaging mode. This generally causes scanning faults and other imaging artefacts. Therefore it usually coated with an ultrathin coating of electrically conducting material, commonly gold deposited on the sample either by low vacuum sputter coating or by high vacuum evaporation [8,9].

2.6 Dielectric properties

Ferroelectric materials are very often dielectrics. For most applications of ferroelectric materials, the dielectric constant (ε_r) and dielectric loss ($\tan\delta$) are important practical parameters. Study of the dielectric properties provides a great deal of information about the suitability of the material for various applications.

2.6.1Dielectric constant (ε_r)

The relative dielectric constant (ε_r) of a material is the ratio between the charge stored on an electrode slab of material brought to a given voltage and the charge stored on a set of identical electrodes, separated by vacuum. It is defined as

$$\varepsilon_r = 1+P/(\varepsilon_o E) \qquad (2.1)$$

Where ε_r = Dielectric constant

P = (Induced dipole moment/volume), under an applied electric field E

ε_o= Permittivity of the free space

And, for an alternating electric field, the dielectric constant can be written as

$$\varepsilon_r = \varepsilon' - i\varepsilon'' \qquad (2.2)$$

Where $\varepsilon'$is the real component of the dielectric constant, in phase with the applied field. ε'' is the imaginary component, 90^o out of phase with the applied field, caused by either resistive leakage or dielectric absorption. For normal substances, the value of ε_r is low, usually under 5 for organic materials and under 20 for most inorganic materials. Generally, ferroelectric ceramics have much higher ε_r, typically several hundred to several thousand [10,11].

2.6.2 Dielectric loss (tanδ)

The charging current in an ideal dielectric leads the applied voltage by $\pi/2$ radians (90^o). However, in real dielectrics in addition to the charging current associated with the storage of electric charge by the dipoles, a loss current must also be considered. The loss current arises

from the long-range migration of charges, e.g., dc ohmic conduction and the dissipation of energy associated with the rotation or oscillation of dipoles [11]. As the dielectric is not loss free, it is generally represented by a complex dielectric constant, defined in equation 2.2**.** The total current in the real dielectric is a complex quantity which leads the voltage by an angle (90-δ), where δ is called the loss angle. Dielectric loss (tanδ) also known as dissipation factor is defined as tanδ= ε"/ ε'. The inverse of the loss tangent, Q = (1/tanδ), is used as a figure of merit in high frequency applications [11]

2.6.3 Curie temperature (T_c)

It is the temperature above which the spontaneous polarization (P_s) of the ferroelectric materials vanishes and it goes into paraelectric state. It is also known as Curie point, denoted as T_c. When the temperature increases across the Curie point, a ferroelectric crystal undergoes a structural phase transition from a ferroelectric (non-centrosymmetric) phase to paraelectric (symmetric) phase and above T_c the material does not exhibit ferroelectricity. When the temperature is in the vicinity of T_c , thermodynamic properties including dielectric, elastic, optical and thermal constants show an anomalous behavior [10]. If there are two or more ferroelectric phases in a material, the Curie point only specifies the temperature at which a ferroelectric - paraelectric phase transition occurs.

2.7 P-E Hysteresis loops

Ferroelectrics have reversible spontaneous polarization. The word spontaneous means that the polarization has a nonzero value in the absence of an applied electric field. The word reversible refers to the direction of the spontaneous polarization that can be reversed by an

applied electric field in opposite direction. The spontaneous polarization P_s usually increases with the increase of applied field and then gradually reaches a saturation value at these electric field. The most prominent features of ferroelectric properties are hysteresis and nonlinearity in the relation between the polarization P and the applied electric field E. The simplest method for measuring P-E behavior is the Sawyer and Tower method, as shown in Fig 2.5, in which C is the capacitance of the ferroelectric specimen and C_o is a standard capacitor. The voltage across C should be sufficiently large to render a saturation in polarization, so V_o should be proportional to the polarization charge, $V_o = AP/C_o$, where A is the area of the specimen. V is the applied voltage, which is usually an AC signal voltage of low frequencies. Thus, the applied field across the specimen, $E = V_c/d = (V-V_o)/d$ [11].

A typical P-E hysteresis loop is shown schematically in Fig 2.6. First the field-induced polarization increases linearly with the field (OA). Polarization increases nonlinearly with increasing field, due to the starting of the orientation of the domains toward the direction of the field (AB). At high fields, polarization reaches a state of saturation in which case most domains are aligned toward the direction of the poling field (BC). By gradually decreasing the field to zero, corresponding polarization decreases, following the path CBD. By extrapolating the linear portion CB to the polarization axis (or zero-field axis) at E, OE represents the spontaneous polarization P_s and OD represents the remanent polarization P_r .Generally P_r is smaller than P_s because when the field is reduced to zero, some domains may return to their original positions due to the strain situation, thus reduces the contribution of these domains to the net polarization [10]

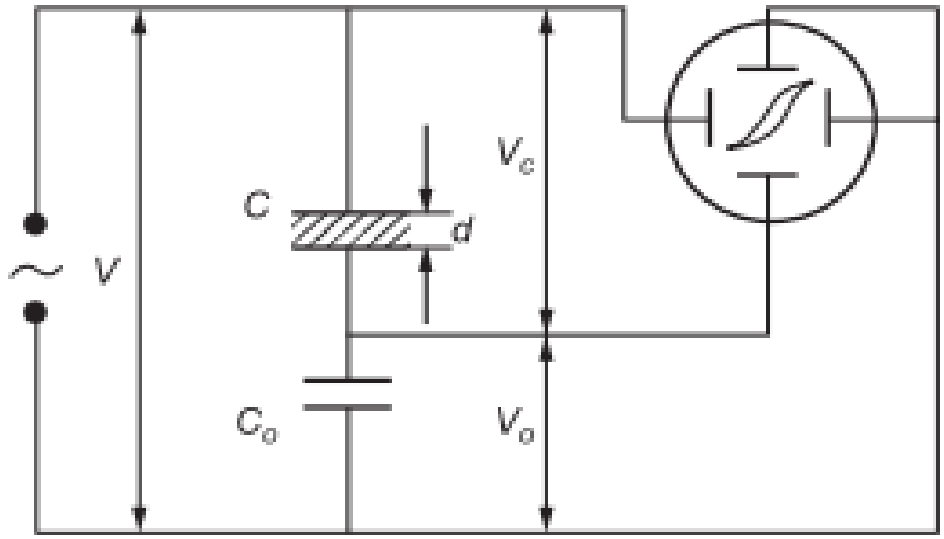

Figure 2.5 The Sawyer–Tower method for the measurement of the polarization-electric field (P–E) characteristics [11].

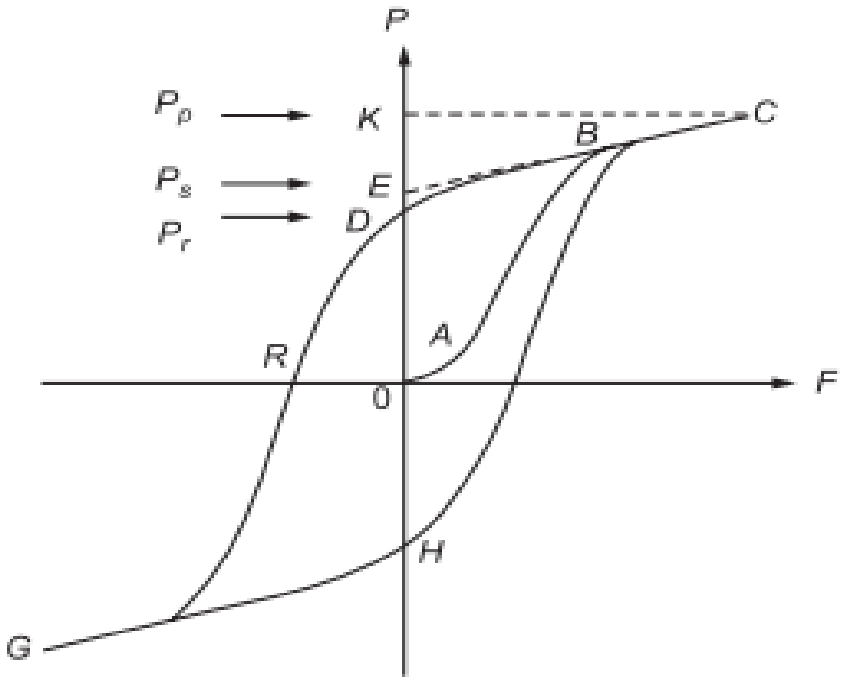

Figure 2.6 Schematic diagram of a typical ferroelectric hysteresis loop.[10]

The field required to bring the polarization to zero is called the coercive field E_c (portion 0R on zero polarization axis). E_c depends not only on temperature, but also on the measuring frequency and the waveform of the applied field. The hysteresis arises due to energy needed to reverse the metastable dipoles during each cycle of the applied field. The area of the loop represents the energy dissipated in the form of heat inside the specimen during each cycle. In general, the hysteresis loop is measured with AC fields at low frequencies, 60 Hz or lower, to avoid heating the specimen.

2.8 Poling

Poling is a process during which a high electric field is applied on the ferroelectric ceramic samples to reorient the domains in the direction of the applied electric field. The poling is possible only in ferroelectric materials and poling steps are shown in Fig 2.7. Pyroelectric or piezoelectric polycrystalline materials, with randomly oriented grains cannot be poled as they lack more than one equilibrium state of the polarization vector. Before poling, the ferroelectric ceramic does not possess any piezoelectric and pyroelectric properties owing to the random orientation of the ferroelectric domains in the ceramics. For domain reorientation, a poling field must be applied on the sample and maintained for a certain length of time [11].

For a given field and poling time, better domain rearrangement results at higher temperature, but less than T_c. This happens because with the increase in poling temperature, crystalline anisotropy and coercive field, E_c, of the ferroelectric materials decreases [11]. Also, with increasing temperature, space charges, which act against domain motion, decreases in the ceramic. However, when the poling temperature is too high, problems arise as the electrical conductivity increases and the consequent increase in leakage current would result in sample breakdown during the period of poling. After poling, the electric field is removed and a

remnant polarization and remnant strain are maintained within the material, and it starts exhibiting piezoelectric and pyroelectric effects [11].

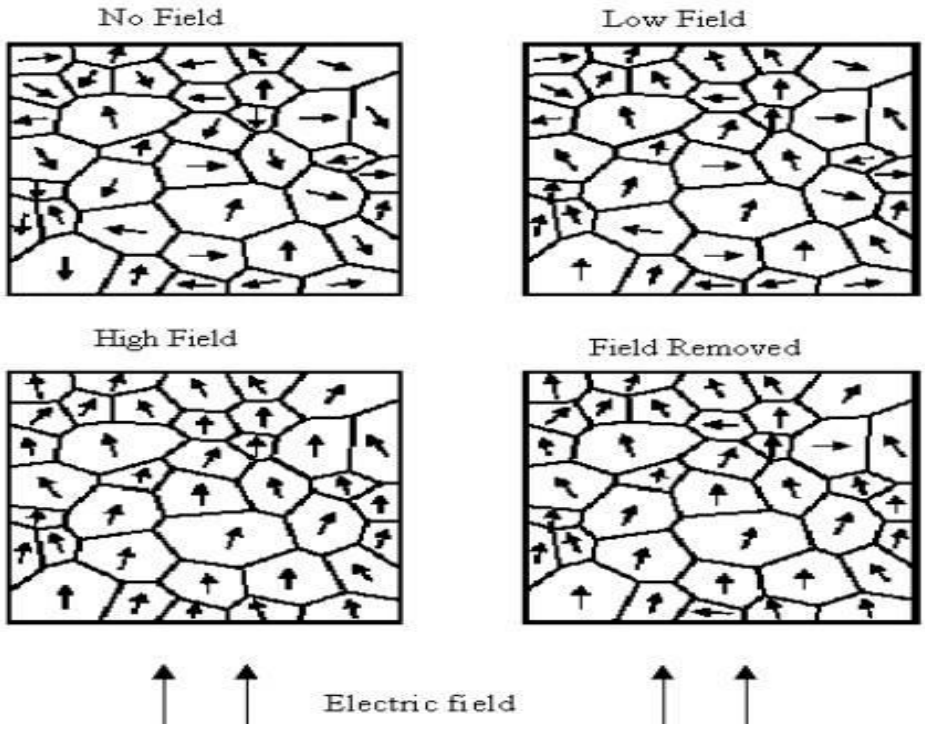

Figure 2.7 Poling steps of a ferroelectric material [11]

2.9 Piezoelectric charge coefficient measurements

Piezoelectric coefficients can be measured using either the direct or converse piezoelectric effects. The piezoelectric coefficients in the direct and converse piezoelectric effects are thermodynamically identical. In order to measure the piezoelectric coefficients using the direct piezoelectric effect, a normal load is applied to a ferroelectric capacitor and the charge on the electrodes is measured. To measure the longitudinal piezoelectric coefficient, the electrical response is parallel to the applied stress. For the transverse piezoelectric coefficient, a

stress is applied in the plane of the material and the induced charge is measured. The most piezoelectric questions use the reduced suffix notation for piezoelectric coefficient

$D_{33} = d_{33}T_3$ (Direct effect)

$S_{33} = d_{33} E_3$ (Converse effect)

Both of the equation can be simplified to the form

$$d_{33} = \frac{Q/A}{F/A} = \frac{Q}{F} = \frac{CV}{F}$$

Where A is the area stressed by the force of F. C is the shunt capacitance which is connected in parallel with the test sample. A quasi-static force (about 0.25N with a frequency of about 110Hz) was applied on the test sample as well as on an internal calibration piezoelectric ceramic element, for which d_{33} of which is known. By comparing the piezoelectric charges developed on the test sample and internal calibration element, the value of d_{33} in (pC/N) of the tested sample was computed and directly displayed on the screen [2,11]

References

[1] John A D. The Analytical Chemistry Handbook.(McGraw Hill New York1995).

[2]Douglas A.S.;Holler F. J.; Nieman A.T. Principles of Instrumental Analysis (Saunders college publication New York1998.)

[3] O'Neill M. J. Anal. Chem.1964,36**,** 1238.

[4] Rahaman M.N. Ceramic processing and sintering (Marcel Dekker New York 1995)

[5]Suryanarayan C. , Norton M. G. X-ray diffraction: a practical approach (Plenum press New York 1998)

[6] Cullity B. D.; Stock S. R. Elements of X-Ray Diffraction (Prentice hall New Jersey 2001)

[7]Suzuki E.J. of Microscopy. 2002, 208, 153.

[8]Goldstein G. I.; Newbury D. E; Echlin,P.; Joy D. C., Fiori C.; Lifshin E. Scanning electron microscopy and x-ray microanalysis.(Plenum Press ,New York 1981).

[9]Effree C. E.; Read N. D. Ambient and Low-temperature scanning electron microscopy (Academic Press London 1991).

[10]Vijaya M.S ,Rangarajan G. material science(Tata McGraw-Hill India2003).

[11]Jaffe B. ;CookW. R.;Jaffe H. Piezoelectric Ceramics (Academic press New York 1971)

Chapter 3

Study of KNN Ceramics Synthesized by Partial Co-Precipitation Technique

Introduction

This chapter explains about the partial co-precipitation synthesis route used for preparing KNN ceramics. The microstructure, ferroelectric, dielectric and piezoelctric properties of the KNN ceramics of different compositions near the three MPB regions are reported in detail.

3.1 Synthesis route used

In the present work we have used partial co-precipitation technique for the synthesis of different MPB compositions of KNN system. It was hypothesized that the properties of ceramic are greatly affected by the properties of the powder such as particle size, morphology purity and chemical composition[1,2] It has been confirmed that the chemical methods like partial co-precipitation, Sol-gel technique, hydrothermal and colloid emulsion techniques control the morphology and the chemical compositions of the prepared powder very efficiently. These methods increase the homogeneity and surface area of the resulting powders which leads to relatively high reactivity and hence low sintering temperature [3,4]. Among these wet chemical techniques sol-gel uses alkoxide whereas hydrothermal and colloid emulsions techniques are time consuming and involve highly unstable alkoxides and also it is difficult to maintain the reaction conditions. Therefore, Partial co-precipitation is one of the most successful techniques for synthesizing ultrafine ceramic powders, having

narrow particle size distribution. The purpose of this study was to prepare ultrafine KNN powder using partial co precipitation technique using simple water soluble inorganic salts. This process avoids complex steps such as refluxing of alkoxides and results in less time consumption compared to other techniques [1-4]

3.2 Procedure for synthesis of $K_XNa_{1-X}NbO_3$ (KNN)ceramics near three MPB regions by partial co-precipitation route

Different MPB compositions of lead free KNN system with general formula $K_xNa_{1-x}NbO_3$(x = 0.52, 0.50, 0.48, 0.35, 0.33, 0.31, 0.20, 0.18, 0.16) were synthesized by partial co-precipitation process. The processing conditions and sequences used in the sample preparation and characterizations are as follows:

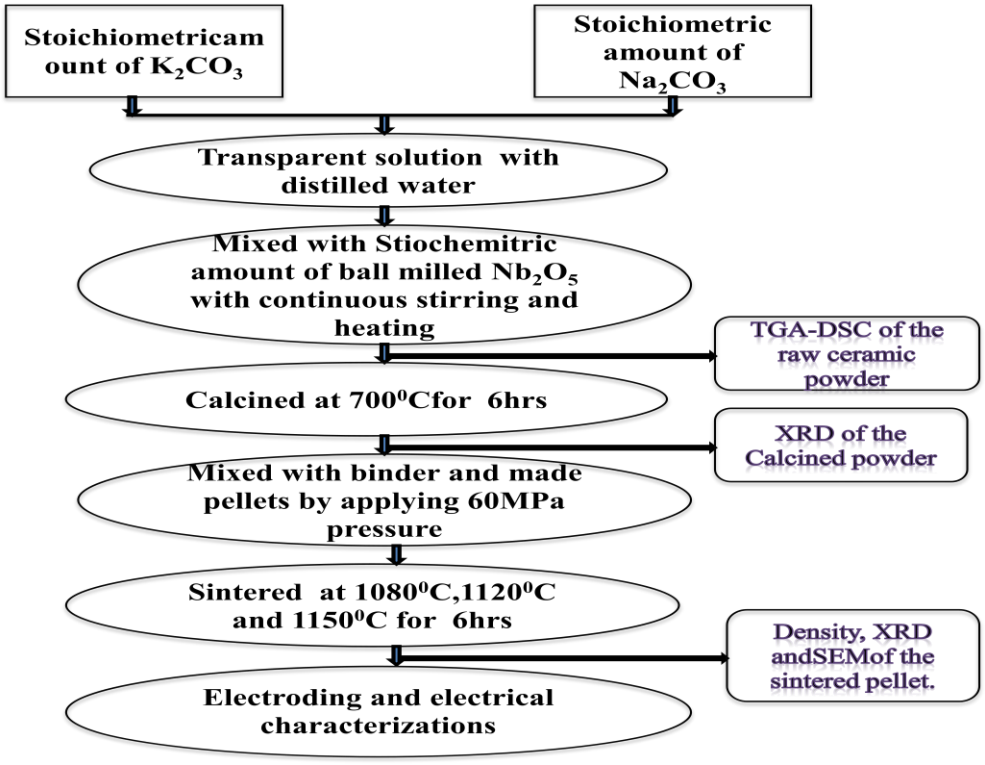

Figure 3.1 Flow chart of the preparation of KNN ceramics by partial co-precipitation synthesis route

The first step in processing is to weigh the staring materials according to the stoichiometric formula. We have to prepare the $K_xNa_{1-x}NbO_3$ ceramic with x = 0.52, 0.50, 0.48,0.35, 0.33, 0.31,0.20,0.18 and 0.16 compositions near the three MPB regions. In this case Sodium Carbonate (Na_2CO_3, 99% purity of Merck Specialist Pvt. Ltd), Potassium Carbonate (K_2CO_3, 99% purity of Merck Specialist Pvt. Ltd) and Niobium Pentoxide (Nb_2O_5, 99% purity of HiMedia Laboraties Pvt.Ltd) were used as the starting precursors. Initially the niobium pentoxide with acetone was ball milled for 14hrs using zirconia balls as a gridding media. The resulting slurry was dried in an oven at 150^0C for 1hr.Then stoichiometric amount of K_2CO_3 and Na_2CO_3 powders with distilled water were mixed in a glass beaker and a transparent solution was prepared. Since K_2CO_3 and Na_2CO_3 are hygroscopic in nature, therefore extra care has been taken. Then stoichiometric amount of Nb_2O_5 powder was weighted and added to the transparent solution of K_2CO_3 & Na_2CO_3 followed by continuous stirring and heating. Stoichiometric formula for mixing of KNN precursors is given below:

$$xK_2CO_3 + (1-x)\ Na_2CO_3 + 1/2Nb_2O_5 + H_2O = K_xNa_{1-x}NbO_3 + 1/2\ CO_2 + H_2O$$

The resulting solution was then dried in an oven for 10 h at 150^0C in order to remove the water. After grinding, the thermal decomposition and crystallization of the powder was investigated by Differential Scanning Calorimeter (TGA-DSC, STA449C, NETZSCH). Thereafter the calcination of the powder was carried out at 700^0C for 6 hrs in an alumina crucible by an indigenous programmable furnace at a heating rate of 5^0C per minute .In order to examine the formation of single pervoskite structure of the KNN

ceramic near the three MPB regions of different compositions , XRD analysis was performed on PW 3020 Philips diffractometer using CuKα (λ=0.15405 nm) radiation. Then the calcined powder was mixed with 2wt% polyvinyl alcohol (PVA) solution and pressed into disks of ~10mm diameter and ~1.5mm thickness under ~60MPa pressure. Sintering of the green disks was carried out at 1080^0C, 1120^0C and 1150^0C for 6hrs for different compositions near 3 MPB regions respectively. The bulk density of the sintered samples was determined using Archimedes method. Again the XRD analysis was carried out by PW 3020 Philips diffractometer using CuKα (λ=0.15405 nm) radiation of the sintered samples in order to examine the structure. Surface morphologies of the sintered samples were studied using JEOL T-330 scanning electron microscope (SEM). A layer of metallic silver in paste form was applied on both circular sides of the sintered pellets of $K_xNa_{1-x}NbO_3$ (x = 0.52, 0.50, 0.48, 0.35, 0.33, 0.31,0.20, 0.18 and 0.16)to perform electrical measurements. The dielectric measurements of samples were conducted as a function of frequency and temperature using a computer interfaced HIOKI 3532-50 LCR-HITESTER. The polarization vs. electric field (P-E) hysteresis loops of the samples were measured by using a computer interfaced conventional Sawyer-Tower circuit. For the piezoelectric coefficient measurements, the samples were poled by corona poling at 150^0C by applying a dc electric field of 3 kV/mm for 30min . The d_{33} value of the sample was measured by Piezo meter(E2730Ad_{33} Meter, APC International Ltd).

3.3 Results and discussion

3.3.1. TGA/DSC study of KNN ceramics

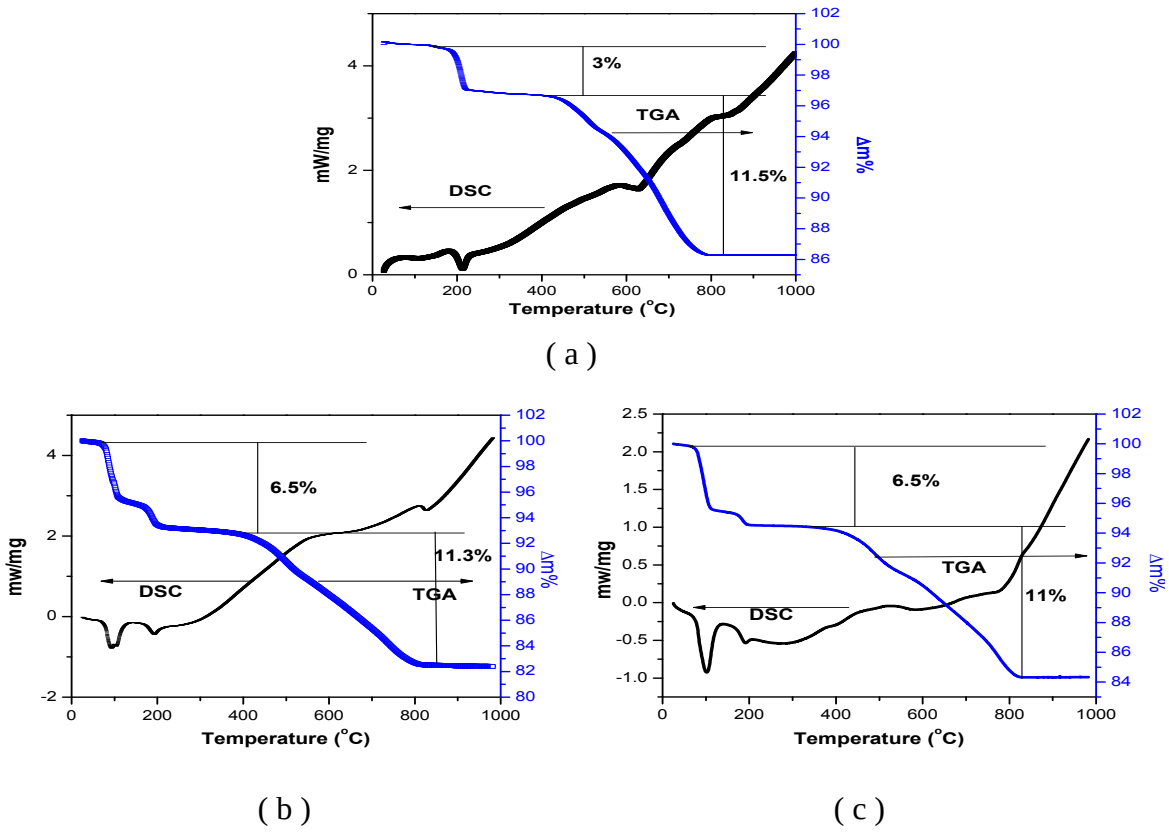

Figure 3.2 TGA/DSC curves of (a) $K_{0.5}Na_{0.5}NbO_3$ (b) $K_{0.33}Na_{67}NbO_3$ & (c) $K_{0.18}Na_{0.82}NbO_3$ MPB compositions

Fig.3.2 (a-c) illustrates the thermal decomposition of the precursors of three compositions of KNN system. The overall weight loss from the room temperature to 1000^0C is ~ 14.5%, ~ 17.8% and~ 17.6% for $K_{0.5}Na_{0.5}NbO_3$, $K_{0.33}Na_{0.67}NbO_3$ & $K_{0.18}Na_{0.82}NbO_3$ compositions respectively. From room temperature to 400^oC, the TGA curve of $K_{0.5}Na_{0.5}NbO_3$ composition shows a weight loss of ~ 3%, whereas the TGA curves of $K_{0.33}Na_{67}NbO_3$ and $K_{0.18}Na_{0.82}NbO_3$ show a weight loss of~ 6.5%. The endothermic peaks upto 200^0C of the DSC curves in Fig.3.2 (a),(b) and (c) correspond to evaporation of water molecules during thermal

decompositions of precursors [5.6]. The endothermic peak above 200^0C in Fig3.2 (a),(b) and (c) corresponds to the elimination of remaining water molecules ,CO and CO_2 molecules originated from the decomposition of oxalate group [6-8]. A weight loss of~ 11% occurred in the temperature range 400^0C to 800^0C in all three MPB compositions shown in Fig 3.2(a) ,(b) and (c) . No further significant weight loss was observed above 800^0C temperature , which conforms the completion of crystallization of the KNN system with an absence of further decompositions and / or volatilizations of sodium and potassium oxides [5-9].

3.3.2. Structural analysis using XRD

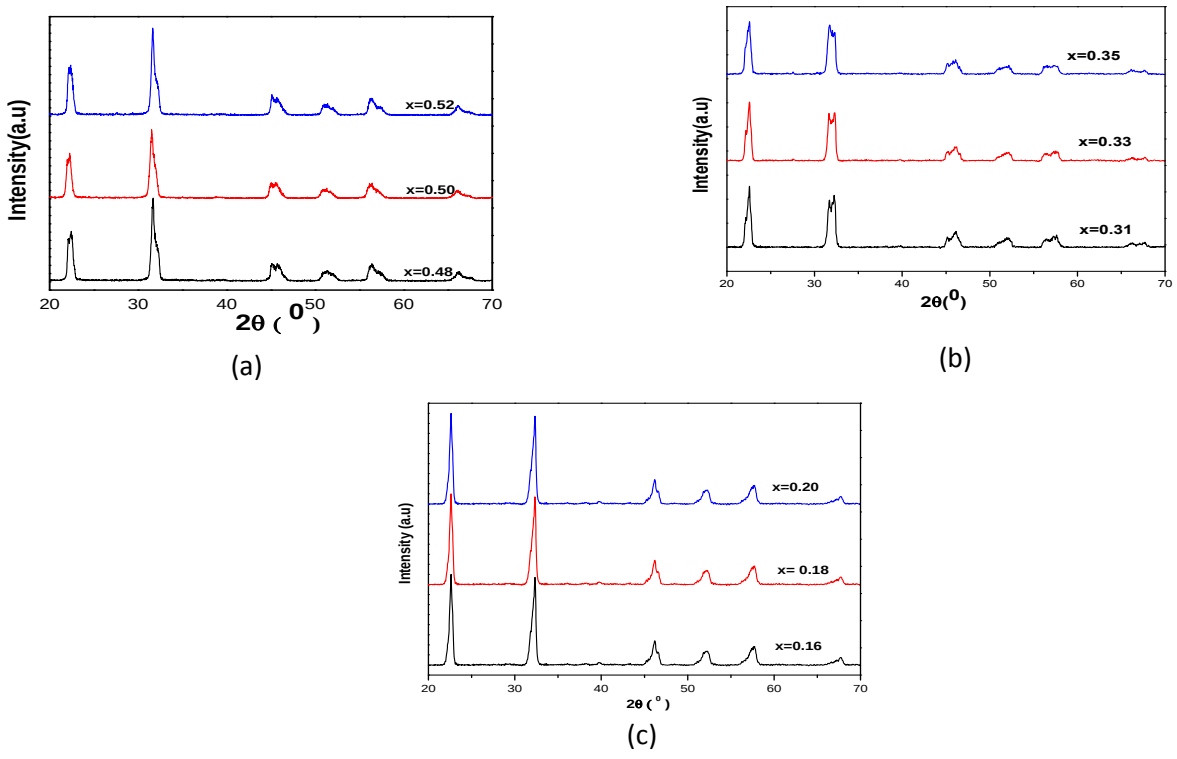

Figure 3.3 XRD of $K_XNa_{1-x}NbO_3$ system calcined at 700^0C for different mol% of potassium near(a) 50/50 MPB (b) 33/67 MPB (c) 18/82 MPB regions

The XRD patterns of KNN ceramics, near three MPB calcined at 700^oC for 6h are shown in Fig.3.3 (a-c). Single perovskite phase peaks were developed in all the KNN ceramics near

three MPBs. Single perovskite phase has been confirmed at a lower calcination temperature at 700^{o}C through the partial co precipitation technique. Whereas, in the same system synthesized by solid state reaction route, single perovskite phase is developed at ~850^{o}C [10]. The basic reason for reduction of processing temperature is that the method increases the homogeneity and surface area of the resulting powders. This leads to relatively high reactivity and hence lowering the processing temperature [11,12].

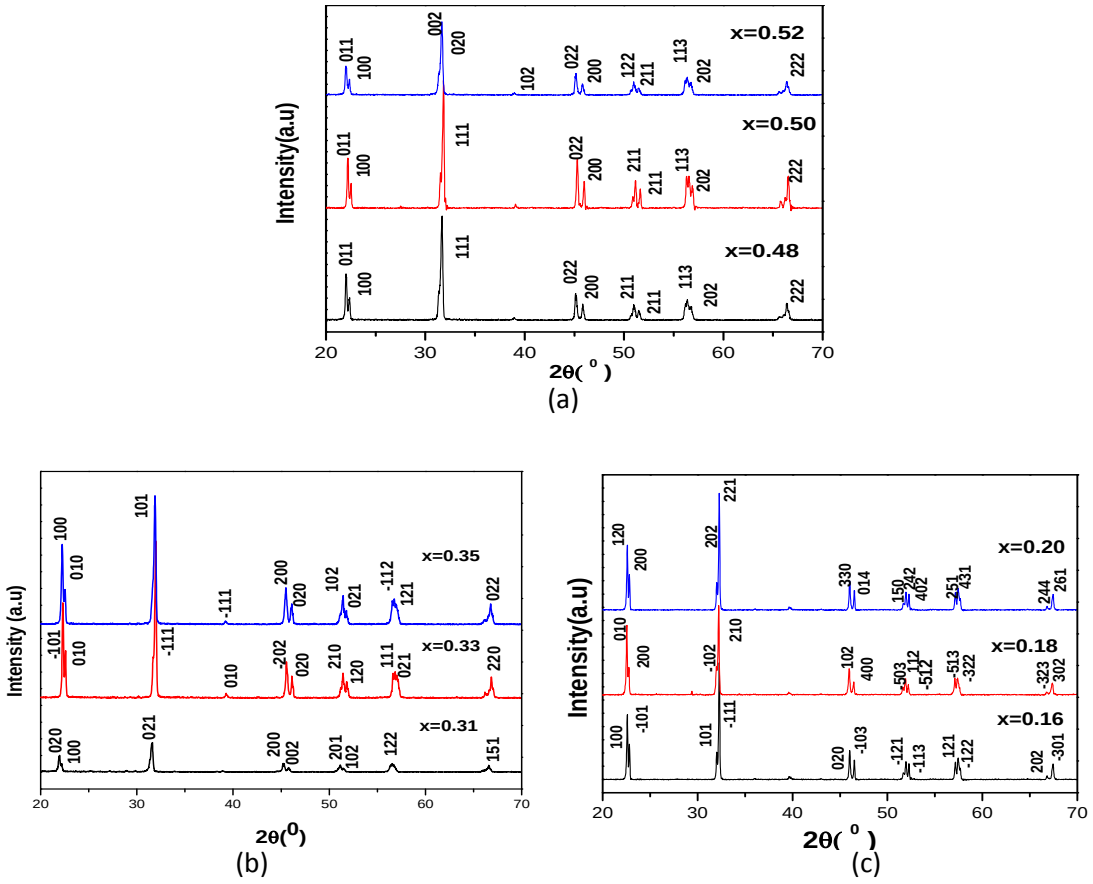

Figure 3.4 XRD of $K_XNa_{1-x}NbO_3$ systems for different mol% of potassium sintered at (a) 1080^{0}C near 50/50 MPB (b) 1120^{0}C near 33/67 MPB (c) 1150^{0}C near 18/82 MPB

Fig.3.4 (a-c) show the XRD patterns of sintered $K_xNa_{1-x}NbO_3$ ceramics near the three MPB regions. The XRD patterns confirm the single perovskite phase formation without any trace of secondary phase. Sharp and distinct XRD peaks of KNN ceramics indicate the good homogeneity and crystallinity of the samples [13, 14].The diffraction lines of these MPB samples are indexed in different crystal systems and unit cell configurations using a computer program package 'Powdmult'. Standard deviations, S.D, $\sum\Delta d = (d_{obs} - d_{cal})$, where'd' is inter-plane spacing, is found to be minimum for different crystal structures, given in Table.3.1. The crystal structure of the compositions corresponding to x=0.48 and x=0.52 exhibit monoclinic and orthorhombic structures, respectively whereas coexistence of orthorhombic and monoclinic structures is found in the composition corresponding to x=0.50 near the50/50 MPB region .Similarly near 33/67 MPB region compositions corresponding to x=0.33 and x=0.35 exhibit only the monoclinic structures , whereas the coexisting of orthorhombic and monoclinic structures is found in the composition corresponding to x=0.31 .However, near 18/82 MPB region, the compositions corresponding to x=0.16, 0.18 and 0.20 exhibit only the single structure of monoclinic, monoclinic and orthorhombic respectively. The existence of double structures suggests that the composition corresponding to x=0.50 and x=0.31are the actual MPB compositions of the KNN system [15].Again with increasing the K concentration we found that the sintering temperature of the KNN system decreases. This explains that potassium was acting as a sintering aid which enhances the liquid phase sintering [16].

Table 3.1 Crystalline structures of $K_XNa_{1-x}NbO_3$ system near three MPB regions.

System	compositions	Structure	Lattice parameter in Å		
			a	b	c
KNN System near 50/50 MPB Composition Sintered at 1080^{0}C	$K_{0.52}Na_{0.48}NbO_3$	Orthorhombic	3.926	8.118	6.045
	$K_{0.50}Na_{0.50}NbO_3$	Monoclinic	5.672	5.642	3.944
		Orthorhombic	5.642	5.673	3.944
	$K_{0.48}Na_{0.52}NbO_3$	Monoclinic	4.132	4.0341	7.354
KNN system near 33/67 MPB composition Sintered at 1120^{0}C	$K_{0.35}Na_{0.65}NbO_3$	Monoclinic	3.987	3.938	3.979
	$K_{0.33}Na_{0.67}NbO_3$	Monoclinic	5.614	3.933	3.981
	$K_{0.31}Na_{0.69}NbO_3$	Orthorhombic	4.312	3.964	5.957
		Monoclinic	3.997	8.098	3.963
KNN System near 18/82 MPB composition Sintered at1150^{0}C	$K_{0.18}Na_{0.82}NbO_3$	Monoclinic	9.796	3.936	5.969
	$K_{0.16}Na_{0.84}NbO_3$	Monoclinic	4.187	3.940	5.909
	$K_{0.20}Na_{0.80}NbO_3$	Orthorhombic	7.765	9.064	7.986

3.3.3 Density

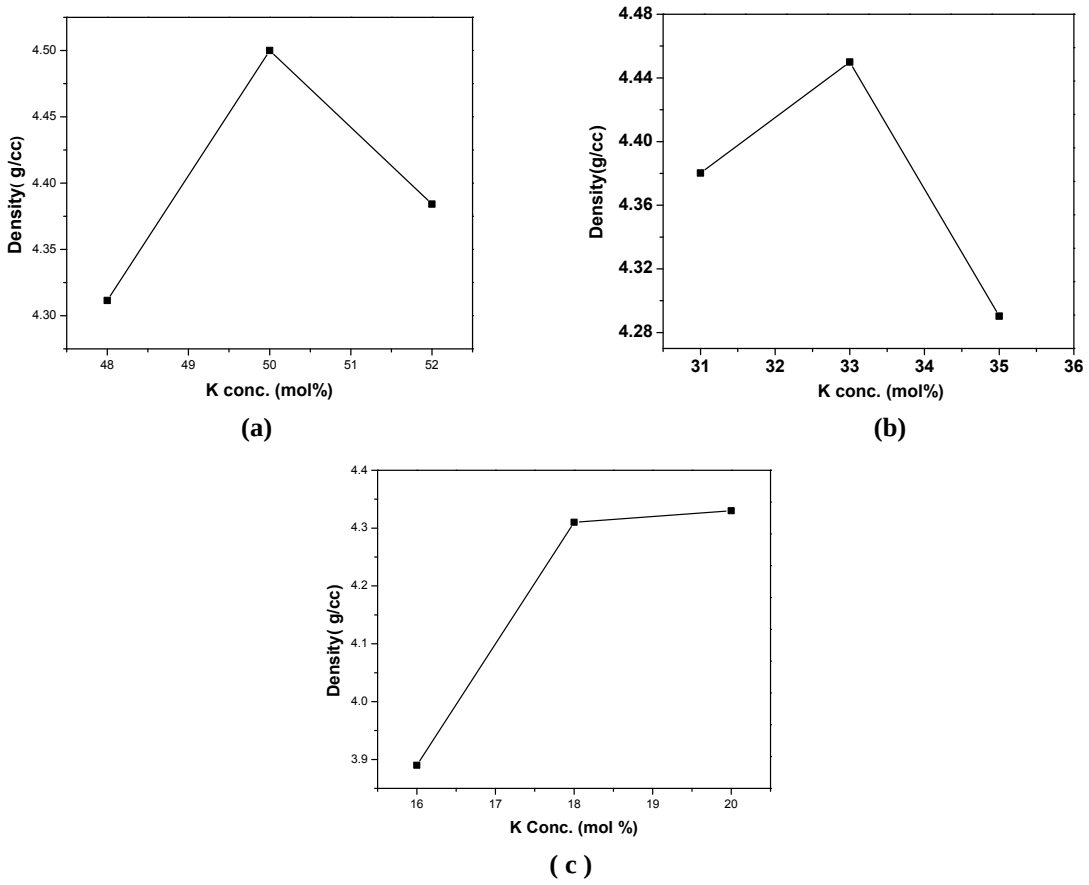

Figure 3.5 Density of $K_XNa_{1-x}NbO_3$system for different mol% of potassium near (a) 50/50 MPB (b) 33/67 MPB (c) 18/82 MPB regions

Fig 3.5 (a-c) shows the variation of measured experimental densities near three MPB regions as a function of K content of the $K_xNa_{1-x}NbO_3$ ceramics. Densities of the sintered $K_xNa_{1-x}NbO_3$ systems were measured using Archimedes' principle. The measured bulk density of KNN samples for the different compositions near three MPB regions sintered at corresponding temperatures are given in Table.3.2.First the experimental density increases with the increase in K content of KNN system, which suggests that excessive K can cause liquid phase sintering and hence leads in the increased density. Therefore, K is acting as sintering aid in KNN system [16]. The apparent density becomes maximum when x =0.5 0.33 and 0.20 near

three MPB regions. Thereafter when x>0.5 and 0.33 near the 50/50 and 33/67 MPBs the apparent density decreases with the further increase of K content. This can be explained on the basis of increasing the volatilization with further increase of K in the compositions near these MPBs [17]. Since near the 3rd MPB region, evaporation of K is less due to its less concentration compared to Na in other compositions. Hence no decrement of experimental density is obtained with the increase of K content in this case [17].

Table 3.2 Measured bulk density of $K_xNa_{1-x}NbO_3$ system sintered at the corresponding temperature for different mol% of potassium near three MPB regions

KNN System near 50/50 MPB region sintered at 1080^0C	**Density (gm/cm^3)**
$K_{0.52}Na_{0.48}NbO_3$	4.4
$K_{0.50}Na_{0.50}NbO_3$	4.49
$K_{0.48}Na_{0.52}NbO_3$	4.31
KNN System near 33/67 MPB region sintered at 1120^0C	
$K_{0.35}Na_{0.65}NbO_3$	4.3
$K_{0.33}Na_{0.67}NbO_3$	4.42
$K_{0.31}Na_{0.69}NbO_3$	4.38
KNN System near 18/82 MPB region sintered at 1150^0C	
$K_{0.20}Na_{0.80}NbO_3$	4.33
$K_{0.18}Na_{0.82}NbO_3$	4.31
$K_{0.16}Na_{0.84}NbO_3$	3.89

3.3.4 Study of surface morphology

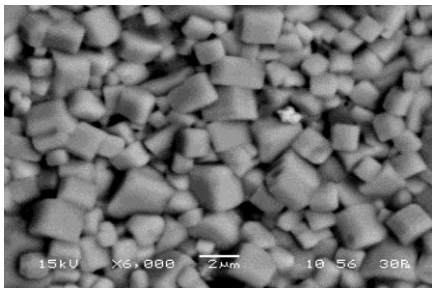

(a)

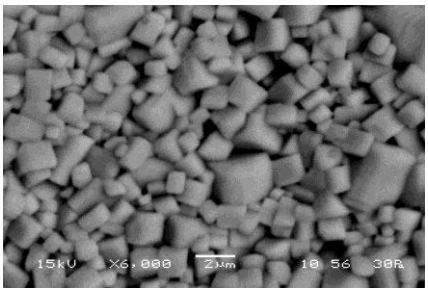

(b)

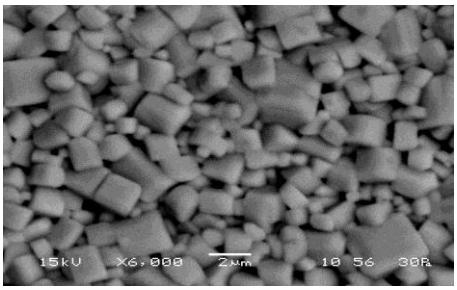

(c)

Figure 3.6 SEM images of (a)$K_{0.48}Na_{0.52}NbO_3$, (b)$K_{0.50}Na_{0.50}NbO_3$ and (c)$K_{0.52}Na_{0.48}NbO_3$ compositions near (50/50) MPB region sintered at 1080^0C

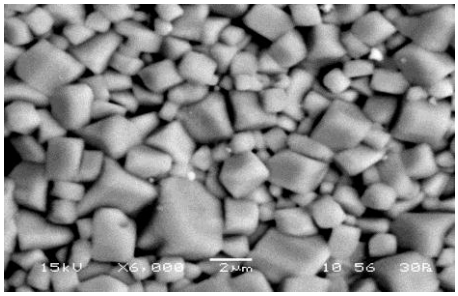

(a)

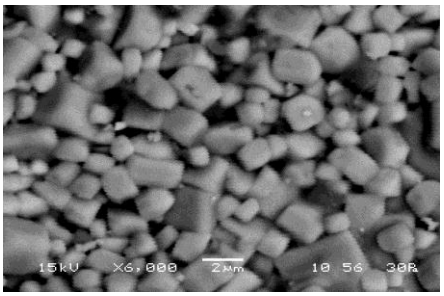

(b)

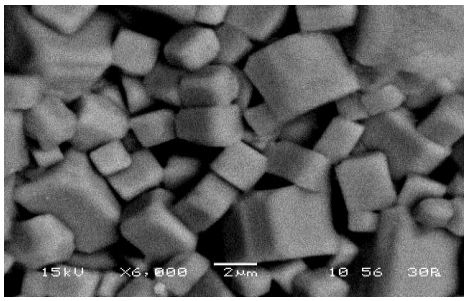

(c)

Figure3.7 SEM micrographs of different (a)$K_{0.31}Na_{0.69}NbO_3$,(b)$K_{0.33}Na_{0.67}NbO_3$ and (c)$K_{0.35}Na_{0.65}NbO_3$ compositions near (33/67) MPB region sintered at 1120^0C

SEM images of $K_x Na_{1-x}NbO_3$ system for different compositions near the three MPB regions are shown in Fig. 3.6, 3.7 and 3.8. The average grain size was calculated by linear intercept method and given in Table.3.3.

Fig. 3.6(a-c) and Fig.3.7 (a-c) shows the presence of uniformly distributed grains with less porosity. As given in Table 3.3. the average grain size increases with the increase of K mol% in KNN system near 50/50 and 33/67MPB regions .This average grain indicates that K is acting as a sintering aid and enhances the grain growth in KNN system near these MPBs compositions [16] .

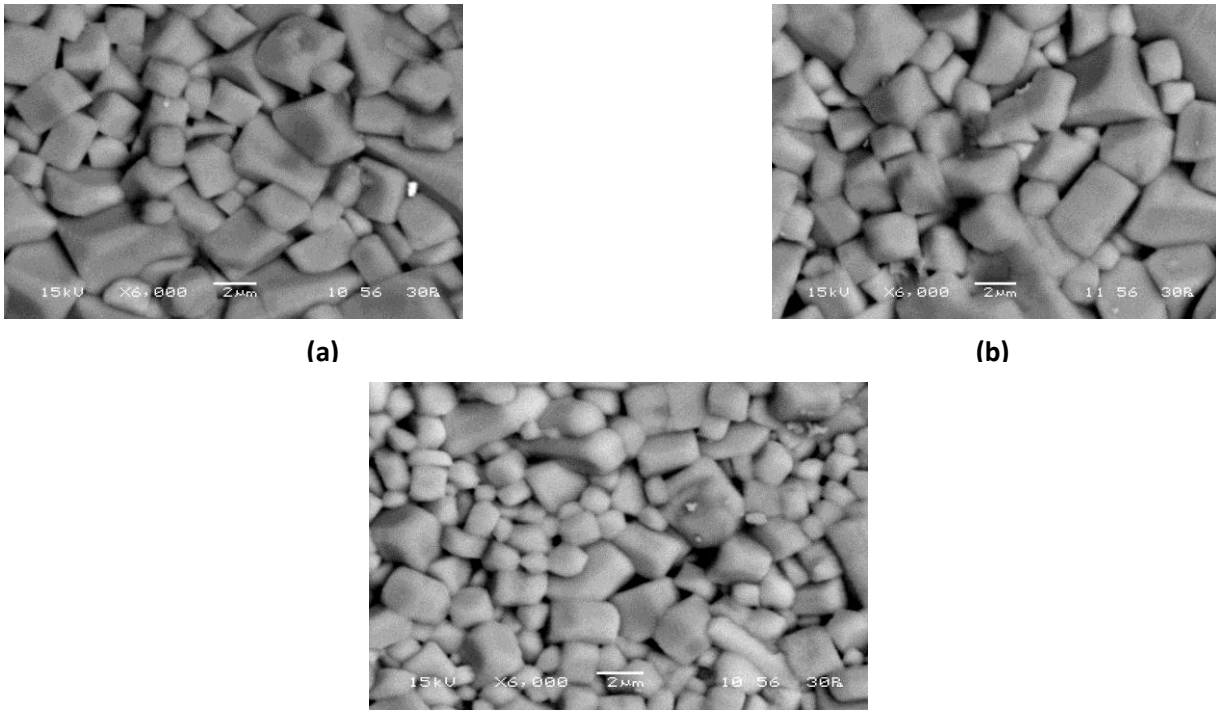

Figure.3.8 SEM micrographs of different (a)$K_{0.16}Na_{0.84}NbO_3$,(b)$K_{0.18}Na_{0.82}NbO_3$ and (c)$K_{0.20}Na_{0.80}NbO_3$compositions near (18/82) MPB region sintered at 1150^0C

Fig.3.8 (a-c) shows the increase of porosity with the increase of K mol% in compositions near 18/82 MPB.As given in the Table.3.3 , the average grain size decreases with the increase of K mol% in KNN compositions near 18/82 MPB region . This indicates that the increase of K mol% in this case acts as inhibiter of grain growth. Since the mol% of K is relatively less, therefore it is not acting as sintering aid [17].

Table 3.3 Average grain size of $K_xNa_{1-x}NbO_3$compositions near three MPBs

KNN System near 50/50 MPB region sintered at 1080^0C	**Avg. Grain Size (μm)**
$K_{0.52}Na_{0.48}NbO_3$	2.17
$K_{0.50}Na_{0.50}NbO_3$	2.1
$K_{0.48}Na_{0.52}NbO_3$	1.90
KNN System near 33/67 MPB region sintered at 1120^0C	
$K_{0.35}Na_{0.65}NbO_3$	7.08
$K_{0.33}Na_{0.67}NbO_3$	3.37
$K_{0.31}Na_{0.69}NbO_3$	2.44
KNN System near 18/82 MPB region sintered at 1120^0C	
$K_{0.20}Na_{0.48}NbO_3$	2.7
$K_{0.18}Na_{0.82}NbO_3$	3.25
$K_{0.16}Na_{0.84}NbO_3$	3.33

3.3.5 Study of Room temperature dielectric proprties

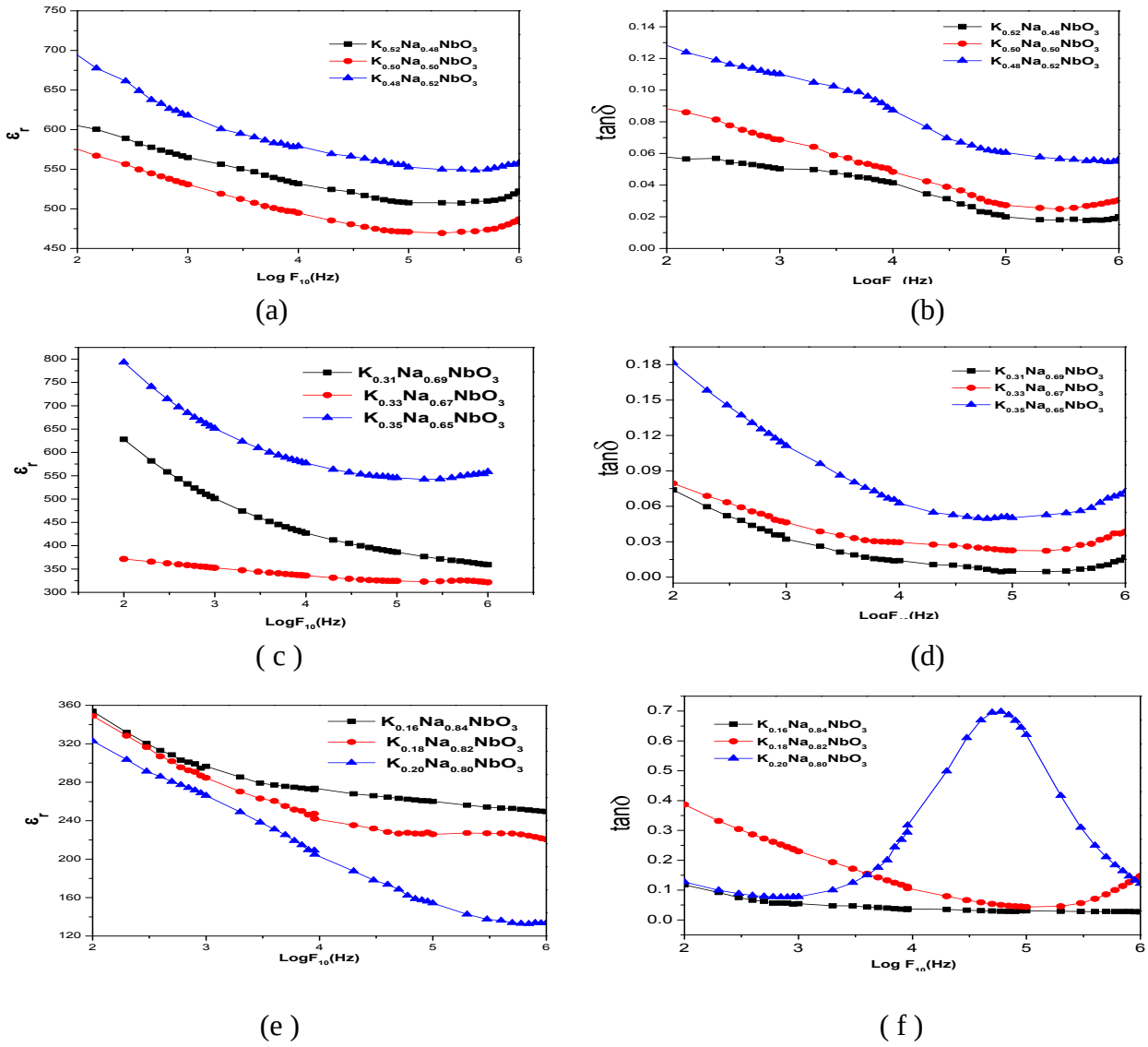

Figure 3.9 Frequency dependence of ε_r and tanδ at room temperature of different MPB compositions of KNN system

Frequency dependence of dielectric constant (ε_r) and dielectric loss (tanδ) at room temperature of different composition of $K_XNa_{1-X}NbO_3$ system near three MPBs are shown in Fig 3.9 (a-f). When a dielectric is subjected to an ac electric field, the displacement of charges, ions and orientation of the dipoles try to follow the direction of the electric field. But the

switching of the displacement and orientations with fast reversal of the electric field becomes more difficult at higher frequencies. As the frequency increases, ionic and orientation sources of polarizability decreases and finally disappear due to the inertia of the molecules and ions. Therefore among the three types of polarizabilities, the electronic polarizability which involves electrons only exists up to very high frequencies [18, 19]. In the above Fig.3.9 (a-f), the dielectric constant shows an expected decrease with increasing frequency because of the damping out of the successive polarization mechanisms. This successive filtration of polarization mechanism causes the corresponding peaks in the loss spectra at different relaxation and resonance frequencies. In the observed frequency range relaxation losses can be associated with the dipolar orientation, ion jump or electron hopping. Space charge polarization losses typically occur at low frequencies and are associated with ion migration and electrode contact losses or in presence of grain boundaries or inhomogeneous phase in dielectric. Contribution to the overall dielectric constant and loss tangent from different polarization mechanisms can be related to the composition, frequency, grain morphology, porosity and temperature of the dielectric and their resultant effect can be held responsible for the observed dielectric behavior of the material for different compositions of KNN system [20-22].

Fig 3.9 (f) shows the variation of dielectric loss with frequency near 20/80 MPB region. For the composition $K_{0.20}Na_{0.80}NbO_3$ the dielectric loss factor increases with increasing frequency followed by the appearance of a resonance peak occurring at higher frequency [23, 24]. The resonance may arise due to the matching of the frequency of the polarization mechanisms with the frequency of the external electric field. This causes the increase of polarization and hence the dielectric loss (tanδ) [18, 25].

3.3.6 Variation of dielectric properties with temperature

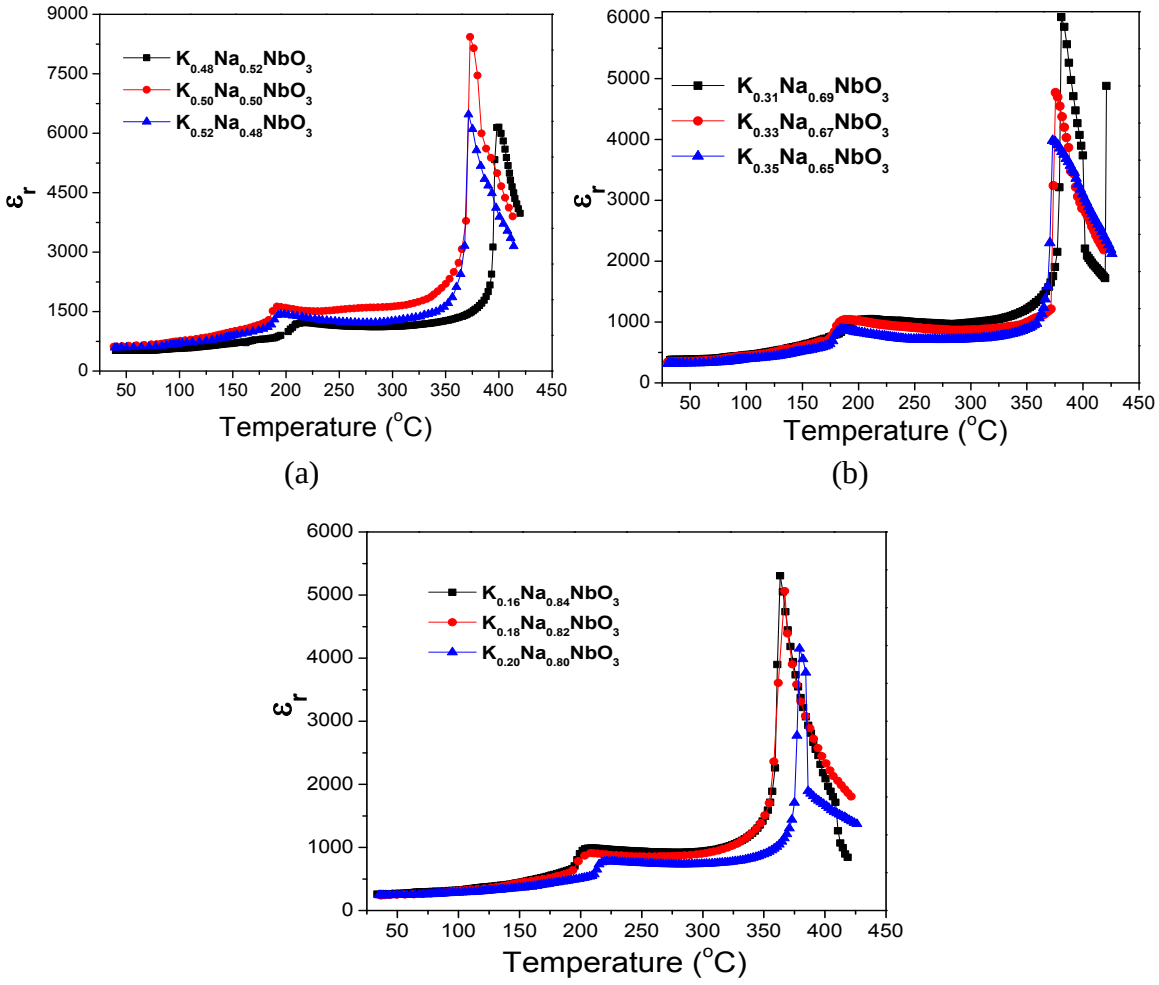

Figure 3.10Temperature dependence of dielectric constant of $K_XNa_{1-x}NbO_3$system for different mol% of potassium near (a) 50/50 (b) 33/67 (c) 18/82 MPB regions at 100kHz

Temperature dependence of ε_r and loss (tanδ) at 100 kHz frequency of different $K_xNa_{1-x}NbO_3$ compositions near three MPB regions are shown in Fig 3.10(a-f). Above the RT, different MPB compositions of KNN system are undergoing two phase transitions, first one ~ 200^0C and second one ~ 400^0C .It is observed that value of ε_r increases with the increase of temperature and shows anomalous behavior near the phase transition temperatures (T_c). The

increase in the value of ε_r with temperature can be explained on the basis of increase in domain wall mobility. Generally the phase transition in perovskite type materials generally occurs due to instability of temperature dependent low frequency optical soft mode frequency [20, 26-28].

At T_c, frequency of the soft mode tends to zero and the lattice displacement associated with it becomes unstable and leads to phase transition [20, 21]. With the increase of potassium concentration, the orthorhombic / monoclinic – cubic phase transition (T_c) is shifted to lower temperature side near three MPBs. The decrease in T_c with the increase in concentration of K in KNN system near 50/50 and 33/67 MPB regions can be attributed to the increase in internal stress in the system. Since the size of K is bigger than that of Na, so there is an increase in internal stress with the increase of K concentration in the KNN system. As reported earlier, we can consider a relationship to be presented between internal stress and pores [15, 29-31]. As pores can relieve internal stresses, which do not constrain grains. It can be seen in the SEM microstructures that with increasing K concentration in KNN system, the porosity of the samples decreases and the grain size increases which leads to an increase in internal stress in the samples. Since the T_c is inversely proportional to the internal stress, consequently the decrease in T_c with increase of K concentration in KNN system seems to be the result of increase in internal stress [15, 29-31]. Near 18/82MPB region the transition temperature T_c increases with the increase in concentration of K in KNN system. Since the SEM microstructures shows that with increasing K concentration in KNN system near this MPB , the porosity of the samples increases and the grain size decreases, it leads to the decrease in internal stress in the samples. As T_c is inversely proportional to the internal stress, it results the increase in T_c near this MPB region.

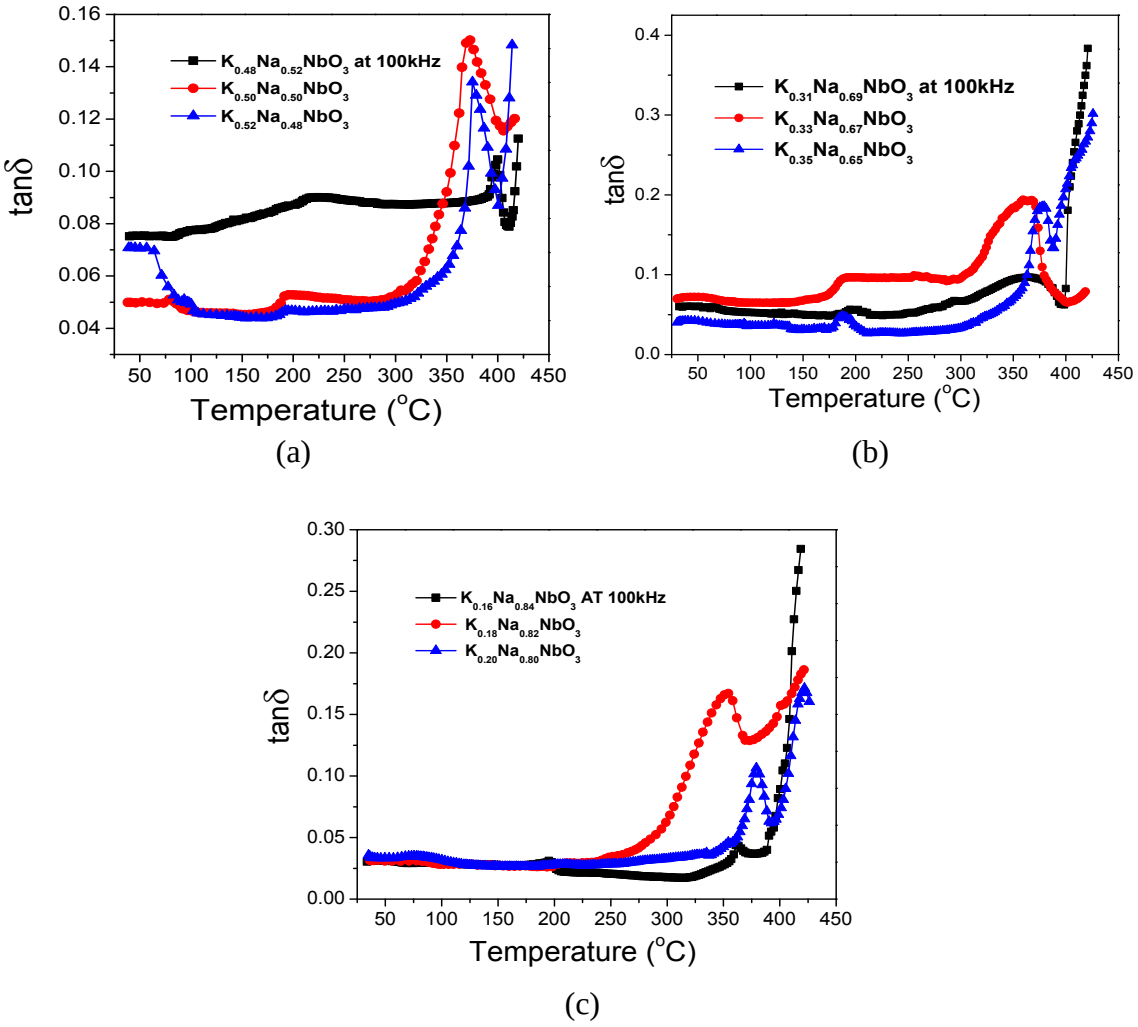

Figure 3.11 Temperature dependence of dielectric loss of $K_XNa_{1-x}NbO_3$system for different mol% of potassium near (a) 50/50 (b) 33/67 (c) 18/82 MPB regions at 100 kHz

Fig.3.11 (a-c) shows the temperature dependence of the dielectric loss (tanδ) at 100kHz of sintered KNN samples near three MPBs. The behaviour of tanδ is very much similar to ε_r i.e. two similar kind of transition peaks are also observed here. The RT value of ε_r and tanδ, T_c and $\varepsilon_{r\ (max)}$ at a frequency of 100kHz are given in Table.3.4 for different compositions near three MPBs. The MPB compositions with x =0.5 0.33 and 0.20 in KNN system near three MPBs

shows low loss with high dielectric constant at room temperature. The dielectric data in Table.3.4 conforms that $K_{0.5}Na_{0.5}NbO_3$ system shows better dielectric properties (RT ε_r ~614, T_C ~376^oC, RT tanδ ~0.04) among all compositions near the three MPBs.

Table 3.4 Dielectric study of $K_xNa_{1-x}NbO_3$ system for different mol% of potassium near three MPBs

Compositions	**RT ε_r**	**RT Tanδ**	**T_c (^oC)**	**ε_r at T_c**	**1st transition temperature (^0C)**	**ε_r at 1st transition**
$K_{0.52}Na_{0.48}NbO_3$	590	0.07	371	6470	195	1435
$K_{0.5}Na_{0.5}NbO_3$	614	0.04	376	8429	191	1627
$K_{0.48}Na_{0.52}NbO_3$	514	0.08	400	6150	213	1205
$K_{0.35}Na_{0.65}NbO_3$	316	0.04	373	3984	185	878
$K_{0.33}Na_{0.67}NbO_3$	341	0.06	376	4770	192	1038
$K_{0.31}Na_{0.69}NbO_3$	378	0.07	380	6008	199	1032
$K_{0.20}Na_{0.80}NbO_3$	243	0.035	379	4149	217	762
$K_{0.18}Na_{0.82}NbO_3$	240	0.031	365	5038	203	887
$K_{0.16}Na_{0.84}NbO_3$	260	0.03	363	5306	208	990

3.3.7 Study of polarization vs electric field (P-E) hysteresis loop

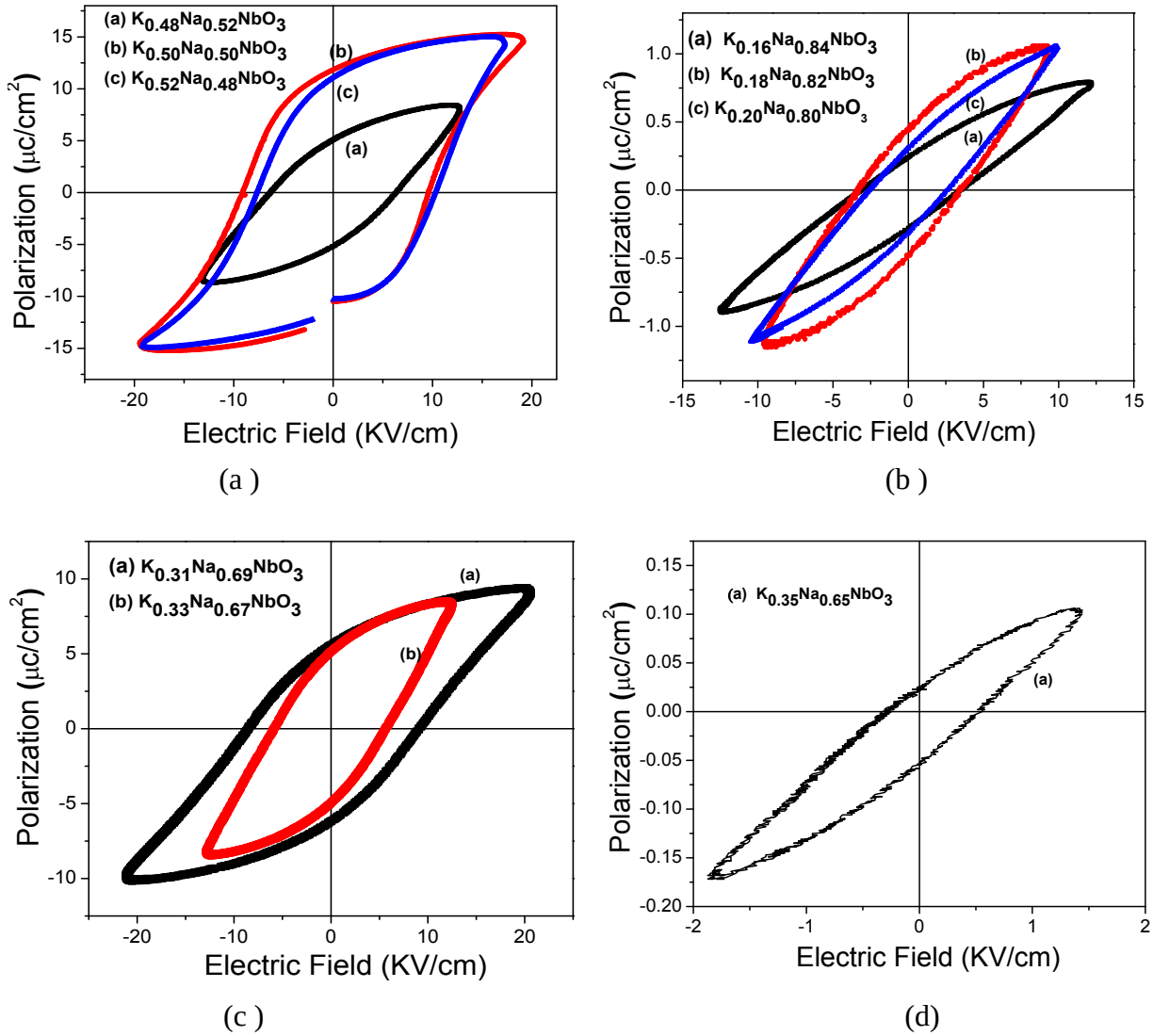

Figure 3.12 PE-Hysteresis loop of $K_XNa_{1-x}NbO_3$system for different mol% of potassium near (a) 50/50 (b) 18/82 (c) and (d) 33/67 MPB regions

The P-E hysteresis loops of different compositions of KNN system near three MPB regions are shown in Fig.3.12 (a-d). The development of well saturated hysteresis loops of different compositions of KNN system near 50/50 MPB confirms the ferroelectric nature .The compositions with potassium concentration X=0.50 and 0.31 have maximum remanent polarization of ~ 11.7 μC/cm^2 and 5.8 μC/cm^2 and coersive electric field of 9.8 kV/cm and 8.8

kV/cm respectively. The occurrence of maximum P_r in these compositions can be explained by the presence of mixed structures. The presence of double structures in these compositions allows the maximum number of polar directions, which helps in maximizing ferroelectric properties. [32]. Therefore the dipole within these samples can easily re-orientate themselves compared to those of the system having single structure [15,33]. The RT value of P_r, E_c, P_s and E_{max} are given in Table.3.5 for different compositions of KNN system near three MPBs .The P-E hysteresis loop study confirms that $K_{0.50}Na_{0.50}NbO_3$ composition of the KNN system shows the better ferroelectric properties (P_r~11.76μC/cm^2 , E_c~ 9.80kV/cm) among all MPB compositions.

Table3.5 P-E hysteresis loop data of $K_XNa_{1-x}NbO_3$ system for different mol% of potassium near three MPBs

Compositions	E_{max}(kV/cm)	P_s(μC/cm^2)	E_c (kV/cm)	P_r (μC/cm^2)
$K_{0.52}Na_{0.48}NbO_3$	17.2	14.2	9.8	10.9
$K_{0.5}Na_{0.5}NbO_3$	19.0	14.8	9.8	11.7
$K_{0.48}Na_{0.52}NbO_3$	12.6	8.2	6.3	5.1
$K_{0.35}Na_{0.65}NbO_3$	1.4	0.1	0.4	0.04
$K_{0.33}Na_{0.67}NbO_3$	12.3	8.4	5.6	4.9
$K_{0.31}Na_{0.69}NbO_3$	12.6	8.9	8.8	5.8
$K_{0.20}Na_{0.80}NbO_3$	9.8	1.05	2.5	0.3
$K_{0.18}Na_{0.82}NbO_3$	9.2	1.01	3.3	0.3
$K_{0.16}Na_{0.84}NbO_3$	12.1	0.8	3.6	0.4

3.3.8 Study of piezoelectric properties near three MPB regions.

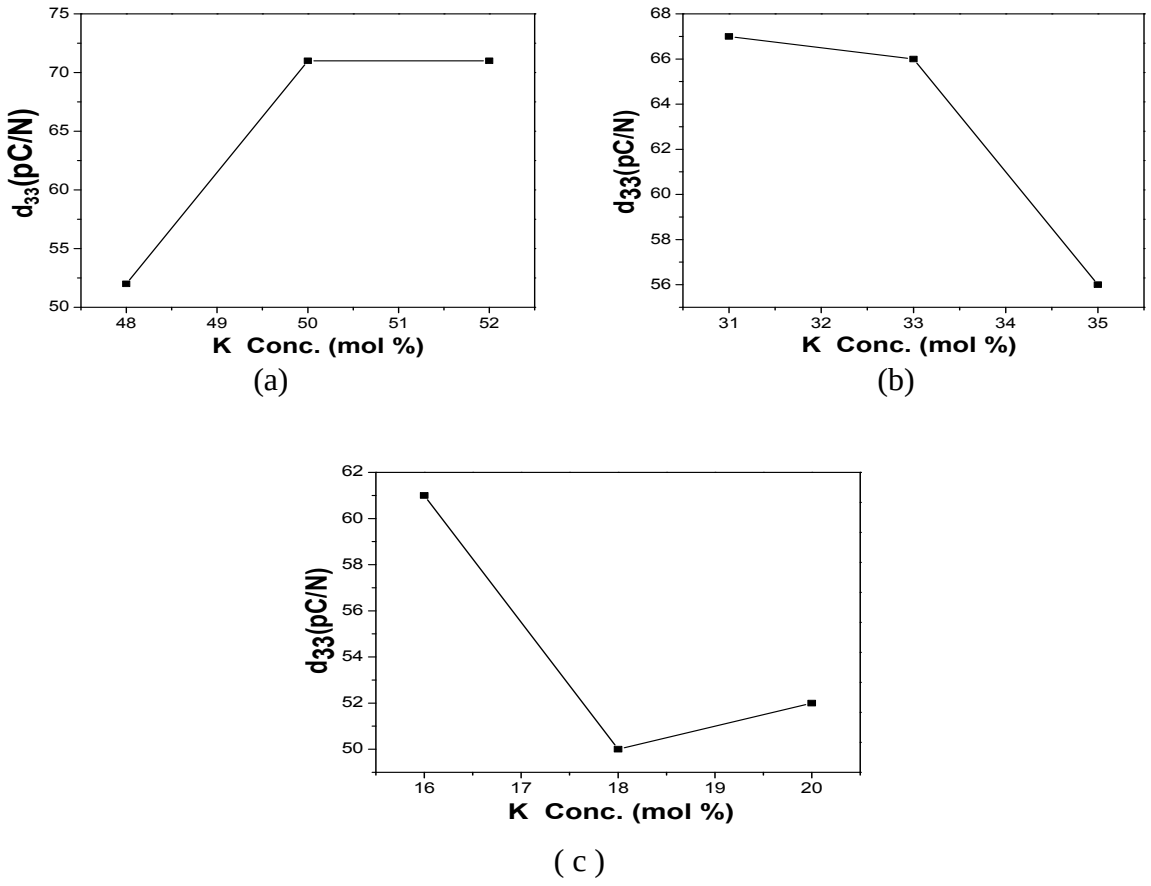

Figure 3.1 3Piezoelectric Coefficient of $K_XNa_{1-x}NbO_3$ system of different mol% of potassium at room temperature near (a) 50/50 (b) 33/67 and (c) 18/82 MPB regions

The piezoelectric coefficient (d_{33}) for the KNN samples near three MPB regions is measured and shown in Fig.3.13 (a-c). Piezoelectric charge coefficient (d_{33}) for the compositions with potassium concentration X=0.50, 0.31 and 0.16 is found to be 71 pC/N, 67 pC/N and 61 pC/N respectively. The maximum value of piezoelectric charge coefficient for x=0.5 and 0.31 compositions is due to the existence of the double structures [15]. In Fig.3.13 (a) we observed that d_{33} value increases with increase of the potassium concentration in KNN system. The increase in d_{33} in the system can be attributed to the MPB nature of the system.

Whereas near 33/67 and 18/82 MPB regions shown in Fig 3.13(b) and (c), d_{33} value decreases with increase of the potassium concentration [1,15]. The RT value of d_{33} are given in Table.3.6 for different compositions of KNN system near three MPBs

Table 3.6 Piezoelectric coefficient (d_{33}) of $K_XNa_{1-x}NbO_3$ system for different mol% of potassium near three MPBs

KNN System near 50/50 MPB region	**d_{33}(pC/N)**
$K_{0.52}Na_{0.48}NbO_3$	71
$K_{0.5}Na_{0.5}NbO_3$	71
$K_{0.48}Na_{0.52}NbO_3$	52
KNN System near 33/67 MPB region	
$K_{0.35}Na_{0.65}NbO_3$	56
$K_{0.33}Na_{0.67}NbO_3$	66
$K_{0.31}Na_{0.69}NbO_3$	67
KNN System near 18/82 MPB region	
$K_{0.20}Na_{0.80}NbO_3$	53
$K_{0.18}Na_{0.82}NbO_3$	23
$K_{0.16}Na_{0.84}NbO_3$	61

3.4 Conclusions

We have successfully synthesized the lead free KNN ceramics near three MPB regions by partial co precipitation technique. Comparing with conventional synthesis methods such as hot pressing, spark plasma synthesis and texturing which are complex and expensive, the partial co-precipitation technique is proven to be simple, in expensive and effective in the synthesis of densified KNN ceramics near 3 MPBs.

KNN system with different compositions near the three MPBs has been successfully synthesized in a single perovskite phase by partial co-precipitation technique. XRD analysis has been carried out in order to investigate the structure of the KNN ceramics. XRD studies showed the presence of mixed structures in the compositions corresponding to x=0.5 and 0.31 mol% of K in KNN system. SEM images of the KNN samples near three MPBs have shown the uniform distribution of grains with dense packing .The bulk density increased with the increase of K content in KNN system. This suggests that K is acts as sintering aid in KNN system. For lower concentration of K in KNN system the sintering aid nature is not effective. The room temperature dielectric and piezoelectric properties of the KNN samples near three MPBs were investigated. It was found that the dielectric and the piezoelectric properties are superior for the compositions corresponding to x=0.5, 0.31and 0.16 mol% of K in KNN system near the three MPBs. The P-E hysteresis loop study of KNN was carried out which shows well saturated hysteresis loops and confirmed the ferroelectric nature of these materials. It was investigated that among the nine MPB compositions $K_{0.5}Na_{0.5}NbO_3$ system showed the best dielectric, ferroelectric and piezoelectric properties which makes it usefull for various applications.

References

[1] Gaikwad S. P.;Dhesphande S. B.;Khollam Y.; Samuel V. ;Ravi V. Mater. Lett. 2004, 58,3474

[2.]Samuel V. ; Gaikwad A.B. ; Ravi V. Bull. Mater.Sci. 2006, 29, 123.

[3]Murugan A. V.; Gaikwad A. B.; SamueL. V.; Ravi V. Bull. Mater.Sci. 2006, 29, 221.

[4] Dhage S R.; Ravi V.; Date S K. Bull. Mater. Sci. 2003, 26 ,215

[5]Nobre M.A.L.;Lanfredi S.; Catalysis Today.2003,78, 529.

[6]Lanfredi S.;Dessemond L.;Rodrigues A.C. M. J. Eur. Ceram. Soc.2000,20 ,983.

[7] Jarupoom P.; Pengpat K.; Eissayeam S.; Intatha U.; Rujijanagul G.; Tunkasiri T. Ferr. Lett. 2008,35,119 .

[8]Pornsuda B.; Winai S.;Supasarote M.;Steven M. J. J. Sci. Technol.2007, 29, 441.

[9] Nopsiri C.;Anucha R.;Rangson M.; Niemcharoen S.; Sanseub A.;Saowanee T. , Sunanta L.;Wanwilaic V.; Naratip V. Ferroelec.2009, 383,8.

[10] Matsubara M.; Kikuta K. ; Hirano S. Jpn. J. Appl. Phys. 2005, 44 ,6618.

[11]. Kuo C.L.; LiWang C.; Chen T.Y.; Chen G.J.; Hung I.M.; Shih C.J.; Fung K.Z. J. Alloys and Compounds.2007,440, 367.

[12] Mayo M.J. Int. Mater. Rev. 1996, 41, 85.

[13] Schroeter C.;Wessler B. ; Meng L. J. Eur. Ceram. Soc. 2007,27, 3785.

[14] Shiratori Y.; Magrez A. ; Pithan C. J.Eur.Ceram. Soc. 2005,25, 2075.

[15] Kumar P.; Singh S.;Thakur O.P.; Prakash C. ; Goel T. C. Jpn.J.Appl. Phys. 2004, 43,1501.

[16] MatsubaraM.; Yamaguchi T. ; KikutaK. ; HiranoS.I. J. Appl. Phys. 2005, 44, 258.

[17] Bo Z. J.; Liang D. H.; Bo Q. S.; Mei Z. H. ; Zhuo X. , Chin. Phys. B 2011, 20,067701.

[18] Shaikh P.A.; Kambale R.C.; Rao A.V.; Kolekar Y.D.J. of Alloys and Compounds.2009,482, 276.

[19] Vijaya M.S.; Rangarajan G. Material science(Tata McGraw-Hill Publishing India 2003).

[20] Khandari A. S.;Bhandari A.;Baurai A.A.;Panwar N.S. Ferroelectrics. 2009,386,139.

[21]Lingwal V.; Semwal B.S.;Panwar N.S. Bull. Mater. Sci. 2003,26 ,619.

[22]Goodman G.;Buchanan R.C.;Reynold T.G. Ceramic materials for electronic processing, properties and applications(Marcel Dekker New York1991)

[23] YamadaS.; Otsuki E. J. Appl. Phys. 1997,81, 4791.

[24] Chand J.; Singh M. J. of Alloys and Compounds 2009, 486, 376

[25] Kadam S.L.; Patankar K.K.; Kanamadi C.M.; Chougule B.K. Mater. Res. Bull. 2004,39,2265.

26] singhK.;Lingwal V.;Bhatt S.C.;Panwar N. ; Semwal S.B.S. Mater.res. bull. 2001,36,2365.

[27] Rahgavender.M.; Kumar G.S ;Prasad G. Ferroelectrics.2005,324,43.

[28] Pytte E.phys.Rev.B. 1972,5, 3758.

[29]KangS.;LeeJ. H.;KimJ. J.;Lee H. Y. ;KimuraS. H. C. J. Eur. Ceram. Soc. 2004,24 1031.

[30]Khiroshima T. T. ;KimuruT. J. Am. Ceram. Soc. 1996,79, 3235.

[31]Kimura T.;MiyamotoS. ;YamaguchiT. J. Am. Ceram. Soc. 1990,73, 123.

[32]Swatz S.L. IEEE transactions on electrical insulation 1990,25,935.

[33]Yoon K. H.;Lee B. D.;Park J. ; Park J. H. J. Appl. Phys. 2001,90 , 1968.

Chapter 4

Study of $K_{0.5}Na_{0.5}NbO_3$ Ceramic Synthesized by Combustion Technique

Introduction

This chapter explains the synthesis of $K_{0.5}Na_{0.5}NbO_3$ (KNN) ceramic by Combustion synthesis Technique. A brief discussion about the microstructure, ferroelectric, dielectric and piezoelectric properties of the KNN ceramics is reported in detail.

4.1 Synthesis route used

Piezoelectric ceramics are the most important and widely used materials for piezoelectric transducers, transformers, sensor, actuator, buzzers and other electronic devices due to their excellent electrical properties. However these ceramics are mostly lead based materials which are toxic in nature. Thus recently lead free ferroelectrics have a great attention which is environmental friendly. Among all lead free ferroelectrics $K_{0.5}Na_{0.5}NbO_3$have attracted much attention because of its high Curie temperature and high piezoelectric properties. From the literature it was found that the synthesis techniques use like hot pressing and spark plasma sintering produce dense $K_{0.5}Na_{0.5}NbO_3$ ceramics with relatively better ferroelectric properties compared to the KNN ceramics synthesized by the conventional solid state route (CSSR) . But still it is obvious that normal /pressureless sintering of these materials is more suitable for mass production. It is well known that with the use of ultrafine powders the densification of a ceramic can be enhanced. Hence, recently researchers have tried to synthesize ultra-fine powders by wet chemical methods. Among the wet chemical methods, sol–gel

method is usually employed to prepare KNN powders in which alkoxides of niobium are generally used as Nb sources. However, certain inherent problems are associated with Nb alkoxides, such as inflammability, relatively high cost, and higher sensitivity to moisture [1]. It has been reported that combustion synthesis(CS) is an attractive technique for the synthesis of different materials, such as $BaTiO_3$ etc., which involves a self-sustained reaction between reactive materials and fuel (e.g., urea), and the reaction converts the initial mixture typically to fine well crystalline powders of desired compositions [2]. Combustion synthesis has emerged as an important technique for synthesis and processing of advance ceramics (structural and functional), catalyst composites, alloys, intermetallics and nanomaterials. In Combustion synthesis, the exothermicity of redox (reduction –oxidation or electron transfer) chemical reaction is used to produce useful materials. This synthesis process is characterized by high temperature, fast heating rate and short reaction times .These features make CS as an attractive method for the manufacturing of the useful materials at lower costs compared to conventional process. Some other advantages of CS process are the use of relatively simple equipment, formation of high purity products and stabilization of metastable phases [3,4].

It was also reported that sintering of the KNN based ceramics in the oxygen rich environment can be very effective to obtain high experimental density and better ferroelectric properties [5,6]. Hence, in the present work to obtain an ultrafine KNN powder at lower calcination temperature, the combustion technique has been used, which is a fast, energy-efficient and environmental friendly chemical process. The effect of oxygen environment sintering on the microstructral and electrical properties has been studied and discussed in detail.

4.2 Synthesis process of $K_{0.5}Na_{0.5}NbO_3$ (KNN) ceramic by combustion synthesis method using urea as a fuel

MPB compositions of lead free $K_{0.5}Na_{0.5}NbO_3$ (KNN)system was synthesized by combustion synthesis process using urea as a fuel. The processing conditions and sequences used in the sample preparation and characterizations were as follows:

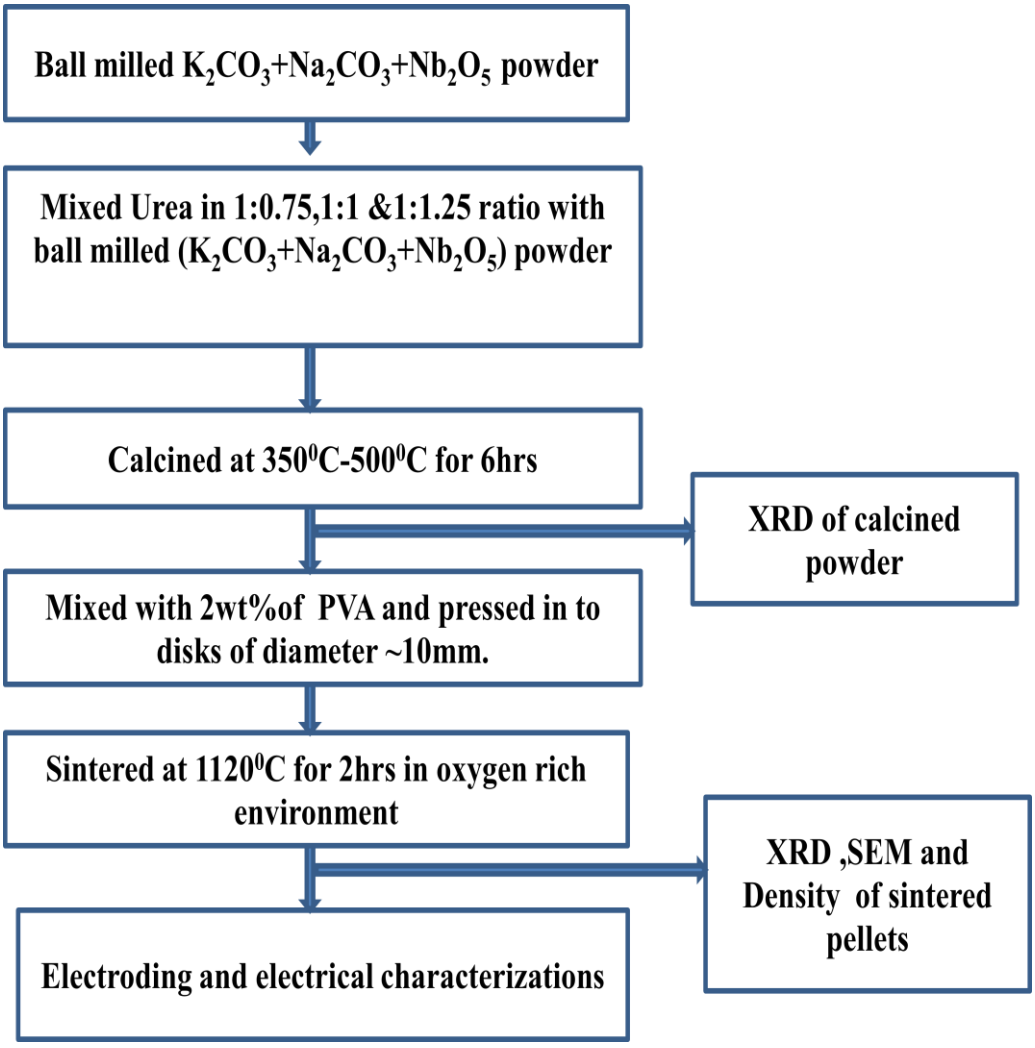

Figure.4.1 Flow chart of the preparation of KNN ceramic by combustion synthesis route using urea as a fuel

Lead free KNN samples were synthesized by combustion synthesis method using urea as a fuel. Sodium carbonate (Na_2CO_3, 99.9% purity), potassium carbonate (K_2CO_3, 99.9% purity), niobium pentoxide (Nb_2O_5,99.9% purity) and urea were used as starting materials. Stoichiometric weights of Na_2CO_3, K_2CO_3 and Nb_2O_5 powders were mixed and ball milled with acetone for 8h, using zirconia balls as the grinding media. The obtained oxide powder was mixed with urea with a weight ratio varying from 1:0.75 to 1:1.25 (KNN: Urea) and wet ball-milling for 2 h. After drying the obtained slurry in an oven, the calcination was carried out at four different temperatures ranging from 350^0C to 500^0C for 6h. The calcined powder was mixed thoroughly with 2wt% polyvinyl alcohol (PVA) binder and pressed into disks of diameter ~10 mm and thickness of ~1.5 mm under a pressure of ~60Mpa. The sintering of the samples was carried out at 1120^0C for 2 h in oxygen rich environment with a heating rate of 5^oC/min. XRD of the sintered KNN samples was performed on a PW 3020 Philips diffractometer using Cu Kα (λ=0.15405 nm) radiation. The microstructures of sintered samples were observed using a JEOL T-330 scanning electron microscope (SEM). The experimental densities (d_{ex}) of the samples were measured by the Archimedes method. Silver paste was applied on both sides of the samples for carrying out the electrical measurements. Dielectric constant (ε_r) and dielectric loss ($\tan\delta$) were measured as a function of temperature using a computer interfaced HIOKI 3532-50 LCR-HITESTER. A conventional Sawyer–Tower circuit was used to measure the electric field Vs polarization hysteresis (P–E) loop at 20 Hz frequency. For measuring the piezoelectric property, the samples were poled using corona poling at 150^0C by applying a dc electric field of 3 kV/mm for 30min. The d_{33} value of the samples was measured by Piezo meter.

4.3 Result and discussion

4.3.1Structural analysis from XRD peaks

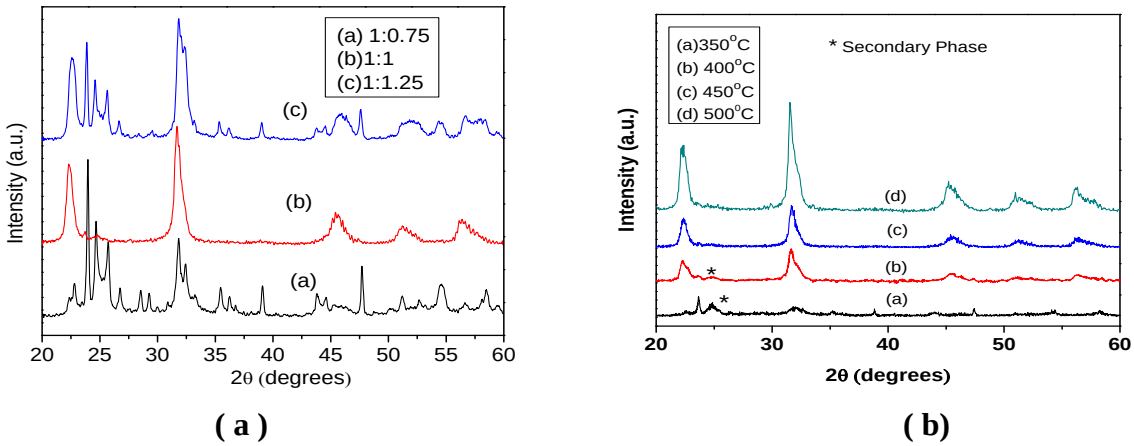

Figure.4.2 (a) XRD patterns of urea mixed KNN powders mixed with varying weight ratio of urea calcined at 450°C and (b) XRD patterns of KNN powder mixed with 1:1 weight ratio of urea calcined at different temperatures

The XRD patterns of urea mixed KNN samples calcined at 450°C for 6h with different weight ratios (1:0.75 to 1:1.25) are shown in Fig.4.2. Single perovskite phase has been developed in case of 1:1 weight ratio of KNN powder and urea, whereas in other cases secondary phases were detected. This may be due to the fact that the uniformity of oxide mixture varies with the variation of urea ratio [1]. Fig.4.2 (b) shows the XRD patterns of urea mixed KNN powders (1:1) calcined at different temperatures starting from 350°C to 500°C for 6h. It can be understood from the fig. that, the phase purity and crystallinity of the urea mixed KNN (1:1) samples increase with the increase in calcination temperature. At lower calcination temperature, secondary phase peaks were detected, but single perovskite phase has been confirmed at 450°C. Whereas, in the same system synthesized by solid state reaction route, single perovskite phase was developed at ~850°C [7]. This shows the importance of using urea

as a fuel for the low temperature synthesis of KNN powder. The basic principle of reduction of processing temperature by using fuel is that when an organic compound combusts within a mixture, it gives out heat that can be effectively supplied to the raw powders in the mixture. The energy supplied in this way accelerates the chemical reaction between raw powders which reduce the reaction temperature.

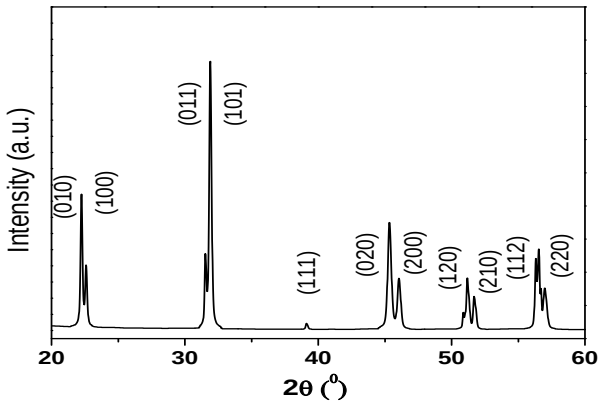

Figure.4.3 XRD pattern of 1:1 urea mixed KNN sample sintered at 1120°C for 2h.

XRD patterns of the 1:1 urea mixed KNN sample sintered at 1120°C for 2h in the oxygen rich environment is shown in Fig 4.3. The diffraction lines are indexed in different crystal systems and unit cell configuration using a computer program package 'Powdmult'. Standard deviations, S.D, $\sum\Delta d = (d_{obs}-d_{cal})$, where'd' is inter-plane spacing, was found to be minimum for orthorhombic structure. The lattice parameters and unit cell volume were found to be a=3.9435Å, b=4.0019Å, c=4.0122Å and V=63.32Å^3 whereas the X-ray density (d_x) of the sample was found to be ~4.508 g/cc. The X-ray density of the sample was calculated by using the formula; $d_x = \frac{(\sum A/N)}{V}n$; where d_x is the X-ray density, ΣA is the sum of the atomic weights of all the atoms in the unit cell, N is the Avogadro's number, V is the volume of the unit cell and n is the number of atoms per unit cell of the crystal structure.

4.3.2 Study of surface morphology

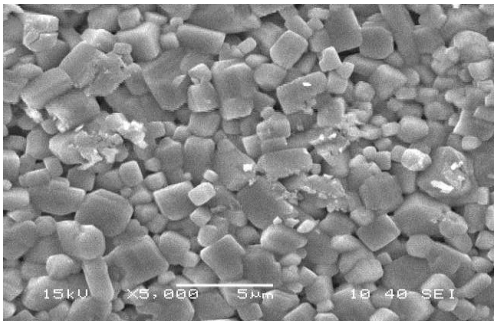

Figure 4.4 SEM image of KNN sample sintered at 1120^{o}C

SEM image of the $K_{0.5}N_{0.5}NbO_3$ sample sintered at 1120^{o}C for 2h in the oxygen rich environment. Surface morphology shows the rectangular size grains with dense packing. The average grain size of this sample was calculated by linear intercept method and found to be ~1.45μm. The experimental density (d_{ex}) of the sample was found to be ~4.398 g/cc which is ~ 97.6% of the d_x. It is also seen that the oxygen sintered KNN sample is denser than the same system sintered in air by the conventional solid-state method [8].

4.3.3 Study of dielectric properties with temperature

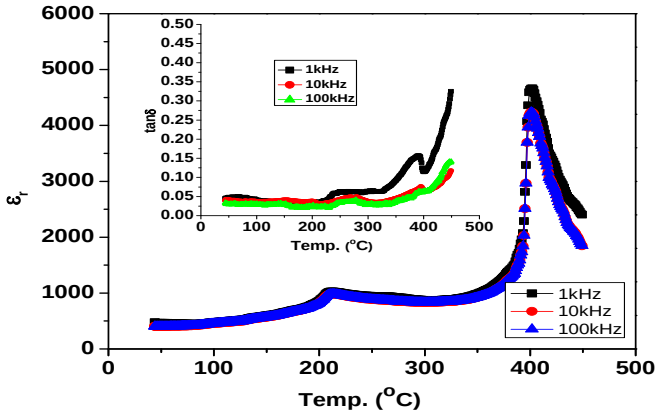

Figure.4.5 Temperature dependence of dielectric constant and dielectric loss of KNN sample.

Temperature dependence of the dielectric constant (ε_r) at different frequencies of oxygen sintered KNN sample is shown in Fig.4.5. The room temperature (RT) ε_r value of KNN sample

at 1 kHz frequency is found to be ~490. Two phase transitions are clearly observed in the dielectric permittivity vs. temp curve corresponding to the orthorhombic to tetragonal (~220^{o}C) and tetragonal to cubic (~420^{o}C) . The phase transition occurred at ~220^{o}C is the ferroelectric transition whereas the transition occurred at ~420^{o}C is called as the ferroelectric – paraelectric transition also known as (Curie temperature). The maximum value of ε_r at Curie temperature (T_c) at 1kHz frequency is found to be ~4637. In perovskite type materials, ferroelectric to paraelectric phase transition occurs due to the instability of temperature dependent lowest frequency optical soft mode [9,10]. At T_c, the lowest frequency soft mode tends to zero and the lattice displacement associated with it becomes unstable. This leads to phase transition from ferroelectric to paraelectric region with max. ε_r at T_c , which can be explained by Lyddane-Sachs-Teller (LST) relation. The LST relation is given as follows

$$\frac{\omega_T^2}{\omega_L^2} = \frac{\varepsilon(\infty)}{\varepsilon(0)} \qquad (4.1)$$

Here static dielectric constant ($\varepsilon(0)$) increases when the transverse optical phonon frequency (ω_T) decreases. Therefore, the higher values of ε_r near T_C is due to the condensation of soft mode frequency ($\omega_T \rightarrow 0$) [11]. The higher value of ε_r near T_c is also supported by the Curie Weiss relation.

The inset Fig.4.5 shows the temperature dependence of the dielectric loss (tanδ) at different frequencies of oxygen sintered KNN sample. The behavior of tanδ is very much similar to ε_r i.e. two similar kind of transition peaks are also observed here. It is observed that a higher value of tanδ is obtained with increasing temperature which may be due to the increase in the mobility of ions and imperfections in the material [12]. The RT tanδ value at 1kHz frequency is found to be ~0.041. It can also be seen form Fig. 4.5 that the temperatures

corresponding to peak dielectric loss and peak dielectric constant do not coinside. Kramers–Kronig relation describes that this can be the consequence of temperature dependent relaxation near Curie temperature [13].

4.3.4 Polarization vs electric field (P-E) hysteresis loop study

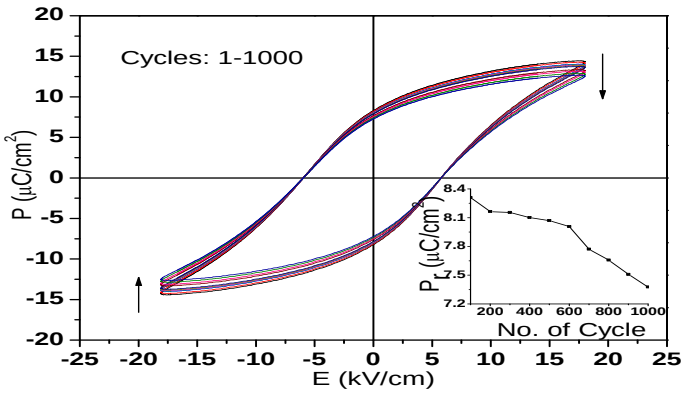

Figure.4.6 Polarization vs electric field (P-E) loop of KNN sample.

(In set Fig.4.6 shows normalized polarization vs switching cycle)

The bipolar polarization vs electric field (P-E) hysteresis loops as a function of no. of switching cycles of KNN samples are shown in Fig.4.6. The development of well saturated hysteresis loops confirms the ferroelectric nature of the material. It can also be noticed that the KNN samples exhibits fatigue behavior i.e. the spontaneous and remnant polarizations (P_r) are found to decrease by 11% with increase in switching cycles. It is known that bipolar fatigue generates microscopic defects and defect clusters in bulk samples, effectively pinning 90° domain wall motion, resulting in the loss of the value of P_r during continuous electric field switching [14]. Inset Fig.4.6 shows the remnant polarization as a function of switching cycle for KNN ceramic, where a logarithmic decay in the value of P_r with increase in switching cycle is

observed. It is found that the value of P_r is decreased from 8.31 to 7.40μC/cm^{2}when the switching cycle increased from 100-1000.

The piezoelectric constant (d_{33}) of this sample was found to be 84pC/N, which is higher than the value reported by conventional process. This may be attributed to the observed higher value of d_{ex} and improved microstructure in the presence of oxygen environment as oxygen sintering facilitates the domain wall switching and give rise to higher piezoelectric properties with lower coercive field [15].

4.4 Conclusions

The XRD confirms the formation of Pure and single perovskite phase KNN samples at lower calcinations temperature (~450^{o}C) using urea as a fuel through the combusion synthesis method, when the urea: KNN is at 1:1 ratio. The presence of urea reduces the processing temperature by supplying heat effectively to the raw powders in the mixture, which accelerates the chemical reaction between them. This enhanced the rate of reaction and obtained single perovskite phase at a lower temperature of 450^{o}C. Dense and uniform distribution of grains was obtained by sintering the sample in the oxygen environment at 1120^{o}C for 2h. Sintering of the samples in the oxygen environment helped to reduce the grain growth and enhanced the density of the samples. The experimental density (d_{ex}) of the sample is found to be ~4.398 g/cc which is ~ 97.6% of the theoretical density. The room temperature dielectric and piezoelectric properties of the $K_{0.5}Na_{0.5}NbO_3$ sample were investigated. It was found that the dielectric and the piezoelectric properties (ε_r ~ 4637, d_{33} = 84pC/N) are superior to the conventionally prepared KNN samples. The P-E hysteresis loop of $K_{0.5}Na_{0.5}NbO_3$ was measured which shows the well saturated hysteresis loop and confirmed the ferroelectric nature of the material.

It was noticed that $K_{0.5}Na_{0.5}NbO_3$ sample exhibits fatigue behavior with increase in switching cycles. Because of the microscopic defects and defect clusters in bulk samples, the value of P_r was decreased from 8.31 to 7.40μC/$cm^2$when the switching cycle has increased from 100-1000. So the results in this study indicate that combustion synthesis process can be used as an effective technique to synthesize ferroelectric materials at lower calcinations temperature.

References

[1] Yang H. B.;Lin Y.; Zhu J. F.;Wang F.;Luo H. J.Mater. Manuf. Process. 2008,23, 489.

[2] Deshpande K.;Mukasyan A.;Varma A. Chem. Mater. 2004,16, 4896.

[3] PATIL K. C. Bull. Mater.Sci.1993,16,533.

[4]Munir Z. A.Am. Ceram. Soc. Bull. 1988, 67, 342.

[5] Yang H.;Lin Y.;Zhu J.;Wang F. Powder Technology.2009,196,233.

[6] Vendrell X. ;Mestres L. Physics Procedia.2010,8, 57.

[7] Chang Y.;Yang Z.;Chao X.;Zhang R.;Li X.Mater.Lett.2007,61,785.

[8] Dua H.L.;Tang F.S.;Liu D.J. Mate. Sci. Eng. B. 2007,136,165.

[9]EgertonL.;DillonM.;J. Am. Ceram. Soc.1959,42, 438.

[10] Cohran W. adv. Phys. 1960 ,9,387.

[11] Kandari A. S.; Bhandari A.; Bauria A.A.; Panwar N.S. Ferroelectrics. 2009,386,139.

[12] Kumar P.; Singh S.; Thakur O.P.; Prakash C.; Goel T.C. J. J. Appl. Phys. 2004,43, 1501.

[13] Lines M.E.;Glass A.M. Applications of Ferroelectrics and Related Materials (Clarendon Press, Oxford, 1977).

[14] Zhang S.; XiaR; Hao H.; Liu H.;Shrout T.R. Appl. Phys. Lett. 2008,14,152904.

[15] Hagh N. M.; Jadidian B.;Safari A. J. Electroceram. 2007,18 , 339.

Chapter 5

Conclusion and Future Scopes

5.1 Conclusions

The majority of currently used high performance piezoelectric and ferroelectric materials contain lead oxide. But due to the biological and environmental concerns the scientific community is interested in developing alternative lead free material with high performance and large operating temperature ranges for electromechanical transducer applications. According to the reported work the KNN family currently shows superior properties than that of the other lead free systems. Similar to PZT system, in KNN system three morphotropic phase boundaries (MPB) exist for K mole % of around 47.5, 32.5 and 17.5 . The compositions near these MPBs are expected to exhibit better electrical properties. A major problem of undoped KNN is that it is fairly difficult to sinter it in the air using the conventional uniaxial pressing technique due to the limited phase stability. Therefore, the work proposed in this thesis was centered around the challenging task for developing the lead free KNN system with better electrical properties .A new chemical process has been used in the synthesis of these KNN ceramics near the three MPB regions and different measurement techniques have been employed to characterize the structure, dielectric, ferroelectric and piezoelectric properties of these materials.

For improving the sinterbility of KNN and thereby enhancing its properties partial co-precipitation technique has been used. Lead free KNN ceramics in single perovskite phase near three MPB regions has been successfully synthesized by partial co-precipitation technique at a low calcination temperature (700^0C). XRD analysis has been carried out in order to investigate the structure of the sintered KNN ceramics which shows the presence of mixed structures in the compositions corresponding to x=0.5 and 0.31 mol% of K in KNN system. The SEM images revealed that the ceramics sintered with higher concentration of K were less porous and have uniform distribution of grains. Potassium (K) acts as a sintering aid to produce the dense KNN ceramics near 50/50 and 33/67 MPB regions. Whereas for lower concentration of K in KNN system the sintering aid nature is not effective. The room temperature dielectric and piezoelectric properties of the KNN samples near three MPBs were investigated, which shows superior properties for the compositions corresponding to x=0.5, 0.31and 0.16 mol% of K in KNN system. The P-E hysteresis loops study of KNN was carried out which shows the well saturated hysteresis loops and confirms the ferroelectric nature of the materials. It was observed that among the nine MPB compositions $K_{0.5}Na_{0.5}NbO_3$ showed the best dielectric, ferroelectric and piezoelectric properties which makes it useful for various applications.

To obtain an ultrafine KNN powder, combustion technique has been used , which is a fast, energy-efficient and environment-friendly chemical process. In the present work, lead-free $K_{0.5}Na_{0.5}NbO_3$ ceramic near 50/50 MPB region was successfully synthesized by the combustion technique and sintered at low processing temperature (450^0C) , using urea as a fuel. The effect of oxygen environment sintering on the microstructural and electrical properties has also been studied and discussed in detail. The XRD analysis confirmed the formation of pure and single perovskite phase in KNN system in presence of 1:1 ratio of urea through the

combustion synthesis method. Dense and uniform distribution of grains was obtained by sintering $K_{0.5}Na_{0.5}NbO_3$ceramics in the oxygen environment. The relative density of the sample is found to be ~ 97.6%. The room temperature dielectric and piezoelectric properties of the $K_{0.5}Na_{0.5}NbO_3$ sample were investigated, which show superior properties than conventionally prepared KNN ceramics. The P-E hysteresis loop of $K_{0.5}Na_{0.5}NbO_3$was measured which shows the well saturated hysteresis loop, confirms the ferroelectric nature of the material. It exhibits fatigue behavior due to microscopic defects and defect clusters in bulk samples, which effectively pinning the 90° domain wall motion. Therefore, the results in this study indicate that combustion synthesis technique can be effectively used to synthesize ferroelectric materials at lower calcination temperature with superior properties.

5.2 Future scopes

The sintering problem of KNN ceramics is very important in the development of lead free materials as high quality material are essential for various applications. KNN is one of the most promising environmental-friendly ferroelectric systems. The ability to overcome the sintering issue of KNN system has opened up new opportunities for device applications. Currently used sintering methods such as hot pressing and texturing are complicated and expensive processes. Compared to these methods partial co-precipitation and combustion techniques are seemed to be simple and cost effective, and also lead to improved properties. In addition to that the calcinations of KNN system which is done by conventional solid state route (CSSR) till date, can also be done by micro wave processing (MW). Although the KNN system near 50/50 MPB region show good electrical properties in the case of partial co-precipitation and combustion techniques, still the size effect of nano size particles on the MW synthesis, dielectric and

piezoelectric properties are yet to be studied. Again the various other characterizations such as pyroelctric, strain vs electrical field, resistivity vs temperature measurements are domains that are not yet studied .These studies will help in exploring their potential for various applications. Further the particle size effect of nano size particles synthesized by the conventional route of KNN systems near the three MPBs, on dielectric and piezoelectric properties is yet to be discussed.

Publications

[1] Synthesis and Characterization of Lead Free $K_{0.33}Na_{0.67}(NbO_3)$ MPB System, M. Pattnaik, & P. Kumar , AIP Conf. Proc.1313 (2010) 284-287.

[2] Effect of Oxygen Sintering on the Structural and Electrical Properties of KNN Ceramics, P. Palei, M. Pattnaik, & P. Kumar, Ceramic International (In Press).

[3] Synthesis and Characterizations of KNN Ferroelectric Ceramics Near 50/50 MPB, M. Pattnaik, & P. Kumar, Bulletin of Material Science (Communicated).

Curriculum Vita

Mausumi Pattanaik

GA-29, Niladri Vihar

Bhubaneswar

Dist. Khurda , Orissa, India

Phone No 8763665396

Email Mausumi.pat@gmail.com

Date of Birth: 7th July 1984

Date of Place: Banpur , Khurda

Father's Name: Himansu Kumar Pattanaik

Husband's Name: Saumya Ranjan Mahapatra

Education: Msc (Physics), Ravenshaw (Auto.) College, Cuttack.

Research Experience:

Project Work: M Tech (R) (2008 – 2011)

Broad Area of Research: - Material Science

Working on synthesis and characterization of Potassium sodium niobate (KNN) lead free ferroelectric system.

Conference

- ✓ International conference
  Physics of Emerging Functional Material , BARC, Mumbai.